Colofon

ISBN: 978-94-6295-125-9

Cover design: Remko van Vught
Printed by: Proefschriftmaken.nl || Uitgeverij BOXPress
Published by: Uitgeverij BOXPress, 's-Hertogenbosch

The research presented in this thesis was performed at the department of Genetics at the Erasmus MC.

Ubiquitin-Mediated Regulation of Damage Recognition in Nucleotide Excision Repair

Regulatie van schadeherkenning in nucleotide excisie herstel door ubiquitine

Proefschift

ter verkrijging van de graad van doctor aan de
Erasmus Universiteit Rotterdam
op gezag van de
rector magnificus

Prof.dr. H.A.P. Pols

en volgens besluit van het College voor Promoties.
De openbare verdediging zal plaatsvinden op
vrijdag 17 april 2015 om 13.30 uur

door

Loes Maria Adriana van Cuijk
geboren te Oosterhout, Nederland

ERASMUS UNIVERSITEIT ROTTERDAM

Promotor:	Prof.dr. W. Vermeulen
Overige leden:	Prof.dr. C.L. Wyman Prof.dr. T.K. Sixma Prof.dr. L.H.F. Mullenders
Copromotor:	Dr. J.A.F. Marteijn

Voor Oma

Table of contents

Scope of the thesis

The integrity of our genetic information is continuously threatened by endogenous metabolites and environmental agents that can generate a variety of DNA lesions. Accumulation of DNA damage can induce genetic changes or cell death, which may result in the onset of cancer or premature ageing. To deal with these adverse effects a network of DNA repair mechanisms and damage signaling pathways, known as the DNA Damage Response (DDR), has evolved. Nucleotide Excision Repair (NER) is responsible for the repair of a wide variety of helix distorting lesions, including those induced by UV-light. NER is a multistep process, which requires the action of more than 30 proteins that need to be tightly controlled to function at the right time and place to warrant efficient repair. Complex cellular processes are commonly regulated by various post translational modifications. Most notably, protein ubiquitylation has emerged as a key regulator of NER. The aim of the work presented in this thesis is to understand the regulation and dynamic properties of NER factors and the UV-DDR in general by ubiquitylation. **Chapter 1** provides the necessary background and the current knowledge on ubiquitin-mediated regulation of the DNA damage recognition steps of NER.

Mass spectrometry (MS) can be used to study the ubiquitylation status of proteins on a proteome wide scale. Since ubiquitylation is transient and solely occurs on a small fraction of proteins, methods to enrich for these proteins are required to study them with MS. In **chapter 2**, a quantitative proteomics approach was combined with the isolation of ubiquitylated peptides to identify UV-regulated ubiquitylation sites on proteins. In addition to the well-known ubiquitylated NER factors, XPC and DDB, we identified UV-responsive ubiquitylated proteins that are active in different biological pathways including, DNA repair, chromatin remodeling, transcription, mRNA splicing, translation and the ubiquitin proteasome system. The most UV-induced peptides were identified for Histone H1. UV-induced H1 ubiquitylation was validated by biochemical experiments.

Chapter 3 describes the identification and characterization of a new ubiquitin E3 ligase - RNF111 - required for efficient NER. RNF111 belongs to the class of SUMO-targeted ubiquitin ligases (STUbLs), which provide direct crosstalk between SUMOylation and ubiquitylation. RNF111 specifically recognizes proteins modified with poly-SUMO2/3 chains, and promotes UBC13-dependent K63-linked ubiquitylation. We demonstrate that RNF111 targets SUMOylated XPC, a DNA damage recognition factor in NER. In **chapter 4** we have studied the function of the RNF111 mediated XPC ubiquitylation *in vivo*. Using a combination of DNA repair assays, immunofluorescence and live cell imaging experiments, we show that RNF111-mediated ubiquitylation stimulates the release of XPC from DNA lesions. This step is required for the stable incorporation of the NER endonucleases XPG and ERCC1/XPF to efficiently complete the NER reaction.

In **chapter 5** we further focus on XPC dynamics. In contrast to other NER factors, XPC shows a non-linear immobilization in response to increasing UV-doses. XPC binding is inhibited at low UV-C doses (0-4 J/m^2), which is dependent on Cul4a and XPC ubiquitylation. NER comprises two damage recognition sub-pathways: global genome NER (GG-NER), involving XPC, and transcription coupled NER (TC-NER). We propose a model in which cells switch between suppression of stable binding of XPC to DNA lesions at low UV-doses and release of this inhibition at higher doses. This bimodal switch allows cells to prioritize repair of transcription

blocking DNA lesions under mild genotoxic stress (low UV-dose, ≤ 4 J/m^2).

Chapter 6 describes the dynamic behavior of RPA in replication and NER. In contrast to other replication factors, RPA does not cluster in replication foci due to a very short residence time at single stranded DNA. During NER, RPA is involved in both the pre- and post-incision steps of NER. RPA binding to the pre-incision complex could only be visualized in the absence of incision without a substantial increase in residence time. Our data show that RPA is an intrinsically highly dynamic protein. In **chapter 7** the main findings of this thesis are wrapped up and the perspectives derived from these data to obtain a more in depth view on the regulation of NER are being discussed.

Chapter 1

General introduction

van Cuijk L, Vermeulen W, Marteijn JA

Adapted from:
Ubiquitin at work: The ubiquitous regulation of the damage recognition step of NER
Published in Experimental Cell Research 2014 November; 329(1):101-109

DNA damage

DNA encodes the genetic instructions required for the development and functioning of every living organism. Preservation of the genetic code is needed for proper cell function and to warrant the correct transmission of the genetic information to progeny and daughter cells. However, the integrity of DNA is constantly threatened by both endogenous and environmental DNA damaging agents that eventually may alter the genetic information (Fig. 1)[1]. During normal cellular metabolism reactive oxygen species (ROS) are produced as byproducts and induce several different types of oxidative DNA lesions. In addition, spontaneous hydrolysis of nucleotide residues results in abasic sites. Approximately 10,000-50,000 DNA lesions per cell per day originate from these endogenous sources[2]. In addition, DNA lesions can be generated by environmental DNA damaging agents, for example from the UV-component in sunlight, ionizing radiation, genotoxic compounds in cigarette smoke and food or man-made chemicals.

DNA lesions directly interfere with vital cellular processes, including transcription and replication[3]. Lesions located in the transcribed strand of active genes may block RNA polymerase II and can thereby inactivate gene expression. Transcription inhibition can eventually induce senescence or cell death, which contributes to premature ageing. DNA lesions also affect the progression and fidelity of replication, which may cause mutations and chromosomal aberrations that increase cancer risk[4].

Damaged DNA cannot be replaced in contrast to other biological molecules and thus completely relies on repair to preserve its genetic information. Through evolution organisms have evolved a network of repair mechanisms and signaling pathways, collectively known as the DNA Damage Response (DDR)[5], to overcome the deleterious effect of DNA damage. The important signaling kinases ATM[6] and ATR[7] can activate cell cycle checkpoints to halt cell proliferation, providing an extended time window for repair. When DNA damage is beyond repair, persistent DNA damage signaling can lead to genome instability, cellular senescence or cell death.

DNA repair

DNA damage sensors monitor DNA to counteract the adverse effects of DNA damage. Upon damage recognition DNA repair mechanisms are initiated to restore DNA to its original state. Multiple DNA repair mechanisms exist, each dedicated to the repair of a specific subset of DNA lesions. Which pathway is triggered does not only depend on the type of lesion, but can also be determined by the cell cycle stage of the cell and the genomic location of the damage (Fig. 1)[8].

Chemical alterations of nucleotides that do not significantly interfere with base-pairing and single strand breaks (SSBs), which both occur frequently - as they originate from endogenous stress - are recognized by Base Excision Repair (BER). The damaged nucleotide is recognized by one of the different DNA glycosylases that cleaves it from the DNA backbone. The remaining abasic (AP)-site is cleaved, generating a single strand break that can be further processed by the BER-specific DNA polymerase β that also re-synthesizes the 1-2 nucleotide gap, which is finally sealed by DNA ligases[9].

DNA double strand breaks (DSBs) can be caused by ionizing radiation (e.g. X-rays) or clastogenic chemicals and are repaired by two mechanistically distinct pathways[10]. Non-homologous end joining simply ligates the two ends of the DSB together. During this process

nucleotides can be lost or added to the broken ends, which results in error-prone repair[11]. Homologous recombination only takes place in S- and G2-phase as it relies on the presence of the intact sister chromatid. The breaks are processed by a series of tightly regulated nucleases to create 3' single-stranded overhangs that invade into the homologous part of the sister. DNA strand exchange and DNA replication in this joint molecule allows the copying of the proper information from the sister, resulting in error-free repair[12].

Interstrand Crosslinks (ICLs) covalently connect the two strands of the DNA double helix and block its unwinding, which therefore interferes with transcription and replication. ICLs are a unique challenge, because their repair involves joined forces of multiple DNA repair pathways. First, ICLs are recognized and processed by the Fanconi Anemia pathway proteins, i.e. a group of 15 or more proteins that are implicated in a damage-induced ubiquitylation of some crucial ICL repair factors to activate specific endonculeases to unhook the ICL. Next via a complex coordination of homologous recombination, nucleotide excision repair and translesion synthesis the repair reaction is completed[13].

Errors, including DNA mismatches, insertions and deletions introduced by the replication machinery are typically recognized by the DNA mismatch repair machinery. This pathway can discriminate the original template strand from the newly synthesized DNA, enabling the removal of the error and incorporation of the correct nucleotides[14,15].

Despite the network of diverse DNA repair mechanisms and cell cycle checkpoints, some lesions may escape removal before entering replication. Some types of lesions may eventually stall the replication machinery and may induce replication fork collapse.

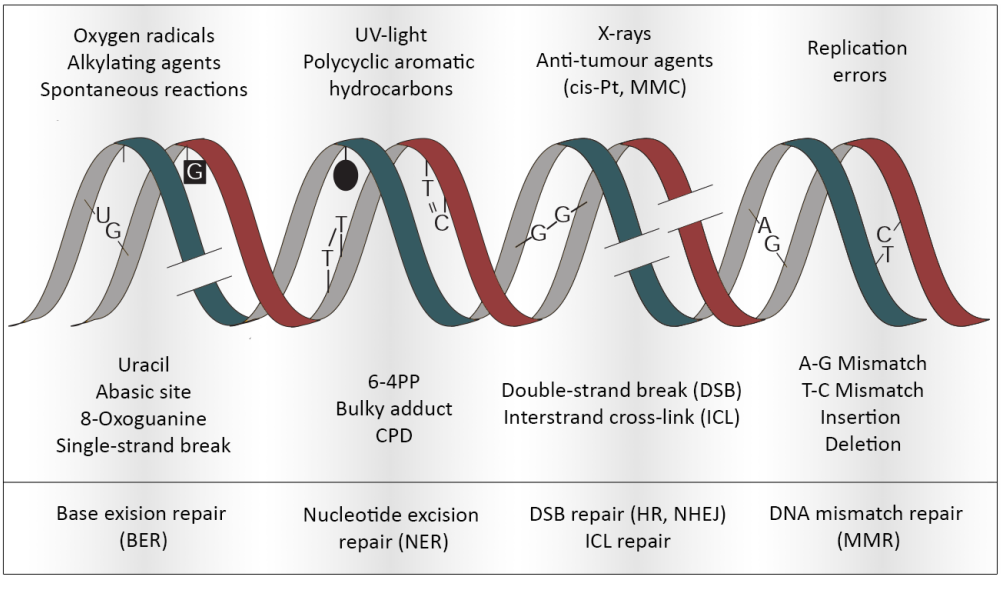

Figure 1. DNA damage and repair mechanisms. Endogenous and environmental DNA damaging agents (top) generate various types of DNA lesions (middle), which are repaired by distinct repair mechanisms (bottom). Abbreviations: cis-Pt, cisplatin; MMC, mitomycin C; 6-4PP, 6-4 pyrimidine-pyrimidone photoproducts; CPD, cyclobutane pyrimidine dimer; HR, homologous recombination; NHEJ, non-homologous end joining; ICL repair, interstrand crosslink repair. Adapted from Hoeijmakers[1].

To overcome these replication blocks mammalian cells express specialized TLS DNA polymerases that can replicate over damaged DNA. However, lesion bypass comes with a prize, since these polymerases are more error-prone. The importance of this pathway is illustrated by the severe skin cancer-prone phenotype associated with the genetic disorder Xeroderma Pigmentosum Variant (XPV)[16,17], which carry inactivating mutations in one of these polymerases.

One important DNA repair pathway is not yet mentioned, which is the topic of this thesis: Nucleotide Excision Repair (NER). The characteristics and regulation of this mechanism is discussed below in further detail.

Nucleotide excision repair

NER removes a remarkable wide variety of DNA lesions, including UV-induced cyclobutane pyrimidine dimers (CPDs) and 6-4 pyrimidine-pyrimidone photoproducts (6-4PPs), chemically induced bulky adducts and some types of endogenously generated oxidative lesions[18,19]. Within NER there are two different modes of damage recognition, which are dependent on the genomic location of the DNA lesion. Global genome NER (GG-NER) detects damage throughout the genome, whereas transcription coupled NER (TC-NER) specifically targets lesions in the transcribed strand of active genes. Both pathways involve four basic steps; including (1) damage recognition, (2) DNA unwinding and damage verification, (3) excision of damaged DNA and, (4) DNA synthesis and ligation (Fig. 2). Inherited defects in NER are associated with different UV-light hypersensitivity recessive autosomal disorders, illustrating its biological significance. Mutations in genes encoding proteins involved in GG-NER cause xeroderma pigmentosum (XP), which is characterized by extreme sun (UV)-sensitivity and a ~2000 fold increased risk of skin cancer[20]. Defects associated with TC-NER can result in Cockayne syndrome (CS) or UV-sensitive syndrome (UV^sS). Whereas the phenotype of UV^sS patients is mainly restricted to UV-hypersensitivity, CS patients present premature aging, developmental and neurological abnormalities[20,21].

Global genome NER

The main damage recognition complex in GG-NER is the heterotrimer XPC-RAD23-Centrin2[22]. XPC is the DNA binding subunit, which constantly probes the DNA for helix distorting lesions[23]. When XPC encounters a damage-induced helix distortion it binds at the junction between the double-strand and damage-induced unpaired part within the undamaged strand opposite to the damage[24]. This striking feature of recognizing the consequence of the damage, rather than the lesion itself also explains the remarkable broad class of different lesions targeted by NER as this partial destabilized helix is a common feature for all types of NER-inducing lesions. Although XPC is the major DNA damage sensor of GG-NER it does not recognize the major UV-induced lesion; CPD, as these hardly destabilize the DNA helix[25]. In this case XPC depends on the UV-DDB complex, which consists of DDB1 and DDB2 (XPE)[26]. The latter subunit has high affinity for UV-induced DNA damage and is required for CPD repair, but also facilitates the repair of 6-4PPs. Structural studies have shown that the WD40 domain of DDB2 binds the lesion. A DDB2 hairpin is inserted into the minor groove, flipping out the photodimer and kinks the DNA by 40^o, facilitating XPC binding[27].

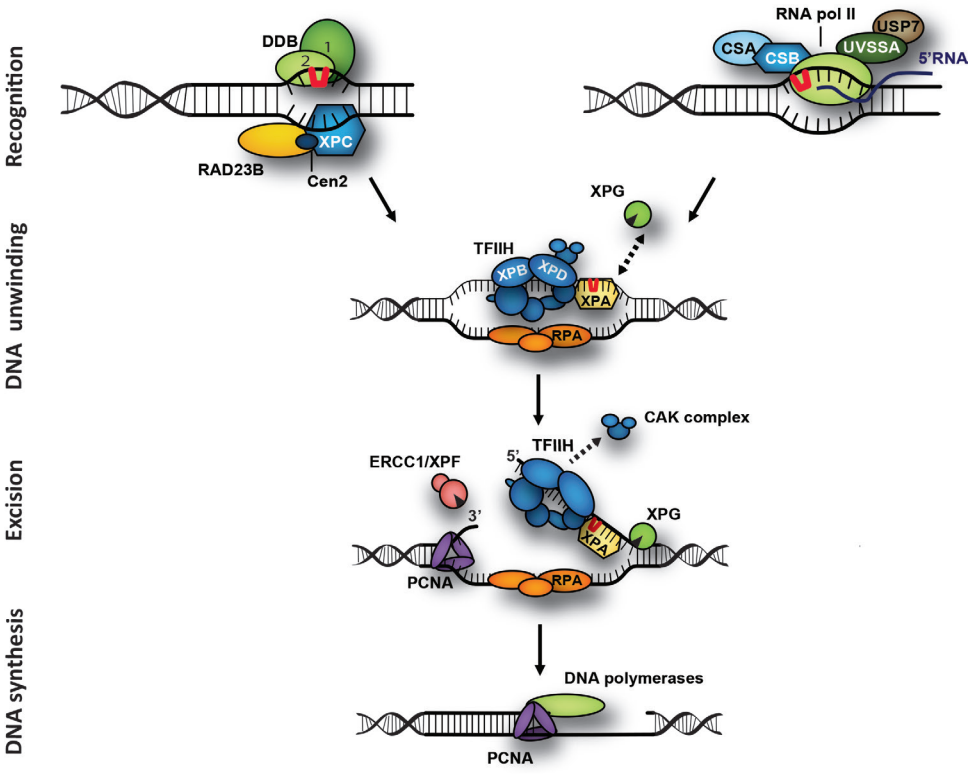

Figuur 2. Model for nucleotide excision repair. NER removes a wide variety of helix distorting DNA lesions. NER comprises two damage recognition sub-pathways, which utilize the same machinery to remove DNA damage. In GG-NER (left) lesions are recognized through the concerted action of the UV-DDB complex (DDB1 and DDB2) and the heterotrimeric XPC complex (XPC, RAD23B and centrin2). TC-NER (right) is initiated by stalling of RNA pol II on a transcription blocking lesion in actively transcribed strands, and requires the proteins CSA, CSB, UVSSA and USP7. Following damage recognition TFIIH is recruited, resulting in the release of its CAK sub-complex and further opening of the DNA double helix. Next RPA and XPA are recruited to stabilize the repair complex and orientate the endonucleases ERCC1/XPF (at the 5' side) and XPG (at the 3' side). After damage excision the DNA is re-synthesized by PCNA and the DNA polymerase δ, ε or κ . The NER reaction is completed by sealing of the final nick by DNA ligase I or III.

Transcription coupled NER

Bulky DNA lesions block transcription elongation and may eventually trigger cell death. This cytotoxic effect of transcription-blocking DNA lesions is counteracted by TC-NER, which specifically removes DNA lesions from the transcribed strand, thereby allowing the restart of the blocked transcription[28]. TC-NER is initiated by stalling of elongating RNA pol II on lesions. The first proteins to interact with lesion stalled RNA pol II are the TC-NER proteins UVSSA and CSB. UVSSA is required for stabilization of CSB, which will be discussed in more detail below[29,30]. CSB recognizes stalled RNA pol II and is responsible for the recruitment of CSA and core NER factors upon initiation of TC-NER[31]. Efficient TC-NER requires the subsequent recruitment of HMNG1, XAB2 and TFIIS, which most likely assist the remodeling of the stalled RNA Pol II complex, thereby generating access for NER proteins to repair the damage[31].

Core NER

After the damage recognition, TFIIH is recruited by a direct interaction with XPC[18]. TFIIH was initially identified as a transcription factor consisting of 10 subunits, including two DNA helicases XPB and XPD and the trimeric CAK complex. Upon DNA damage the CAK complex is released from TFIIH facilitating the switch between its function in transcription and repair[32]. The smallest subunit of TFIIH - TTDA (p8) - is essential for NER, although dispensable for transcription[33]. XPC binds multiple DNA structures, but the NER reaction can only be finalized upon damage verification most likely depending on the helicase activity of XPD assisted by the XPA protein[34-36]. XPA binds also the damage strand and interacts with all NER proteins, defining XPA as the central factor that positions the NER factors at the right place[18]. RPA binds the undamaged strand and positions the endonucleases ERCC1/XPF and XPG on the 5' and 3' side of the damage respectively[37]. First, XPG is recruited independently or through its interaction with TFIIH. Subsequently, ERCC1/XPF is recruited which can only incise the DNA in the presence of XPG. Only after the 5' incision has been completed by ERCC1/XPF, the 3' incision by XPG is triggered. After the coordinated incision[38] the lesion containing oligonucleotide is removed and the undamaged strand is used as a template for DNA repair synthesis performed by PCNA and the DNA polymerase δ, ε or κ[18,39]. This gap filling takes place even in the absence of the 3' incision'[38]. This mechanism most likely protects against accumulation of ssDNA gaps, which induce damage signaling[40]. Finally the DNA gap is sealed by Ligase I or ligase III/XRCC1, which completes the NER reaction[41].

Ubiquitylation

NER involves the action of more than 30 proteins to recognize, verify and repair the damage. The repair factors have to assemble into functional repair complexes and dissociate at the right time and location for proper repair. Intricate molecular processes, such as NER, require a tight regulation, which is commonly achieved by post translational modifications (PTMs) to ensure proper complex assembly and control the function of different protein activities. Their swift induction, reversibility and ability to regulate activity and binding of other proteins make PTMs a very suitable regulator. Phosphorylation, ribosylation and SUMOylation have been reported to play a role in the DNA damage response, including NER[42,43]. Based on recent literature ubiquitylation seems to be a key regulator for NER [42]. Ubiquitin is a highly conserved protein of 76 amino acid that modifies protein substrates, thereby regulating its stability and function[42,43]. Ubiquitin is covalently attached via its C-terminal glycine residue to the ε-amino group of lysine residues in substrates through the concerted action of three enzymes. Ubiquitin is activated in an ATP-dependent manner by an ubiquitin-activating enzyme (E1). Subsequently ubiquitin is transferred to an ubiquitin-conjugating enzyme (E2), which together with an ubiquitin-ligating enzyme (E3) links ubiquitin to the substrate with a high specificity (Fig. 3A)[44]. There are approximately 2 E1, 40 E2 and > 600 E3 proteins encoded in the human genome, which illustrates the complexity and determines the specificity of ubiquitylation[43]. After linkage to one or more sites in the substrate (mono- or multi-ubiquitylation) ubiquitin can use one of its 7 internal lysine residues (K6, K11, K27, K29, K33, K48 and K63) or its N-terminus to form ubiquitin chains (polyubiquitylation)[45]. Ubiquitin chains have distinct structures and properties; consequently they have a different impact on the fate of the target protein.

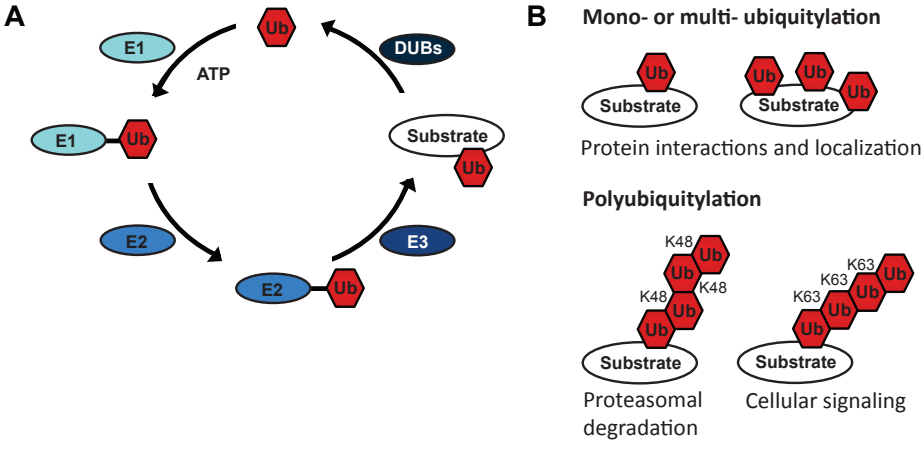

Figure 3. Ubiquitylation. (A) Ubiquitin (Ub) can be covalently attached to itself or other substrates. Ubiquitin is targeted to the ε-amino group of lysines residues in substrates by a serie of enzymatic reactions. The Ub activating (E1) enzyme binds ubiquitin through hydrolysis of ATP to AMP. Subsequently, Ubiquitin is transferred to a Ub conjugating (E2) enzyme, which together with a Ub ligase (E3) enzyme targets substrates. Ubiquitylation is reversible as indicated by deubiquitylating enzymes (DUBs). **(B)** Substrates can be modified by mono-, multi- and polyubiquitylation. Distinct polyubiquitylation chains can be formed, using one of the seven internal lysine residues (K6, K11, K27, K29, K33, K48 and K63) or the N-terminus. Ubiquitylation has different regulatory functions depending on the type of ubiquitylaton or chain. Only the best known ubiquitylation forms are depicted.

For example K48-linked chains result in proteasomal degradation, whereas K63-linked chains are involved in cellular signaling (Fig. 3B)[45]. In addition, ubiquitylated proteins can be recognized by chain specific ubiquitin-binding proteins ("readers"), thereby for example regulating protein-protein interactions[46]. Like most other PTMs ubiquitylation is transient and can be reversed by approximately 100 different deubiquitylating enzymes (DUBs)[47]. The large number of enzymes involved in ubiquitylation and the different ubiquitin chains that can be formed illustrates the diversity of regulation with ubiquitin. Advanced quantitative proteomics in combination with purification methods for ubiquitylated proteins or peptides revealed many UV-induced differential ubiquitylated proteins, confirming the significant involvement of ubiquitin in DNA repair[29,48]. Even though different factors involved in the UV-induced DNA damage response are known to be ubiquitylated e.g. XPA[49] and histone H2A[40], the largest UV-induced ubiquitylation increase was observed for the damage recognition factors of GG-NER and TC-NER, underlining the high regulation of NER initiation. Therefore, in this review we will focus on the role of ubiquitylation in the damage recognition steps of NER.

Ubiquitylation in GG-NER

UV-DDB

The UV-DDB heterodimer (DDB1 and DDB2) is part of a multi-subunit ubiquitin E3 ligase complex that contains the scaffold protein CUL4 and the E2-binding subunit RBX-1/ROC1. DDB1 is the adaptor subunit, which can interact with different DCAF proteins (DDB1- and CUL4-associated factors). DCAFs are characterized by their WD40 repeats that serve as substrate receptor[50].

DDB2 is one of the best characterized DCAFs and targets this Cullin-RING containing ubiquitin ligase complex ($CRL4^{DDB2}$) to sites of UV-induced DNA damage. The ubiquitin ligase activity of $CRL4^{DDB2}$ is tightly regulated by the COP9 signalosome (CSN), a multisubunit-protease[51]. Under unperturbed conditions the CSN is associated with the $CRL4^{DDB2}$ complex, thereby inhibiting its activity by removing the ubiquitin-like protein Nedd8 from CUL4. In addition, it was shown *in vitro* that CSN has also deubiquitylating activity, which might target ubiquitin chains formed on this CRL ligase complex itself[51]. Upon UV-damage infliction CSN dissociates from the $CRL4^{DDB2}$ complex, stimulating the neddylation of CUL4, thereby activating the E3 ligase activity of this CRL[51]. Several $CRL4^{DDB2}$ substrates have been identified, including XPC and DDB2 itself[52,53]. In addition, to these damage recognition factors the $CRL4^{DDB2}$ complex ubiquitylates the core histones H2A[54,55], H3 and H4[56]. The UV-induced ubiquitylation of H3 and H4 followed the kinetics of the 6-4PP repair and weakens the interaction between the histones and DNA, which may aid access of NER proteins to DNA lesions[56]. It was shown *in vitro* that the UV-induced histone H2A mono-ubiquitylation at K119/K120 by the $CRL4^{DDB2}$ complex also results in nucleosome destabilization[55].

In response to UV-damage DDB2 is auto-ubiquitylated, leading to its proteasomal degradation[53,57]. In addition, *in vitro* experiments suggested that DDB2 ubiquitylation might also reduce the binding affinity of the E3 ubiquitin complex for damaged DNA[52]. DDB2 is mainly ubiquitylated at multiple N-terminal lysine residues[52]. Deletion of the DDB2 N-terminus (aa 1-40) as well as mutation of the first 7 N-terminal lysine residues into arginine resulted in stabilization of DDB2 after UV[52,58]. Ubiquitylated DDB2 is recognized by the ATP-driven molecular chaperone VCP/p97, which facilitates proteasomal degradation or recycling of ubiquitylated proteins[59]. More information on the role of VCP/p97 in the DNA damage response can be found a review by *Dantuma et al. 2014*[60]. The recruitment of p97 to sites of DNA damage depends, in addition to CRL ligase activity, on the substrate specific ubiquitin binding-adaptors NPL4, UFD1, and UBXD7. P97 extracts ubiquitylated DDB2 from the chromatin bound $CRL4^{DDB2}$ complex and channels it into the 26S proteasome for degradation (Fig. 4). Knockdown of p97 resulted in an increased recruitment, prolonged residence time of DDB2 and XPC at lesions and a reduced repair activity, suggesting that ubiquitylated DDB2 needs to be removed from the chromatin for efficient NER[59]. In line with this, siRNA mediated knockdown of CUL4A in human cells resulted in an increased retention time of DDB2 at lesions in combination with reduced CPD removal[61]. In contrast, CUL4A knockout mice exhibit enhanced GG-NER activity and increased UV-resistance in combination with increased DDB2 and XPC protein levels[62]. These contradicting observations may be explained by the different species in which these studies were performed that are characterized by different DDB2 expression levels[63]. However, together these observations show that CUL4A-dependent DDB2 ubiquitylation not only stimulates damage recognition, but also induces the subsequent p97-dependent clearance of DDB2 that is required to promote the downstream repair reaction. Moreover, it appeared that expression levels of DDB2 need to be under tight control to warrant efficient NER[64]. It was recently found that the steady state level of DDB2 is regulated by the DUB USP24, which interacts with DDB2 and might counteract CUL4A under unperturbed conditions[65]. The recently identified PARylation of DDB2 adds another level of regulation and complexity to the DDB2 function in NER. It was shown that PARP1-dependent PARylation of DDB2 resulted in its prolonged binding to chromatin and

its delayed degradation[66]. This PARylation dependent stabilization of DDB2 thus counteracts CUL4A induced ubiquitylation and the subsequent degradation of DDB2 (Fig. 4). The crosstalk between DDB2 ubiquitylation and PARylation is most likely based on competition of lysine residues. Since both ubiquitylation and PARylation are targeted to lysine residues at the 40 N-terminal amino acids of DDB2[66].

XPC

Next to DDB2, also XPC protein levels are controlled by the ubiquitin-proteasome system. High levels of XPC are found to be cytotoxic, most likely caused by its ability to bind a wide variety of DNA structures, thereby interfering with DNA metabolism[67]. An important XPC regulator is its binding partner RAD23. Mammalian cells express two RAD23 paralogs, RAD23A and RAD23B. Both proteins encode two ubiquitin-associated (UBA) domains, which recognize ubiquitylated proteins, and an ubiquitin-like (UBL) domain, which can interact with the proteasome, thereby targeting bound ubiquitylated proteins for degradation[42]. Although XPC can bind both proteins, it is predominantly associated to the more abundant RAD23B. Interestingly, deletion of both RAD23 paralogs severely reduced steady-state levels of XPC, causing reduced UV-resistance and DNA repair synthesis comparable with $XPC^{-/-}$ cells[67]. Thus contrary to the expected proteasomal shuttling function of RAD23B, this protein stabilizes XPC rather than targeting XPC for degradation. Overexpression of Rad4, the yeast ortholog of XPC, in rad23 yeast strains only partially complemented the UV-sensitivity, suggesting additional roles of RAD23 during NER[68]. Indeed, FRAP analysis of XPC in RAD23 double knock out cells showed that RAD23 is required for XPC binding to UV-induced DNA damage. Although RAD23 is essential for XPC loading, it is not detectable at DNA lesions, since it dissociates from XPC upon damage recognition[69]. This suggests that RAD23 delivers XPC at UV-lesions, but is not required to stabilize lesion-bound XPC. XPC is also a well described target of the $CRL4^{DDB2}$ complex upon UV-damage[50,52]. Interestingly, in contrast to DDB2, XPC polyubiquitylation did not result in degradation (Fig. 4). Whether the $CRL4^{DDB2}$ complex forms different polyubiquitin chains on DDB2 (K48-linked) and XPC (unknown) is currently not known. However, it has been noted that XPC is modified by K48- as well as K63-linked chains[59,70]. It is suggested that the K48-linked ubiquitylated XPC- like DDB2- is recognized by the ATPase p97 and channeled into the proteasome for degradation[59]. In a yeast-two hybrid screen OTUD4, a deubiquitylating enzyme was identified as an interaction partner of XPC[71]. Knockdown of OTUD4 resulted in an increase of the ubiquitylated form of XPC after UV. Although the exact function of OTUD4 is currently unknown, it may function to trim down CUL4-induced polyubiquitin chains protecting XPC form degradation[71].

XPC is not only ubiquitylated, but also modified by the ubiquitin like modifier SUMO upon UV-damage in a DDB2 dependent manner. The XPC SUMOylation was suggested to result in its stabilization[72]. Recently, another XPC regulating E3 ubiquitin-ligase was identified: RNF111[70]. It belongs to the class of SUMO-targeted ubiquitin ligases (STUbLs), which provide direct crosstalk between SUMOylation and ubiquitylation. RNF111 specifically binds the UV-induced SUMOylated form of XPC, which results in the RNF111 dependent formation of UBC13-dependent K63-linked chains on XPC (Fig. 4)[70]. Although both the $CRL4^{DDB2}$ complex and RNF111 ubiquitylate XPC in response to UV, they have opposite effects on the damaged DNA binding kinetics of XPC. Whereas knockdown of RNF111 increased the accumulation of

1

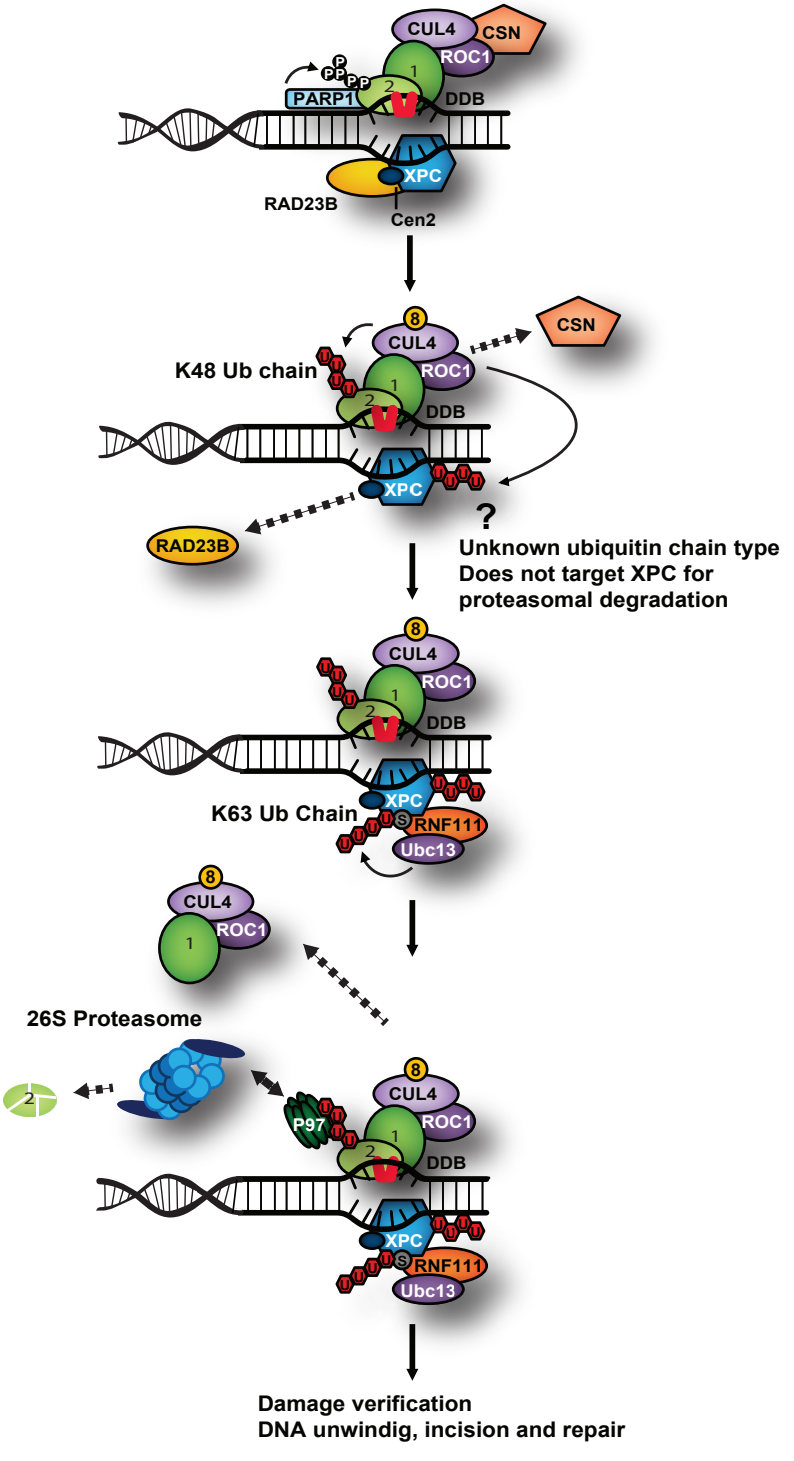
CUL4
CSN
ROC1
PARP1
DDB
XPC
RAD23B
Cen2
8
K48 Ub chain
?
Unknown ubiquitin chain type
Does not target XPC for
proteasomal degradation
K63 Ub Chain
RNF111
Ubc13
26S Proteasome
P97
Damage verification
DNA unwindig, incision and repair

Figure 4. The Role of ubiquitin in the regulation of global genome NER.
GG-NER repairs helix distorting lesions in the entire genome. UV-induced DNA damage can be recognized by DDB2 and XPC. In response to UV, DDB2 is PARylated by PARP1, which stabilizes DDB2 at the site of DNA damage. DDB2 forms an E3 ligase complex with DDB1, Cul4 and Roc1 ($CRL4^{DDB2}$). The E3 ligase activity is tightly regulated by the COP9 signalosome (CSN). Upon damage binding CSN dissociates form the complex, stimulating the neddylation of CUL4, thereby activating the E3 ligase. This results in polyubiquitylation of DDB2 and XPC. Ubiquitylated DDB2 is extracted from the $CRL4^{DDB2}$ complex by p97 and channeled into the 26S proteasome for degradation. XPC, associated with RAD23B and CEN2, binds the undamaged strand and is ubiquitylated by the $CRL4^{DDB2}$ complex, which is a signal to increase its binding affinity for damaged DNA. RAD23 is required for efficient XPC loading and contains two ubiquitin-binding domains and an ubiquitin-like domain. Upon binding of XPC to the damaged DNA, RAD23 is released from the complex. XPC is in response to UV SUMOylated, which results in the recruitment of RNF111 by its SIM domains. This SUMO-targeted E3 ligase subsequently modifies XPC with K63-linked ubiquitin chains, which is crucial for efficient NER.

XPC-GFP on local UV-induced damage, knockdown of DDB2 resulted in a decrease of XPC-GFP accumulation[70]. Despite this opposing effect on XPC kinetics knockdown of either DDB2 or RNF111 resulted in reduced DNA repair synthesis (a measure for GG-NER), indicating that both E3 ligases are required for efficient GG-NER[70]. Future research is required to elucidate the interplay between these different E3 ligases, DUBs and ubiquitin binding proteins to provide insight in their exact roles during NER.

Ubiquitylation in TC-NER

CSA and CSB

Like DDB2, CSA belongs to the family of DCAF proteins and forms an E3 ubiquitin complex with DDB1-CUL4-ROC1 ($CRL4^{CSA}$)[51]. Whereas the DDB2 containing CRL4 complex is required for proper GG-NER, the CSA containing CRL4 complex is essential for TC-NER and the subsequent transcription restart. The ubiquitin ligase activity of $CRL4^{CSA}$ is also regulated by the CSN[51]. However, CSN remains associated to the $CRL4^{CSA}$ shortly after UV-irradiation and only dissociates at later time points as compared to $CRL4^{DDB2}$ complex[51]. It was shown that CSB is polyubiquitylated and degraded 3h after UV-irradiation, coinciding with the dissociation of the CSN from $CRL4^{CSA}$ [73]. This CSA-mediated CSB degradation was suggested to occur after repair has been completed and the subsequent CSB-clearance was proposed to allow transcription restart[73]. Next to $CRL4^{CSA}$ also the heterodimer BRCA1-BARD1 E3-ligase complex was suggested to be implicated in TC-NER[74]. Knockdown of BRCA1 resulted in a reduced ubiquitylation and degradation of CSB and inhibited CPD repair by TC-NER[74]. The existence of two independent pathways resulting in CSB degradation might either indicate redundancy or reflect different roles for CSA and BRCA1 mediated ubiquitylation in TC-NER. The C-terminus of CSB contains an ubiquitin-associated (UBA) domain that can interact with ubiquitin, with the highest affinity for K63-linked chains[75]. Although deletion of the UBA domain does not interfere with TC-NER complex assembly, repair does not occur. Live cell imaging experiments revealed that deletion of the UBA domain completely immobilizes CSB after UV and thereby traps TC-NER complexes at the site of DNA damage, most likely blocking the TC-NER reaction[75]. This suggests that the UBA domain is involved in the release of CSB, indicating that this is a crucial step during repair. However the ubiquitylated interaction partner of the UBA domain, which most likely serves as signal for CSB dissociation, is still unknown.

UVSSA

Next to exome sequencing of UV^{S}S group A patient cells[76] and correction cloning by chromosome transfer to UV^{S}S-A cells[30], the TC-NER factor UVSSA was recently identified in a quantitative proteomics screen to detect differences in protein ubiquitylation upon UV-induced DNA damage [29]. UVSSA was found to be ubiquitylated itself; however this ubiquitylation was independent of DNA damage. Further research suggested that UVSSA co-purifies with ubiquitylated RNA pol II upon UV-damage and interacts with the TC-NER factors CSA and CSB[29,30,76]. In addition, UVSSA forms a complex with the DUB USP7 in a UV-independent manner[29,30]. Depletion of USP7 resulted in a similar TC-NER deficiency as seen for UVSSA knockdown. In the absence of UVSSA or USP7 a strong increase in the proteasomal degradation of CSB was observed in response to UV. One of the key functions of UVSSA during TC-NER is to recruit the pleiotropic DUB USP7, which has multiple roles both in as well as outside the DNA Damage Response[77], to TC-NER complexes and thereby counteracting CSB ubiquitylation. Most probably this de-ubiquitylation results in an increased window of opportunity for CSB to assemble the TC-NER complexes before CSB is degraded. Together UVSSA, USP7, CSA and BRCA1 tightly regulate the fate of CSB and thereby the completion of TC-NER (Fig. 5, left side).

RNA polymerase II

UVSSA encodes two conserved, poorly characterized domains: a C-terminal DUF2043 domain and an N-terminal Vps27-Hrs-STAM (VHS) domain both required for functional TC-NER. Like the UBA domain of CSB, the VHS domain was suggested to interact with ubiquitylated proteins. Indeed it was shown that UVSSA interacts with ubiquitylated RPB1 (the large subunit of the RNA pol II complex)[76]. While the VHS domain is crucial for its function in TC-NER, the exact biological relevance of the ubiquitin binding capacity of UVSSA remains to be discovered. Finally, while UVSSA together with USP7 plays an important role in the de-ubiquitylation of CSB, UVSSA is also important for the ubiquitylation of RPB1. In response to UV, an UVSSA-dependent ubiquitylation of RPB1 was observed, which interestingly does not target it for proteasomal degradation. Not only the precise function of this ubiquitylation event is unknown, also the molecular mechanism how UVSSA can be responsible for this ubiquitylation needs to be uncovered.

When TC-NER cannot be executed successfully, for example due to mutations in CSA or CSB proteins, lesion-stalled RNA Pol II cannot be properly resolved. It was shown that when lesion-stalled RNA pol II cannot be efficiently processed by TC-NER, RPB1 gets poly-ubiquitylated and degraded[78]. Several ubiquitin E3 ligases were proposed to be involved in the ubiquitylation of RPB1, including CSA[79], BRCA1-BARD1[80] and NEDD4[81]. In CS-A and CS-B cells ubiquitylation of RPB1 is remarkably reduced[79]. Since CSA is part of an ubiquitin E3 complex, it was suggested that CSA ubiquitylates RNA pol II. However, more recently, it was shown that this defect in UV-induced RNA pol II ubiquitylation and degradation in CS-A and CS-B cells is most likely indirect and can be explained by the absence of transcription recovery in these cells[81]. The von Hippel-Lindau tumor suppressor protein (pVHL) has also been implicated in the degradation of elongating RNA pol II. pVHL-associated complex was shown to interact with the elongating RPB1, targeting it for ubiquitylation and proteasomal degradation[82,83].

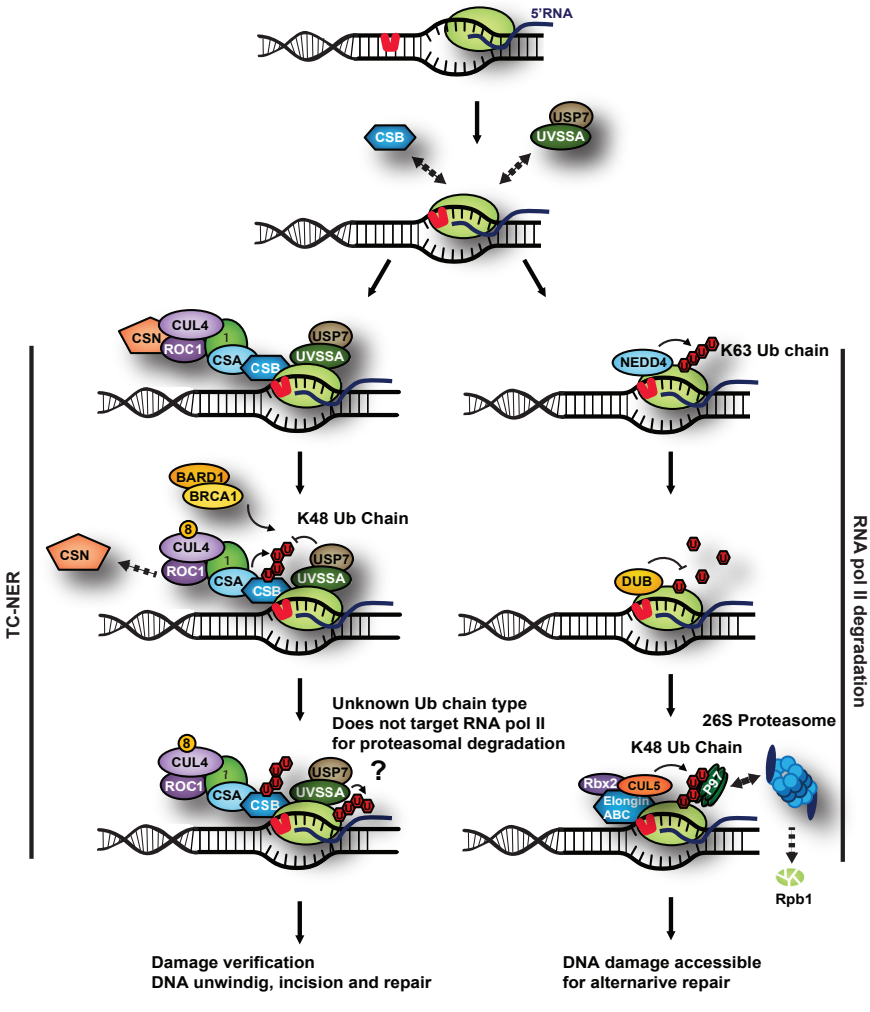

Figure 5. The Role of ubiquitin in the regulation of transcription coupled NER.
Transcription blocking lesions are repaired by TC-NER. Upon stalling of elongating RNA pol II at the DNA lesion, it is bound by CSB and UVSSA. CSB recruits CSA, which forms an E3 ligase complex together with DDB1, Cul4 and Roc1 (CRL4^{CSA}) (Left panel). Upon dissociation of the CSN, the CRL4^{CSA} complex is activated, resulting in ubiquitylation and proteasomal degradation of CSB. This ubiquitylation is counteracted by the DUB USP7, which is recruited to the stalled RNA polymerase by UVSSA, to stabilize CSB during the TC-NER reaction. In addition to the CRL4^{CSA} complex, also other proteins are involved in the ubiquitylation of TC-NER proteins. UVSSA mediates ubiquitylation of stalled RNA pol II, the function of this event is unknown, but it does not result in proteasomal degradation of RNA pol II. Furthermore, BRCA1-BARD1 is described to ubiquitylate CSB and RNA pol II. If TC-NER fails to repair the damage, stalled RNA pol II can be degraded "as a last resort" to remove RNA pol II from the lesion (right panel). This pathway is initiated by NEDD4, which promotes K63-dependent ubiquitylation of the large subunit RPB1 of RNA pol II. These K63-linked chains are trimmed down to a mono-ubiquitylated form of RNA pol II, which is a substrate for Elongin ABC-Cul5-RBX2. This E3 ligase complex induces K48-linked ubiquitylation of RPB1, which is recognized by the p97, resulting in the extraction of the RPB1 subunit from the stalled RNA pol II, which subsequently leads to its degradation by the 26S proteasome.

However, the exact role of RPB1 ubiquitylation by pVHL remains to be established. In addition, it was shown that the BRCA1-BARD1 complex interacts with RNA pol II[80]. Overexpression of the BRCA1-BARD1 complex stimulated UV-induced ubiquitylation of the hyperphosphorylated form of RPB1, which results in its degradation[84]. Also RPB8, a common subunit in all three RNA polymerases, was shown to be ubiquitylated in response to UV by BRCA1-BARD1[85]. Interestingly, ubiquitylation of RPB8 does not result in proteasomal degradation, but is implicated in UV survival. Cells expressing an ubiquitin-resistant form of RPB8 were extremely UV-sensitive, which might suggest that the ubiquitylation of RPB8 is an important step in RNA pol II disassembly or dissociation from the transcription blocking lesion. However, *Anindya et al. 2007*[81] found out that only knockdown of NEDD4, but not of BRCA1, significantly reduced the RPB1-ubiquitylation and subsequent proteasomal degradation. NEDD4 co-immunopreciptates with RNA pol II in a UV-dependent manner and is able to ubiquitylate RNA pol II *in vitro*[81]. Interestingly, NEDD4 is only capable of catalyzing mono- or K63 polyubiquitylation, which does not target the substrate protein for proteasomal degradation. This suggests that, another E3 ligase must be involved. It was shown that the Elongin ABC-Cul5-RBX2 complex can form K48-linked chains on RNA pol II, however only when RPB1 is already ubiquitylated by NEDD4[86]. In S. cerevisiae the DUB, Ubp2, is associated to Rsp5, the yeast homolog of NEDD4 and trims the K63-linked ubiquitin chains down until a mono-ubiquitin modification remains on RPB1[86]. The mammalian ortholog of Ubp2 is currently unknown. This concerted action of the E3 ligase NEDD4, an unknown DUB and the Elongin ABC-Cul5-RBX2 complex to modify RPB1 represents a nice example of ubiquitin chain editing (Fig. 5, right side). Elongating RNA pol II is very stably associated to the DNA template even in the presence of UV-induced ubiquitylation[78]. Interestingly, in yeast cells deficient for the ATPase CDC48 K48-linked ubiquitylated RNA pol II accumulates in response to UV, as it is not degraded anymore[87]. Whether the VCP/p97 ubiquitin segregase, the mammalian ortholog of CDC48, is involved in the extraction and degradation of RPB1 in currently unknown; see for more details on the role of p97 *Dantuma et al. 2014*[60]. The balance between NEDD4, the Elongin ABC-Cul5-RBX2 complex and de-ubiquitylating enzymes determine the fate of RNA pol II, as soon the K48-linked chain becomes long enough it is recognized by VCP/p97 and stripped from the elongating complex resulting in its degradation by the proteasome. This degradation pathway of RBP1 is more common in TC-NER deficient cells, suggesting that TC-NER is the preferred pathway to deal with lesion-stalled RNA pol II and that degradation and removal of RNA pol II is an important pathway of "last resort" to overcome the highly cytotoxic blocked transcription complexes[78,79].

Concluding remarks

In this review we summarize the multiple ubiquitylation events implicated in regulating the different damage recognition steps of NER. Ubiquitin modifications are not only important for regulating protein-protein interactions, facilitating the transition through the different NER reaction-steps, but appeared also to function in clearing repair factors from chromatin when their activity is no longer needed or when repair fails or is aborted. How can this high level and complex ubiquitin-dependent regulation of particularly GG-NER and TC-NER initiating proteins be rationalized? One obvious possibility is that NER initiation needs to be carefully regulated to prevent unwanted NER-mediated excision on non-damaged DNA. For this reason the NER

reaction itself has also an important damage verification step, which is performed by the joint action of TFIIH and XPA[18]. Non-true NER lesions are not further processed and the formed NER pre-incision complex needs to be disassembled. Ubiquitin might play a crucial role in this reversible nature of the damage sensing complexes. In addition, the different ubiquitylation events during TC-NER seem to play a crucial role in pathway choice; either the reaction will proceed through the "conservative" TC-NER pathway, or when TC-NER failed a "destructive" pathway has to take over to remove the stalled RNA pol II from the DNA. It is expected that with the still advancing isolation procedures for ubiquitylated proteins and peptides, improved quantitative proteomics and data analysis tools, new ubiquitylation targets and factors involved in NER will be identified[88]. This will give important new insights in the complex regulation of NER. Furthermore, these proteomics approaches might uncover more examples of the interplay between different PTMs on NER factors, as have been observed for ubiquitin with PAR on DDB2[66] and with SUMO on XPC [70,72]. The current challenge in the field is not only to identify different PTMs, but mainly how these collaborate at each separable step in the repair reaction and how these PTMs facilitate proper repair. Emerging evidence suggests that the "Readers" of modified proteins, which contain specific PTM binding motifs, are important drivers of this process. A nice example is the recognition of SUMOylated XPC by the STUbL RNF111, which will be addressed in chapter 3. Furthermore, it will be interesting to study which proteins are recognized by the Ub-binding domains of RAD23B, CSB and UVSSA and how these proteins are involved in repair?

References

1. Hoeijmakers, J.H. Genome maintenance mechanisms for preventing cancer. *Nature* **411**, 366-74 (2001).
2. Lindahl, T. Instability and decay of the primary structure of DNA. *Nature* **362**, 709-15 (1993).
3. Mitchell, J.R., Hoeijmakers, J.H. & Niedernhofer, L.J. Divide and conquer: nucleotide excision repair battles cancer and ageing. *Curr Opin Cell Biol* **15**, 232-40 (2003).
4. Hoeijmakers, J.H. DNA damage, aging, and cancer. *N Engl J Med* **361**, 1475-85 (2009).
5. Jackson, S.P. & Bartek, J. The DNA-damage response in human biology and disease. *Nature* **461**, 1071-8 (2009).
6. Shiloh, Y. ATM and related protein kinases: safeguarding genome integrity. *Nat Rev Cancer* **3**, 155-68 (2003).
7. Cimprich, K.A. & Cortez, D. ATR: an essential regulator of genome integrity. *Nat Rev Mol Cell Biol* **9**, 616-27 (2008).
8. Giglia-Mari, G., Zotter, A. & Vermeulen, W. DNA damage response. *Cold Spring Harb Perspect Biol* **3**, a000745 (2011).
9. Hegde, M.L., Hazra, T.K. & Mitra, S. Early steps in the DNA base excision/single-strand interruption repair pathway in mammalian cells. *Cell Res* **18**, 27-47 (2008).
10. van Gent, D.C., Hoeijmakers, J.H. & Kanaar, R. Chromosomal stability and the DNA double-stranded break connection. *Nat Rev Genet* **2**, 196-206 (2001).
11. Lieber, M.R. The mechanism of double-strand DNA break repair by the nonhomologous DNA end-joining pathway. *Annu Rev Biochem* **79**, 181-211 (2010).
12. Li, X. & Heyer, W.D. Homologous recombination in DNA repair and DNA damage tolerance. *Cell Res* **18**, 99-113 (2008).
13. Raschle, M. *et al.* Mechanism of replication-coupled DNA interstrand crosslink repair. *Cell* **134**, 969-80 (2008).
14. Jiricny, J. The multifaceted mismatch-repair system. *Nat Rev Mol Cell Biol* **7**, 335-46 (2006).
15. Jiricny, J. Postreplicative mismatch repair. *Cold Spring Harb Perspect Biol* **5**, a012633 (2013).
16. Lehmann, A.R. Replication of damaged DNA by translesion synthesis in human cells. *FEBS Lett* **579**, 873-6 (2005).
17. Gratchev, A., Strein, P., Utikal, J. & Sergij, G. Molecular genetics of Xeroderma pigmentosum variant. *Exp Dermatol* **12**, 529-36 (2003).
18. Scharer, O.D. Nucleotide excision repair in eukaryotes. *Cold Spring Harb Perspect Biol* **5**, a012609 (2013).
19. Marteijn, J.A., Lans, H., Vermeulen, W. & Hoeijmakers, J.H. Understanding nucleotide excision repair and its roles in cancer and ageing. *Nat Rev Mol Cell Biol* **15**, 465-81 (2014).
20. Lehmann, A.R. DNA repair-deficient diseases, xeroderma pigmentosum, Cockayne syndrome and trichothiodystrophy. *Biochimie* **85**, 1101-11 (2003).
21. Spivak, G. UV-sensitive syndrome. *Mutat Res* **577**, 162-9 (2005).
22. Sugasawa, K. *et al.* Xeroderma pigmentosum group C protein complex is the initiator of global genome nucleotide excision repair. *Mol Cell* **2**, 223-32 (1998).
23. Hoogstraten, D. *et al.* Versatile DNA damage detection by the global genome nucleotide excision repair protein XPC. *J Cell Sci* **121**, 2850-9 (2008).
24. Min, J.H. & Pavletich, N.P. Recognition of DNA damage by the Rad4 nucleotide excision repair protein. *Nature* **449**, 570-5 (2007).
25. Sugasawa, K. *et al.* A multistep damage recognition mechanism for global genomic nucleotide excision repair. *Genes Dev* **15**, 507-21 (2001).
26. Wakasugi, M. *et al.* DDB accumulates at DNA damage sites immediately after UV irradiation and directly stimulates nucleotide excision repair. *J Biol Chem* **277**, 1637-40 (2002).
27. Scrima, A. *et al.* Structural basis of UV DNA-damage recognition by the DDB1-DDB2 complex. *Cell* **135**, 1213-23 (2008).
28. Vermeulen, W. & Fousteri, M. Mammalian transcription-coupled excision repair. *Cold Spring Harb Perspect Biol* **5**, a012625 (2013).
29. Schwertman, P. *et al.* UV-sensitive syndrome protein UVSSA recruits USP7 to regulate transcription-coupled repair. *Nat Genet* **44**, 598-602 (2012).
30. Zhang, X. *et al.* Mutations in UVSSA cause UV-sensitive syndrome and destabilize ERCC6 in transcription-coupled DNA repair. *Nat Genet* **44**, 593-7 (2012).

31. Fousteri, M., Vermeulen, W., van Zeeland, A.A. & Mullenders, L.H. Cockayne syndrome A and B proteins differentially regulate recruitment of chromatin remodeling and repair factors to stalled RNA polymerase II in vivo. *Mol Cell* **23**, 471-82 (2006).
32. Compe, E. & Egly, J.M. TFIIH: when transcription met DNA repair. *Nat Rev Mol Cell Biol* **13**, 343-54 (2012).
33. Theil, A.F. *et al.* Disruption of TTDA results in complete nucleotide excision repair deficiency and embryonic lethality. *PLoS Genet* **9**, e1003431 (2013).
34. Sugasawa, K., Akagi, J., Nishi, R., Iwai, S. & Hanaoka, F. Two-step recognition of DNA damage for mammalian nucleotide excision repair: Directional binding of the XPC complex and DNA strand scanning. *Mol Cell* **36**, 642-53 (2009).
35. Mathieu, N., Kaczmarek, N., Ruthemann, P., Luch, A. & Naegeli, H. DNA quality control by a lesion sensor pocket of the xeroderma pigmentosum group D helicase subunit of TFIIH. *Curr Biol* **23**, 204-12 (2013).
36. Camenisch, U., Dip, R., Schumacher, S.B., Schuler, B. & Naegeli, H. Recognition of helical kinks by xeroderma pigmentosum group A protein triggers DNA excision repair. *Nat Struct Mol Biol* **13**, 278-84 (2006).
37. de Laat, W.L. *et al.* DNA-binding polarity of human replication protein A positions nucleases in nucleotide excision repair. *Genes Dev* **12**, 2598-609 (1998).
38. Staresincic, L. *et al.* Coordination of dual incision and repair synthesis in human nucleotide excision repair. *EMBO J* **28**, 1111-20 (2009).
39. Ogi, T. *et al.* Three DNA polymerases, recruited by different mechanisms, carry out NER repair synthesis in human cells. *Mol Cell* **37**, 714-27 (2010).
40. Marteijn, J.A. *et al.* Nucleotide excision repair-induced H2A ubiquitination is dependent on MDC1 and RNF8 and reveals a universal DNA damage response. *J Cell Biol* **186**, 835-47 (2009).
41. Moser, J. *et al.* Sealing of chromosomal DNA nicks during nucleotide excision repair requires XRCC1 and DNA ligase III alpha in a cell-cycle-specific manner. *Mol Cell* **27**, 311-23 (2007).
42. Bergink, S. & Jentsch, S. Principles of ubiquitin and SUMO modifications in DNA repair. *Nature* **458**, 461-7 (2009).
43. Jackson, S.P. & Durocher, D. Regulation of DNA damage responses by ubiquitin and SUMO. *Mol Cell* **49**, 795-807 (2013).
44. Hershko, A. & Ciechanover, A. The ubiquitin system. *Annu Rev Biochem* **67**, 425-79 (1998).
45. Kulathu, Y. & Komander, D. Atypical ubiquitylation - the unexplored world of polyubiquitin beyond Lys48 and Lys63 linkages. *Nat Rev Mol Cell Biol* **13**, 508-23 (2012).
46. Husnjak, K. & Dikic, I. Ubiquitin-binding proteins: decoders of ubiquitin-mediated cellular functions. *Annu Rev Biochem* **81**, 291-322 (2012).
47. Jacq, X., Kemp, M., Martin, N.M. & Jackson, S.P. Deubiquitylating enzymes and DNA damage response pathways. *Cell Biochem Biophys* **67**, 25-43 (2013).
48. Povlsen, L.K. *et al.* Systems-wide analysis of ubiquitylation dynamics reveals a key role for PAF15 ubiquitylation in DNA-damage bypass. *Nat Cell Biol* **14**, 1089-98 (2012).
49. Kang, T.H., Reardon, J.T. & Sancar, A. Regulation of nucleotide excision repair activity by transcriptional and post-transcriptional control of the XPA protein. *Nucleic Acids Res* **39**, 3176-87 (2011).
50. Hannah, J. & Zhou, P. Regulation of DNA damage response pathways by the cullin-RING ubiquitin ligases. *DNA Repair (Amst)* **8**, 536-43 (2009).
51. Groisman, R. *et al.* The ubiquitin ligase activity in the DDB2 and CSA complexes is differentially regulated by the COP9 signalosome in response to DNA damage. *Cell* **113**, 357-67 (2003).
52. Sugasawa, K. *et al.* UV-induced ubiquitylation of XPC protein mediated by UV-DDB-ubiquitin ligase complex. *Cell* **121**, 387-400 (2005).
53. Matsuda, N. *et al.* DDB2, the xeroderma pigmentosum group E gene product, is directly ubiquitylated by Cullin 4A-based ubiquitin ligase complex. *DNA Repair (Amst)* **4**, 537-45 (2005).
54. Kapetanaki, M.G. *et al.* The DDB1-CUL4ADDB2 ubiquitin ligase is deficient in xeroderma pigmentosum group E and targets histone H2A at UV-damaged DNA sites. *Proc Natl Acad Sci U S A* **103**, 2588-93 (2006).
55. Aillet, F. *et al.* Isolation of ubiquitylated proteins using tandem ubiquitin-binding entities. *Methods Mol Biol* **832**, 173-83 (2012).

56. Wang, H. *et al.* Histone H3 and H4 ubiquitylation by the CUL4-DDB-ROC1 ubiquitin ligase facilitates cellular response to DNA damage. *Mol Cell* **22**, 383-94 (2006).
57. Rapic-Otrin, V., McLenigan, M.P., Bisi, D.C., Gonzalez, M. & Levine, A.S. Sequential binding of UV DNA damage binding factor and degradation of the p48 subunit as early events after UV irradiation. *Nucleic Acids Res* **30**, 2588-98 (2002).
58. Fischer, E.S. *et al.* The molecular basis of CRL4DDB2/CSA ubiquitin ligase architecture, targeting, and activation. *Cell* **147**, 1024-39 (2011).
59. Puumalainen, M.R. *et al.* Chromatin retention of DNA damage sensors DDB2 and XPC through loss of p97 segregase causes genotoxicity. *Nat Commun* **5**, 3695 (2014).
60. Dantuma, N.P., Acs, K. & Luijsterburg, M.S. Should I stay or should I go: VCP/p97-mediated chromatin extraction in the DNA damage response. *Exp Cell Res* **329**, 9-17 (2014).
61. El-Mahdy, M.A. *et al.* Cullin 4A-mediated proteolysis of DDB2 protein at DNA damage sites regulates in vivo lesion recognition by XPC. *J Biol Chem* **281**, 13404-11 (2006).
62. Liu, L. *et al.* CUL4A abrogation augments DNA damage response and protection against skin carcinogenesis. *Mol Cell* **34**, 451-60 (2009).
63. Chen, X. *et al.* A kinase-independent function of c-Abl in promoting proteolytic destruction of damaged DNA binding proteins. *Mol Cell* **22**, 489-99 (2006).
64. Alekseev, S. *et al.* Cellular concentrations of DDB2 regulate dynamic binding of DDB1 at UV-induced DNA damage. *Mol Cell Biol* **28**, 7402-13 (2008).
65. Zhang, L., Lubin, A., Chen, H., Sun, Z. & Gong, F. The deubiquitinating protein USP24 interacts with DDB2 and regulates DDB2 stability. *Cell Cycle* **11**, 4378-84 (2012).
66. Pines, A. *et al.* PARP1 promotes nucleotide excision repair through DDB2 stabilization and recruitment of ALC1. *J Cell Biol* **199**, 235-49 (2012).
67. Ng, J.M. *et al.* A novel regulation mechanism of DNA repair by damage-induced and RAD23-dependent stabilization of xeroderma pigmentosum group C protein. *Genes Dev* **17**, 1630-45 (2003).
68. Xie, Z., Liu, S., Zhang, Y. & Wang, Z. Roles of Rad23 protein in yeast nucleotide excision repair. *Nucleic Acids Res* **32**, 5981-90 (2004).
69. Bergink, S. *et al.* Recognition of DNA damage by XPC coincides with disruption of the XPC-RAD23 complex. *J Cell Biol* **196**, 681-8 (2012).
70. Poulsen, S.L. *et al.* RNF111/Arkadia is a SUMO-targeted ubiquitin ligase that facilitates the DNA damage response. *J Cell Biol* **201**, 797-807 (2013).
71. Lubin, A., Zhang, L., Chen, H., White, V.M. & Gong, F. A human XPC protein interactome--a resource. *Int J Mol Sci* **15**, 141-58 (2014).
72. Wang, Q.E. *et al.* DNA repair factor XPC is modified by SUMO-1 and ubiquitin following UV irradiation. *Nucleic Acids Res* **33**, 4023-34 (2005).
73. Groisman, R. *et al.* CSA-dependent degradation of CSB by the ubiquitin-proteasome pathway establishes a link between complementation factors of the Cockayne syndrome. *Genes Dev* **20**, 1429-34 (2006).
74. Wei, L. *et al.* BRCA1 contributes to transcription-coupled repair of DNA damage through polyubiquitination and degradation of Cockayne syndrome B protein. *Cancer Sci* **102**, 1840-7 (2011).
75. Anindya, R. *et al.* A ubiquitin-binding domain in Cockayne syndrome B required for transcription-coupled nucleotide excision repair. *Mol Cell* **38**, 637-48 (2010).
76. Nakazawa, Y. *et al.* Mutations in UVSSA cause UV-sensitive syndrome and impair RNA polymerase IIo processing in transcription-coupled nucleotide-excision repair. *Nat Genet* **44**, 586-92 (2012).
77. Nicholson, B. & Suresh Kumar, K.G. The multifaceted roles of USP7: new therapeutic opportunities. *Cell Biochem Biophys* **60**, 61-8 (2011).
78. Wilson, M.D., Harreman, M. & Svejstrup, J.Q. Ubiquitylation and degradation of elongating RNA polymerase II: the last resort. *Biochim Biophys Acta* **1829**, 151-7 (2013).
79. Bregman, D.B. *et al.* UV-induced ubiquitination of RNA polymerase II: a novel modification deficient in Cockayne syndrome cells. *Proc Natl Acad Sci U S A* **93**, 11586-90 (1996).
80. Chiba, N. & Parvin, J.D. The BRCA1 and BARD1 association with the RNA polymerase II holoenzyme. *Cancer Res* **62**, 4222-8 (2002).
81. Anindya, R., Aygun, O. & Svejstrup, J.Q. Damage-induced ubiquitylation of human RNA polymerase II by the ubiquitin ligase Nedd4, but not Cockayne syndrome proteins or BRCA1. *Mol*

Cell **28**, 386-97 (2007).
82. Kuznetsova, A.V. *et al.* von Hippel-Lindau protein binds hyperphosphorylated large subunit of RNA polymerase II through a proline hydroxylation motif and targets it for ubiquitination. *Proc Natl Acad Sci U S A* **100**, 2706-11 (2003).
83. Aune, G.J. *et al.* Von Hippel-Lindau-coupled and transcription-coupled nucleotide excision repair-dependent degradation of RNA polymerase II in response to trabectedin. *Clin Cancer Res* **14**, 6449-55 (2008).
84. Starita, L.M. *et al.* BRCA1/BARD1 ubiquitinate phosphorylated RNA polymerase II. *J Biol Chem* **280**, 24498-505 (2005).
85. Wu, W. *et al.* BRCA1 ubiquitinates RPB8 in response to DNA damage. *Cancer Res* **67**, 951-8 (2007).
86. Harreman, M. *et al.* Distinct ubiquitin ligases act sequentially for RNA polymerase II polyubiquitylation. *Proc Natl Acad Sci U S A* **106**, 20705-10 (2009).
87. Verma, R., Oania, R., Fang, R., Smith, G.T. & Deshaies, R.J. Cdc48/p97 mediates UV-dependent turnover of RNA Pol II. *Mol Cell* **41**, 82-92 (2011).
88. Vertegaal, A.C. Uncovering ubiquitin and ubiquitin-like signaling networks. *Chem Rev* **111**, 7923-40 (2011).

Chapter 2

Quantitative proteome wide analysis of di-Gly modified peptides to uncover UV-responsive ubiquitylated proteins identifies histone H1 a new ubiquitin target in the UV-DDR

van Cuijk L, Mandemaker IK, Bezstarosti K, Demmers JAA, Vermeulen W, Marteijn JA.

Chapter 3

RNF111/Arkadia is a SUMO-targeted ubiquitin ligase that facilitates the DNA damage response

Poulsen SL, Hansen RK, Wagner SA, van Cuijk L, van Belle GJ, Streicher W, Wikström M, Choudhary C, Houtsmuller AB, Marteijn JA, Bekker-Jensen S, Mailand N

Published in Journal of Cell Biology 2013 June; 201(6):797-807

Abstract

Protein modifications by ubiquitin and small ubiquitin-like modifier (SUMO) play key roles in cellular signaling pathways. SUMO-targeted ubiquitin ligases (STUbLs) directly couple these modifications by selectively recognizing SUMOylated target proteins through SUMO-interacting motifs (SIMs), promoting their K48-linked ubiquitylation and degradation. Only a single mammalian STUbL, RNF4, has been identified. We show that human RNF111/Arkadia is a new STUbL, which used three adjacent SIMs for specific recognition of poly-SUMO2/3 chains, and used Ubc13–Mms2 as a cognate E2 enzyme to promote non-proteolytic, K63-linked ubiquitylation of SUMOylated target proteins. We demonstrate that RNF111 promoted ubiquitylation of SUMOylated XPC (xeroderma pigmentosum C) protein, a central DNA damage recognition factor in Nucleotide Excision Repair (NER) extensively regulated by ultraviolet (UV)-induced SUMOylation and ubiquitylation. Moreover, we show that RNF111 facilitated NER by regulating the recruitment of XPC to UV-damaged DNA. Our findings establish RNF111 as a new STUbL that directly links non-proteolytic ubiquitylation and SUMOylation in the DNA damage response.

Introduction

Protein modification by ubiquitin and the small ubiquitin-like modifier (SUMO) play important, often interconnected, regulatory roles in numerous signaling pathways in eukaryotic cells[1-3]. Similar enzymatic cascades involving activating (E1), conjugating (E2), and ligase (E3) enzymes underlie protein modification by ubiquitin and SUMO[1]. Although no consensus sequences surrounding ubiquitylation sites have been described, SUMOylation is frequently, but not always, targeted to K-X-E/D motifs or an inverted version of this sequence[4]. Three different SUMO isoforms, SUMO1–3, are expressed in cells, and although SUMO2 and SUMO3 are 97% identical and thus often referred to as SUMO2/3, SUMO1 and SUMO2/3 only share ~50% sequence identity[2]. Both ubiquitin and SUMO can be attached to target proteins as single moieties but additionally share the ability to form chains via internal lysine residues. Unlike ubiquitin, only a single lysine residue in SUMO that conforms to the SUMO consensus sequence is used for chain formation, and this ability is exclusive to SUMO2/3[3,5].

Different polyubiquitin chains have distinct cellular functions[3]. Although most of the known ubiquitylation processes generate K48-linked chains, which target substrates for degradation by the 26S proteasome, protein ubiquitylation does not always promote destruction; in particular, K63-linked polyubiquitylation, catalyzed by the E2 enzyme Ubc13 in conjunction with its partner proteins Mms2 or Uev1, is a non-degradative modification used in a range of signaling pathways, including cellular stress responses such as DNA damage and inflammatory responses[3,6,7]. The function of poly-SUMO chains is less well understood, but roles in processes such as chromosome segregation, DNA damage, and heat shock responses have been described[8-10]. Several cellular processes, including the DNA damage response, are intimately co-regulated by ubiquitin- and SUMO-mediated signaling[1,11,12]. The discovery of SUMO-targeted ubiquitin ligases (STUbLs) revealed a further, direct interplay between these modifications. By means of tandem SUMO-interacting motifs (SIMs)[13], STUbLs recognize poly-SUMOylated proteins and target them for K48-linked polyubiquitylation and degradation via their E3 ubiquitin ligase activities[14,15]. Accordingly, although SUMOylation is not a degradative modification per se, it can indirectly promote proteasomal destruction via STUbLs. Only a few STUbLs have been identified so far, including Slx5-Slx8 in Saccharomyces cerevisiae, Rfp1/Rfp2-Slx8 in Schizosaccharomyces pombe, and RNF4 in mammalian cells. All of these enzymes play important roles in maintenance of genome stability[10,14-16], consistent with the extensive involvement of both ubiquitin and SUMO in cellular responses to DNA damage.

In a search for new SUMO-binding proteins, we discovered that the human RNF111 ubiquitin ligase (also known as Arkadia) is a STUbL, which can promote non-proteolytic ubiquitylation of target proteins through cognate E2 enzymes such as Ubc13. We demonstrate that RNF111 has a physiological role in Nucleotide Excision Repair (NER), catalyzing DNA damage–induced ubiquitylation of SUMOylated XPC (xeroderma pigmentosum C). Our findings reveal direct coupling between non-proteolytic ubiquitylation and SUMOylation in the DNA damage response.

Results and discussion

RNF111 recognizes poly-SUMO chains via tandem SIMs

In a search for proteins containing SIMs, we noted that the human RNF111/Arkadia E3 ubiquitin

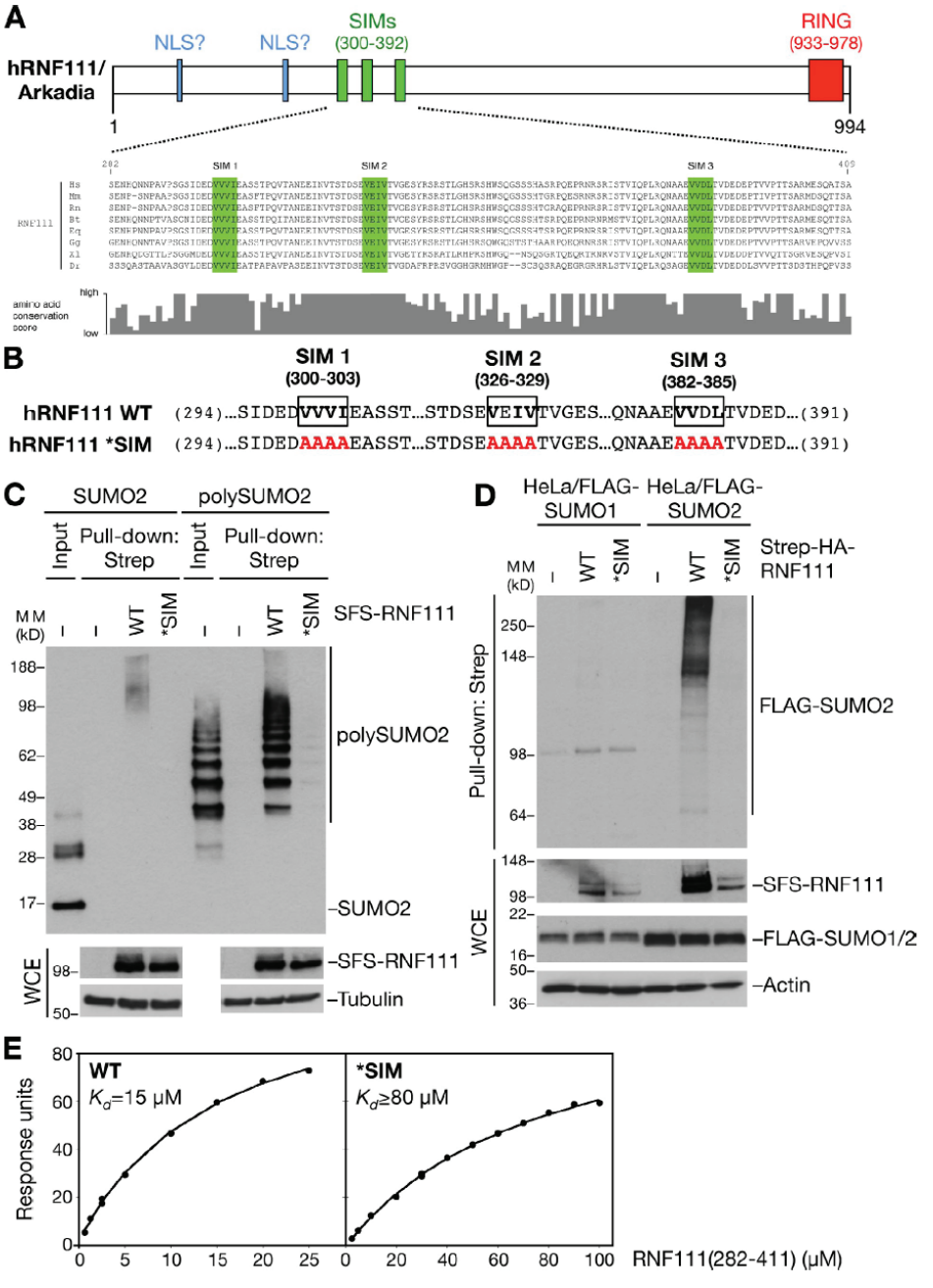

Figure 1. **Human RNF111 binds to poly-SUMOylated proteins via an N-terminal SIM region. (A)** Schematic of human RNF111/Arkadia. The RING domain, two putative NLSs [18]most notably the anterior visceral endoderm (AVE, and three SUMO-interacting motifs (SIMs; top), conserved in higher vertebrates (bottom), are shown. Core hydrophobic SIM residues are highlighted in green. **(B)** Amino acid substitutions (highlighted in red) in the RNF111 SIM region to disrupt its SUMO-binding ability (*SIM). **(C)** S-FLAG-Strep-tagged RNF111 (SFS-RNF111) proteins expressed in U2OS cells were purified on Strep-Tactin Sepharose,

incubated with purified SUMO2 or poly-SUMO2 (3-8), and washed extensively. Bound complexes were immunoblotted with the SUMO2 antibody. WCE, whole-cell extract. **(D)** HeLa cells stably expressing FLAG-SUMO isoforms were transfected with Strep-HA-RNF111 plasmids as indicated. Whole-cell extracts were subjected to Strep-Tactin pull-down and immunoblotting with the FLAG antibody. **(E)** Plasmon surface resonance analysis of poly-SUMO2 binding kinetics of RNF111 fragments spanning the SIMs. Data shown are from a single representative experiment out of three repeats. MW, molecular weight.

ligase, which has been shown to function in amplification of TGF-β signaling pathways[17], contains three highly conserved, potential SIMs in its N-terminal region (Fig. 1A and B). To test whether these putative SIMs are functional SUMO-binding modules, we generated an RNF111 mutant (*SIM) in which the core hydrophobic residues in each of the three SIMs were mutated to alanines, predicted to disrupt their SUMO-binding ability (Fig. 1B)[13]. We first assessed the SUMO-binding ability of ectopically expressed Strep-tagged forms of RNF111 wild type (WT) or *SIM purified on Strep- actin agarose. We found that RNF111 bound purified poly-SUMO2 chains with high affinity *in vitro* but was virtually unable to bind free SUMO2 (Fig. 1C). This was fully dependent on the integrity of the SIM motifs, as the RNF111 *SIM mutant did not interact with poly-SUMO2 (Fig. 1C). To test whether RNF111 binds to SUMOylated proteins in cells, we overexpressed RNF111 WT or *SIM in cells stably expressing FLAG-SUMO1 or 2 and analyzed their interactions in immunoprecipitation (IP) experiments. Consistent with *in vitro* binding experiments, RNF111 interacted with high-molecular weight SUMOylated species, but not free SUMO2, in a SIM-dependent manner (Fig. 1D). Moreover, RNF111 selectively interacted with proteins modified with SUMO2 but not SUMO1 (Fig. 1D), in agreement with the notion that SUMO2, but not SUMO1, forms poly-SUMO chains in vivo[5]. Surface plasmon resonance analysis showed that the RNF111 SIM region bound directly to poly-SUMO2 with a Kd of ~15 μM, whereas the *SIM mutations reduced binding to a Kd > 80 μM (Fig. 1E). These data demonstrate that RNF111 interacts with poly-SUMOylated proteins via three N-terminal SIM motifs, in accordance with recent findings that showed an additive contribution of each SIM to poly-SUMO binding[19] proteins with clustered SUMO-interacting motifs (SIMs.

RNF111 promotes Ubc13–Mms2-dependent ubiquitylation

To gain insight into the functional significance of RNF111 SUMO binding, we performed quantitative mass spectrometry (MS)-based analysis of cellular RNF111-interacting proteins (Fig. 2A and Fig. S1A). Several potential RNF111-binding factors were identified by this approach, including components of the AP2 (clathrin adaptor 2) complex, consistent with the known role of RNF111 in regulating endocytosis via interaction with this complex (Fig. S1A and B)[17]. Among the RNF111-associated proteins, we also found two E2 ubiquitin-conjugating enzymes: Ubc13-Mms2, which specifically catalyzes K63-linked ubiquitin chain formation, and UBE2O, a large E2 enzyme of unknown function (Fig. 2A and Fig. S1B). The presence of both Ubc13 and Mms2 lends strong support to the possibility that this complex is a physiological E2 partner for RNF111. We validated the interactions between RNF111 and Ubc13 or UBE2O by reciprocal co-IP analysis (Fig. 2B and Fig. S2A and B). In contrast, we did not observe binding of RNF4, the known mammalian STUbL, to Ubc13 under a range of conditions (Fig. S2C and D).

Because RNF111 promotes degradation of factors in TGF-β signaling pathways, the interaction with Ubc13-Mms2 was unexpected, and we set out to investigate its physiological

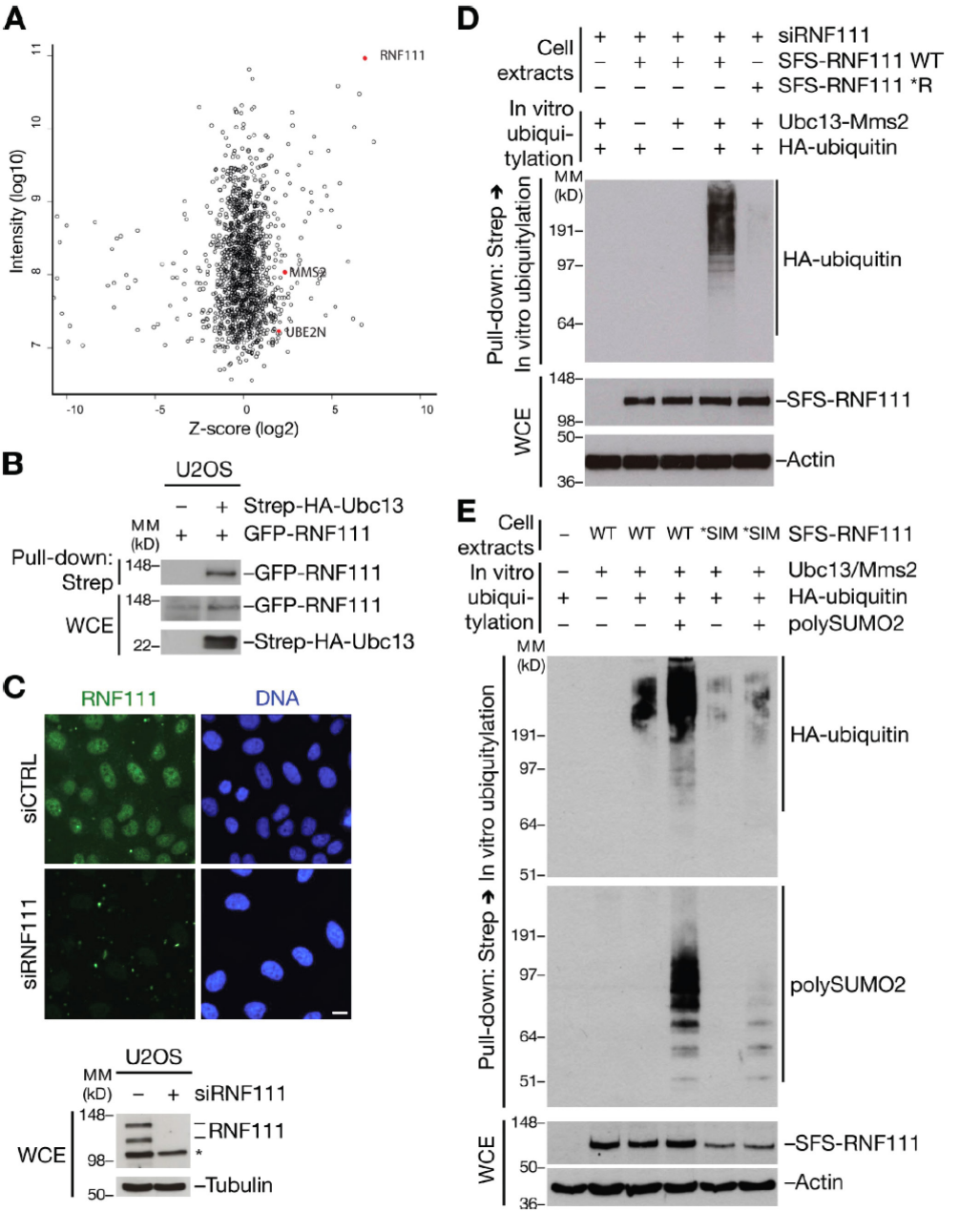

Figure 2. RNF111 has STUbL activity in the presence of Ubc13-Mms2. (A) MS-based analysis of RNF111-interacting proteins. U2OS and U2OS/GFP-RNF111 cells were grown in light and heavy SILAC medium, respectively. GFP-RNF111 and associated proteins enriched on GFP-Trap resin were analyzed by MS. Plot shows z scores (from SILAC heavy/light ratios) and total intensity of identified proteins. RNF111, Ubc13 (UBE2N), and Mms2 (MMS2) are highlighted. See also Fig. S1 (A and B). **(B)** U2OS cells were co-transfected with indicated combinations of GFP-RNF111 and Strep-HA-Ubc13 plasmids. Whole cell extracts (WCE)

were subjected to Strep-Tactin pull-down followed by immunoblotting with GFP and HA antibodies. **(C)** U2OS cells transfected with non-targeting (control [CTRL]) or RNF111 siRNAs were collected 72 h later and processed for immunostaining (top) or immunoblot (bottom) with RNF111 antibody. Asterisk indicates a nonspecific band. Bar, 10 µm. **(D)** Extracts of U2OS cells sequentially transfected with RNF111 siRNA and S-FLAG-Strep-tagged RNF111 (SFS-RNF111) plasmids were subjected to Strep-Tactin pull-down. Bound complexes were incubated with ubiquitylation reaction mixture containing E1, Ubc13-Mms2 complex, and HA-ubiquitin as indicated and washed extensively, and RNF111 E3 ligase activity was analyzed by immunoblotting with the HA antibody. **(E)** As in D, except that ubiquitylation reactions were performed in the presence or absence of poly-SUMO2 (3-8) chains followed by immunoblotting with HA and SUMO2 antibodies. MW, molecular weight.

relevance. We noted that endogenous RNF111 is primarily localized in the nucleus (Fig. 2C), suggesting that in addition to facilitating amplification of TGF-β signaling and endocytosis, RNF111 might have other important nuclear functions. To test whether RNF111 has E3 ligase activity in the presence of Ubc13-Mms2, we performed *in vitro* ubiquitylation assays using ectopic RNF111 immunopurified from cells. Because RNF111 appeared to form homodimers in cells (unpublished data), we depleted endogenous RNF111 to remove background E3 ligase activity of co-purifying endogenous RNF111. We found that RNF111 was highly active as an E3 ligase in the presence of purified Ubc13-Mms2, as judged from its auto-ubiquitylation (Fig. 2D). As expected, this required the integrity of the RNF111 RING domain (Fig. 2D), whereas mutation of the SIMs did not impair intrinsic RNF111 E3 ligase activity (Fig. S2E). In addition to Ubc13-Mms2, RNF111 was active with more generic E2 enzymes, such as UbcH5, as expected (Fig. S2F). To test whether RNF111 has STUbL activity in the presence of Ubc13-Mms2, we analyzed the impact of SUMO2 on RNF111 E3 ligase activity. Strikingly, we found that poly-SUMO2 chains, but not free SUMO2, were efficiently targeted for Ubc13-Mms2-dependent ubiquitylation by RNF111 in a manner fully dependent on the integrity of the SIMs (Fig. 2E and not depicted). We conclude from these experiments that RNF111 functions as a STUbL that employs Ubc13-Mms2 and likely other cognate E2 partners in ubiquitylation of SUMOylated substrates.

RNF111 promotes UV-induced ubiquitylation of XPC

We next attempted to identify physiological substrates for the STUbL activity of RNF111. The NER factor XPC is known to undergo both SUMOylation and ubiquitylation in response to UV-radiation, and the UV-induced ubiquitin chains on XPC do not appear to destine XPC for proteasomal destruction[20,21]. We reasoned that SUMOylated XPC might be a candidate target of the Ubc13-Mms2-dependent E3 ligase activity of RNF111. Indeed, knockdown of RNF111 by any of several independent siRNAs impaired UV-induced ubiquitylation but not SUMOylation of XPC (Fig. 3A and B; and Fig. S3A and B), suggesting that XPC is SUMOylated before ubiquitylation by RNF111. The slow-migrating, UV-inducible XPC species seen in immunoblots represent a mixture of ubiquitin- and SUMO-modified forms; hence, the dramatic decrease in XPC ubiquitylation but not SUMOylation in RNF111-depleted cells manifests less prominently in total XPC blots (Fig. 3A). Consistent with a direct role of RNF111 in ubiquitylating XPC after UV, we found that elevated levels of RNF111 augmented the UV-induced increase in XPC-GFP ubiquitylation (Fig. 3C). In contrast, depletion of RNF4, the known STUbL in mammalian

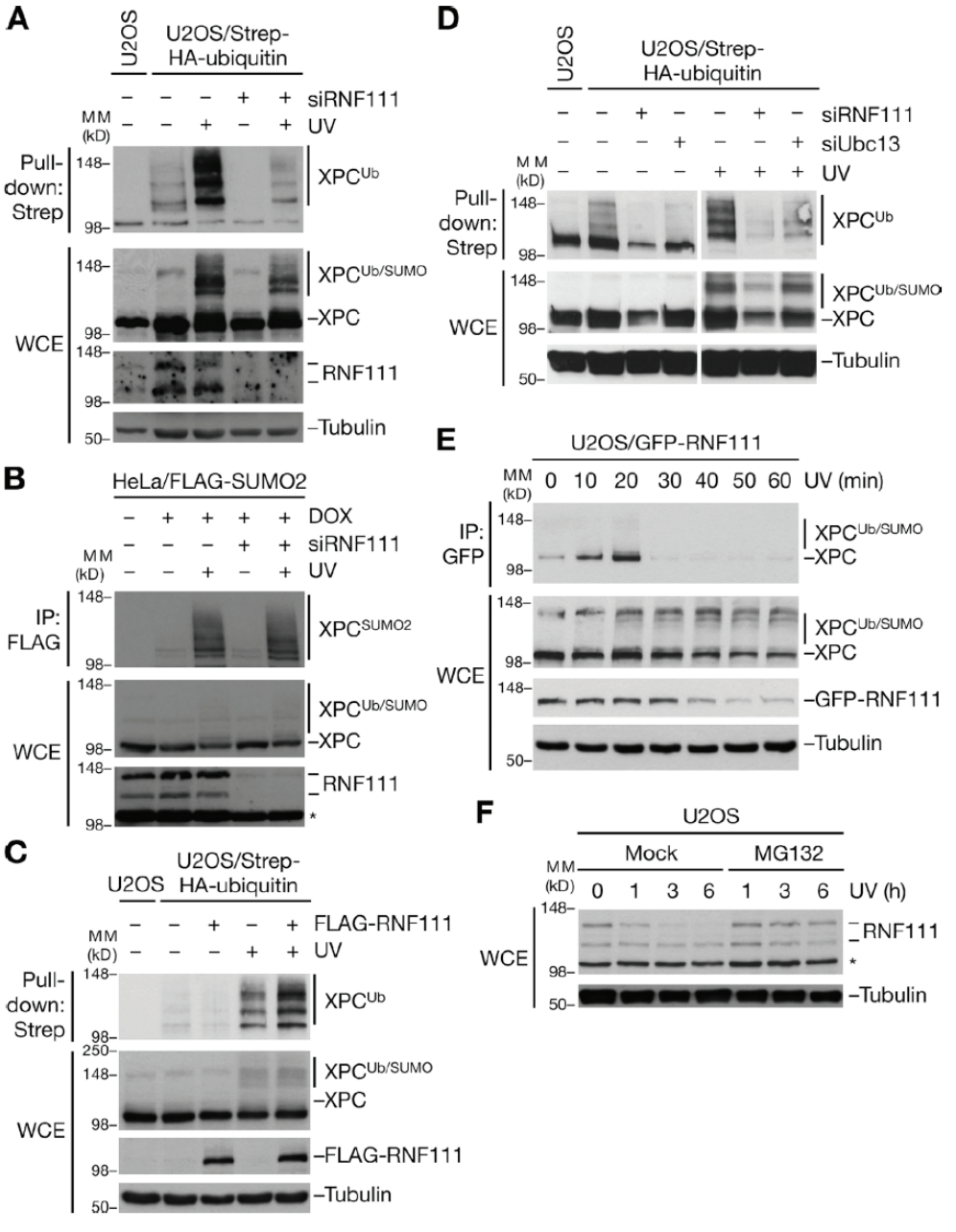

Figure 3. RNF111 promotes UV-induced ubiquitylation of XPC. (A) U2OS or U2OS/Strep-HA-ubiquitin cells transfected with control (-) or RNF111 siRNAs were exposed or not exposed to UV and collected 1 h later, and XPC ubiquitylation was analyzed by immunoblotting Strep-Tactin pull-downs of whole cell extracts (WCE) with the XPC antibody. **(B)** HeLa/FLAG-SUMO2 cells transfected with control (-) or RNF111 siRNAs and left untreated or induced to express FLAG-SUMO2 by addition of doxycycline (DOX) were exposed or not exposed to UV and collected 1 h later. Cells were lysed under denaturing conditions, and XPC SUMOylation was analyzed by immunoblotting of FLAG IPs with XPC antibody. **(C)** U2OS/Strep-HA-

ubiquitin cells transfected with empty vector (-) or FLAG-RNF111 plasmid were exposed or not exposed to UV and collected 1 h later. XPC ubiquitylation was analyzed as in A. **(D)** XPC ubiquitylation in U2OS/Strep-HA-ubiquitin cells depleted of RNF111 or Ubc13 was analyzed as in A. Ubc13 knockdown efficiency is shown in Fig. S3D. **(E)** Extracts of U2OS/GFP-RNF111 cells collected at the indicated times after UV radiation were subjected to GFP IP followed by immunoblotting with XPC antibody. **(F)** Extracts of U2OS cells incubated with or without MG132, exposed to UV 30 min later, and collected at the indicated times after UV were analyzed by immunoblotting with the RNF111 antibody. Asterisks denote a nonspecific band. MW, molecular weight.

cells, had no effect on UV-induced XPC ubiquitylation (Fig. S3C). The ability of RNF111 to promote Ubc13-Mms2-dependent ubiquitylation prompted us to test whether UV-induced XPC ubiquitylation required Ubc13 function. Like RNF111 knockdown, depletion of Ubc13 decreased UV-induced XPC ubiquitylation substantially (Fig. 3D and Fig. S3D), suggesting that RNF111-dependent XPC ubiquitylation after UV-exposure was, at least partially, mediated by Ubc13-dependent, non-proteolytic ubiquitylation.

To further probe the basis of RNF111-dependent XPC ubiquitylation in response to UV, we asked whether RNF111 and XPC interact in cells. Indeed, UV-induced prominent, but transient, interaction between RNF111 and XPC at early time points after UV (Fig. 3E). Interestingly, like several known NER factors, both endogenous and ectopic RNF111 underwent partial degradation after UV in a proteasome-dependent manner, which, however, did not require the intrinsic E3 ligase activity of RNF111 (Fig. 3E and F; and Fig. S3E). In general, the kinetics of UV-induced RNF111 interaction with XPC and degradation correlated with that of XPC ubiquitylation after UV exposure (Fig. 3E and F; and Fig. S3F).

RNF111 selectively ubiquitylates SUMOylated XPC

The aforementioned findings suggested that RNF111 targets SUMOylated XPC for ubiquitylation in response to UV. Hence, we tested whether RNF111 specifically interacts with SUMO- modified XPC via its SIMs, using a strategy wherein GFP-tagged XPC immunopurified from cells was SUMOylated *in vitro* and then incubated with extracts of cells transfected with WT or mutant forms of ectopic RNF111 (Fig. 4A). Under these conditions, RNF111 efficiently interacted with XPC, but only if XPC had been pre-SUMOylated, and this required the integrity of the RNF111 SIMs (Fig. 4B), in agreement with the notion that RNF111 specifically recognizes SUMOylated XPC. We next tested whether RNF111 functions as a STUbL for XPC. To do this, we extended the setup to monitor SUMO-dependent RNF111-XPC binding, by subjecting the bound complexes to an *in vitro* ubiquitylation assay in the presence of Ubc13-Mms2 as an E2 (Fig. 4A). Although a background level of Ubc13-Mms2-dependent ubiquitylation of XPC-GFP could be seen in the absence of ectopically expressed RNF111 (Fig. 4C, compare lanes 1–6), the addition of RNF111 WT markedly enhanced XPC ubiquitylation (Fig. 4C, compare lanes 6 and 7) but only if XPC had been pre-SUMOylated (Fig. 4C, compare lanes 2, 3, and 7). Importantly, this increase in RNF111-dependent XPC ubiquitylation required the functional integrity of both the RNF111 RING and SIM domains (Fig. 4C, compare lanes 7–9). These data suggest that RNF111 acts as a STUbL for XPC, catalyzing its non-proteolytic ubiquitylation in response to UV damage.

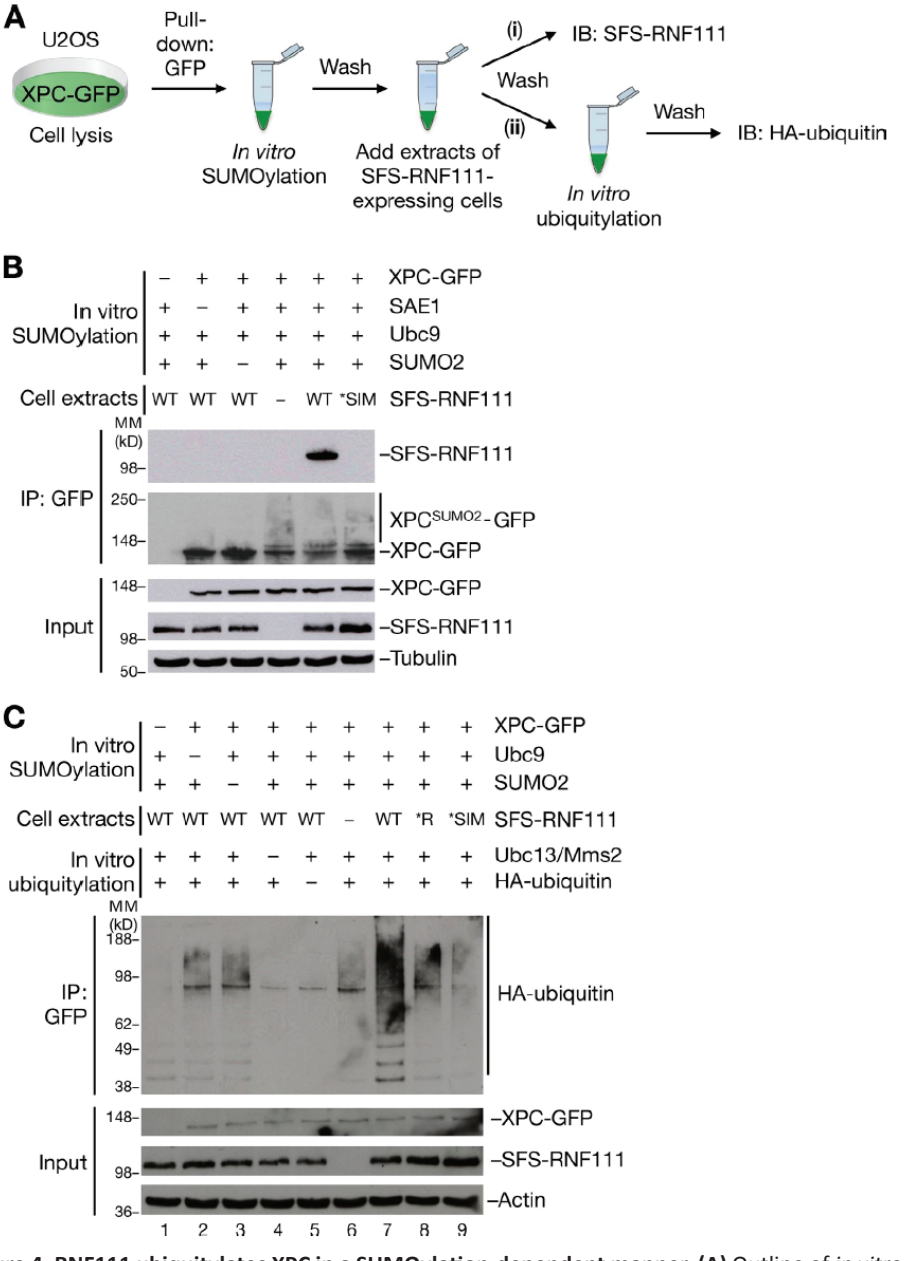

Figure 4. RNF111 ubiquitylates XPC in a SUMOylation-dependent manner. (A) Outline of *in vitro* SUMO-binding and STUbL assays. XPC-GFP expressed in U2OS cells was immunopurified on GFP-Trap resin and subjected to *in vitro* SUMOylation. After washing, the XPC-GFP-containing beads were incubated with extracts of cells transfected or not transfected with S-FLAG-Strep-RNF111 (SFS-RNF111) constructs, washed again, and processed for immunoblotting (IB) of bound SFS-RNF111 with FLAG antibody (i) or subjected to *in vitro* ubiquitylation followed by washing and immunoblotting with the HA antibody to analyze ubiquitin ligase activity (ii). **(B)** SUMOylation-dependent binding of RNF111 to XPC, analyzed as described in A. **(C)** Analysis of SUMOylation-dependent XPC ubiquitylation by RNF111 was performed as described in A. MW, molecular weight.

RNF111 promotes NER by regulating the interaction of XPC with damaged DNA

Because RNF111 promotes ubiquitylation of XPC after UV, we asked whether RNF111 regulates NER. Although UV-induced ubiquitylation of XPC has been suggested to increase its DNA-binding affinity[20], the exact role of this modification in NER is unclear. Previous work suggested that XPC is ubiquitylated by $CRL4^{DDB2}$, an E3 ligase complex functioning as a proximal sensor of UV-lesions in DNA[20]. It is possible that XPC is ubiquitylated by both $CRL4^{DDB2}$ and RNF111 in response to UV. Indeed, using MS, we found that XPC ubiquitylation involves a variety of ubiquitin chains and ≥ 15 individual ubiquitylation sites (unpublished data)[22]; hence, the nature and regulation of XPC ubiquitylation appears to be highly complex, likely involving several E3 ligases. To determine whether RNF111 loss affects NER, we measured UV-induced DNA repair synthesis (UDS) in $RNF111^{-/-}$ mouse embryonic fibroblasts (MEFs)[23]. Strikingly, these MEFs showed a marked reduction in UDS, as was also observed in $XPC^{-/-}$ MEFs (Fig. 5A). Moreover, using two independent siRNAs, we found that RNF111 knockdown resulted in increased accumulation of XPC-GFP to locally UV-irradiated chromatin, whereas knockdown of DDB2 had the opposite effect, as previously observed (Fig. 5B and C)[24]. Hence, although DDB2 and RNF111 have opposing effects on XPC accumulation at UV lesions, interfering with the proper kinetics of XPC interaction with damaged chromatin by inactivation of either E3 reduces the efficiency of NER. These data suggest that RNF111 has a physiological role in promoting NER by regulating ubiquitylation of XPC and its association with damaged DNA.

Our findings show that RNF111 is a STUbL that promotes non-proteolytic ubiquitylation of at least a subset of its substrates, including XPC, implying that STUbL activity is not confined to RNF4 in higher vertebrates and that STUbLs do not always target substrates for proteasomal degradation. Although Ubc13-Mms2 appears to be a major cognate E2 enzyme for RNF111 in cells, RNF111 also interacts with other E2 enzymes and is known to promote ubiquitin-dependent degradation of TGF-β signaling factors[25-27]. Hence, depending on the context, RNF111 may work with different E2s to promote degradative or non-proteolytic ubiquitylation of SUMOylated substrate proteins. Despite the fact that both RNF4 and RNF111 interact with poly-SUMOylated proteins through tandem SIMs, they appear to have largely non-overlapping roles in the cell. For instance, RNF4, but not RNF111, was dispensable for UV-induced ubiquitylation of XPC, whereas RNF111 was not recruited to laser micro-irradiation-induced DNA double-strand breaks, unlike RNF4 (unpublished data)[10,16]. This distribution of labor between RNF4 and RNF111 in targeting distinct subsets of SUMOylated factors may reflect differences in the SUMO-binding properties of their tandem SIMs, which have a distinct configuration, as well as differential target-binding specificity contributed by other domains in these proteins.

Although our comprehensive analysis of RNF111-binding factors in unperturbed cells uncovered several E2 partner proteins, we did not detect any known components of TGF-β signaling pathways, nor XPC. Given the involvement of RNF111 in regulating these proteins, we speculate that processes mediated by the RNF111 STUbL activity may, in many cases, be induced by stimuli such as TGF-β or UV-treatment, which may promote SUMOylation of specific factors and thus trigger their RNF111-mediated ubiquitylation. This is consistent with previous findings that elevated levels of RNF111 only cause degradation of SnoN in TGF-β-stimulated cells[26]. Based on the large and heterogeneous group of proteins identified by MS as putative

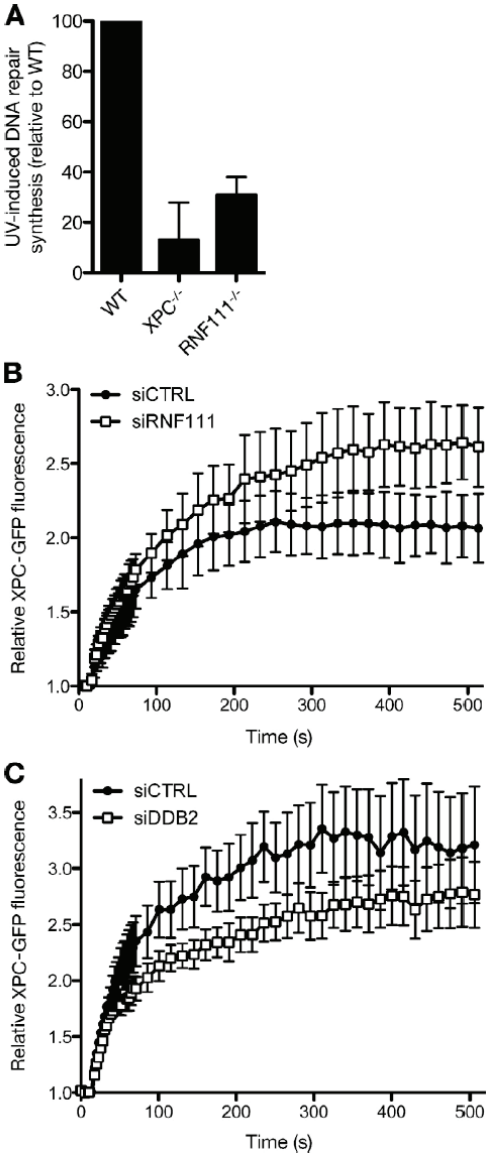

Figure 5. RNF111 promotes NER by regulating XPC recruitment to UV- damaged DNA. (A) UDS of the indicated MEF cell lines, determined by EdU incorporation for 3 h after exposure to 16 J/m2 UV-C. Error bars indicate SDs of three independent experiments. **(B)** Cells stably expressing XPC-GFP were transfected with indicated siRNAs and locally exposed to laser-induced UV-C damage. XPC-GFP fluorescence intensity at the damaged area relative to pre-damage intensity was recorded in time using live-cell confocal imaging (mean of three independent experiments, n=8 cells per experiment, ± SD). **(C)** As in B, except that cells were transfected with control (CTRL) or DDB2 siRNA. Results of a representative experiment (n=8 cells per sample, ± SEM) are shown.

RNF111-interacting proteins, we propose that RNF111, like RNF4, is a multifunctional STUbL regulating a diverse range of cellular signaling processes, determined to a large extent by the SUMOylation state of target proteins. This scenario reconciles the involvement of RNF111 in radically different cellular processes, such as TGF-β signaling and endocytosis[17], and NER. Whether the ability of RNF111 to ubiquitylate proteins in the former processes involves its STUbL activity remains to be addressed. Our findings shed further light on how STUbLs directly couple ubiquitylation and SUMOylation in important cellular signaling pathways.

Materials and methods

Plasmids and siRNA

Full-length human RNF111 cDNA was amplified by PCR and inserted into pEGFP-C1 (Takara Bio Inc.) and pcDNA4/TO (Invitrogen) containing N-terminal Strep-HA or S-FLAG-Strep tags to generate mammalian expression constructs for GFP-, Strep-HA-, and S-FLAG-Strep-tagged RNF111, respectively. The RNF111 *RING (W963A) point mutation was introduced using the site-directed mutagenesis kit (QuikChange; Agilent Technologies). The RNF111 *SIM mutations (VVVI(300–303)AAAA, VEIV(326–329)AAAA, and VVDL(382–385)AAAA) were introduced by replacing part of the coding sequence of human RNF111 (nucleotides 665–1,677 of the RNF111 ORF) with a synthetic gene spanning this region and containing the mutated *SIM sequence using the unique KpnI and EcoNI sites in RNF111. All constructs were verified by sequencing. Constructs expressing Strep-HA-tagged Ubc13 and GFP-XPC were described previously[28]. Plasmid transfections were performed using GeneJuice (EMD Millipore) according to the manufacturer's instructions. siRNA transfections were performed with Lipofectamine RNAiMAX (Invitrogen) as described. siRNA target sequences used in this study were control, 5'-GGGAUACCUAGACGUUCUA-3'; RNF111 (#1), 5'GGAUAUUAAUGCAGAGGAA-3'; RNF111 (#4), 5'-GGAUAUGAAGAGUGAGAUU-3'; Ubc13, 5'-GAGCAUGGACUAGGCUAUA-3'; XPC, 5'-GCAAAUGGCUUCUAUCGAAUU-3'; DDB2, 5'-CCCAGAUCCUAAUUUCAAA-3'; RNF4 (#1), 5'-GCUAAUACUUGCCCAACUU-3'; and RNF4 (#2), 5'-GACAGAGACGUAUAUCUGA-3'.

Cell culture

Human U2OS and HeLa cells were cultured in DMEM containing 10% fetal bovine serum. SV40-immortalized XP4PA cells stably expressing XPC-GFP[29] were cultured in DMEM containing 5% fetal bovine serum and 2 mM L-glutamine. RNF111$^{-/-}$ primary mouse fibroblasts of mixed 129Sv/MF1 genetic backgrounds (provided by V. Episkopou, Imperial College London, London, England, UK)[23], and XPC$^{-/-}$ MEFs in which exons 4–7 of the XPC gene were deleted[30] were cultured in a 1:1 ratio of Ham's F10 and DMEM supplemented with 10% fetal calf serum and 1% non-essential amino acids. To generate cell lines stably expressing GFP-tagged WT and mutant RNF111 alleles, U2OS cells were co-transfected with GFP-RNF111 constructs and pBabe-puromycin plasmid, and positive clones were selected with 1 µg/ml puromycin. A stable U2OS/ Strep-HA-ubiquitin cell line[31] was generated by selecting cells transfected with Strep-HA-ubiquitin expression plasmid in medium containing 400 µg/ml G418 until resistant clones grew out. Stable HeLa cell lines expressing FLAG-SUMO1/2 in a doxycycline-inducible manner[32] were generated by co-transfection of HeLa/FRT/TRex cells (Invitrogen) with pcDNA5/FRT/TO-3×FLAG-SUMO1/2 and pOG44 followed by selection with 200 µg/ml Hygromycin B. Unless stated otherwise, cells were exposed to 30 J/m2 UV and collected 1 h later.

MS-based analysis of RNF111-interacting proteins

For stable isotope labeling by amino acids in cell culture (SILAC) labeling, U2OS or U2OS/ GFP-RNF111 cells were cultured for 14 d in Eagle's minimum essential medium (Sigma-Aldrich) supplemented with L-arginine and L-lysine or L-arginine-U-13C6-15N4 and L-lysine-U-13C6-15N2 (Cambridge Isotope Laboratories), respectively[33]. Cells were lysed in EBC buffer supplemented with protease and phosphatase inhibitor cocktails (Roche), and GFP-RNF111

and its interacting proteins were enriched using GFP-Trap resin. Proteins were resolved by SDS-PAGE and in-gel digested with trypsin. Peptide fractions were analyzed on a quadrupole mass spectrometer (Q Exactive; Orbitrap; Thermo Fisher Scientific) equipped with a nanoflow HPLC system (Thermo Fisher Scientific)[34]. Raw data files were analyzed using MaxQuant software (version 1.2.2.9)[35]. Parent ion and MS2 spectra were searched against protein sequences obtained from the UniProt knowledge base using the Andromeda search engine[36]. Spectra were searched with a mass tolerance of 6 ppm in MS mode and 20 ppm in higher-energy C-trap dissociation MS2 mode, strict trypsin specificity, and allowing up to two missed cleavage sites. Cysteine carbamidomethylation was included as a fixed modification, and N-terminal protein acetylation was included as variable modification. The dataset was filtered based on posterior error probability to arrive at a false discovery rate < 1% for peptide spectrum matches and protein groups. For calculation of z scores, the protein group ratios were logarithmized, and the standard deviation was estimated separately for ratios below and above 0 based on the 0.159 and 0.841 quantile[35].

Immunochemical methods and antibodies

Immunoblotting, IP, and Strep-Tactin pull-downs were performed as previously described[37]. In brief, cells were lysed in EBC buffer (50 mM Tris, pH 7.5, 150 mM NaCl, 1 mM EDTA, 1 mM DTT, and 0.5% NP-40) or denaturing buffer (20 mM Tris, pH 7.5, 50 mM NaCl, 1 mM EDTA, 1 mM DTT, 0.5% NP-40, 0.5% sodium deoxycholate, and 0.5% SDS) supplemented with protease and phosphatase inhibitors and incubated on ice for 10 min, and lysates were cleared by centrifugation for 10 min at 20,000 rpm. Lysates were incubated with FLAG agarose (Sigma-Aldrich), GFP-Trap agarose (ChromoTek), or Strep-Tactin Sepharose (IBA BioTAGnology) for 1.5 h on an end-over-end rotator at 4°C, washed five times with EBC buffer or denaturing buffer, and re-suspended in 2× Laemmli sample buffer.

Antibodies used in this study included mouse monoclonals to RNF111 (M05; Abnova), GFP (sc-9996) and β-actin (sc-130301; Santa Cruz Bio- technology, Inc.), and FLAG (F1804; Sigma-Aldrich), rat monoclonal to HA (Roche), and rabbit polyclonals to XPC (Bethyl Laboratories, Inc.), SUMO1 (ab32058), SUMO2/3 (ab3742), β-tubulin (ab6046; Abcam), and Ubc13 (4919; Cell Signaling Technology). Rabbit polyclonal RNF4 antibody was a gift of J. Palvimo (University of Eastern Finland, Kuopio, Finland).

Immunofluorescence staining, microscopy, and laser microirradiation

Cells were fixed in 4% formaldehyde, permeabilized with PBS containing 0.2% Triton X-100 for 5 min, and incubated with primary antibodies diluted in DMEM for 1 h at room temperature. After staining with secondary antibodies (Alexa Fluor 488 and 568; Life Technologies) for 30 min, coverslips were mounted in Vectashield mounting medium (Vector Laboratories) containing nuclear stain DAPI. Confocal images were acquired on a microscope (LSM 510; Carl Zeiss) mounted on a confocal laser-scanning microscope (Axiovert 100M; Carl Zeiss) equipped with Plan-Neofluar 40×/1.3 NA oil immersion objective. Dual-color confocal images were acquired with standard settings using laser lines 488 and 543 nm for excitation of Alexa Fluor 488 and Alexa Fluor 568 dyes (Molecular Probes/Invitrogen), respectively. Band pass filters 505–530 and 560–615 nm were used to collect the emitted fluorescence signals. Image acquisition and

analysis was performed with LSM ZEN software (Carl Zeiss). Raw images were exported as TIF files, and if adjustments in image contrast and brightness were applied, identical settings were used on all images of a given experiment.

In vitro ubiquitylation, SUMOylation, and binding experiments

To analyze *in vitro* binding of RNF111 to SUMO, S-FLAG-Strep-RNF111 constructs were overexpressed in U2OS cells, purified on Strep-Tactin Sepharose, and incubated with purified free SUMO1, SUMO2, or poly-SUMO chains (3-8; all obtained from Boston Biochem) for 2 h at 4°C. Bound complexes were washed extensively in EBC buffer (50 mM Tris, pH 7.5, 150 mM NaCl, 1 mM EDTA, 1 mM DTT, and 0.5% NP-40), and immobilized material was resolved by SDS-PAGE and analyzed by immunoblotting.

For *in vitro* RNF111 ubiquitylation assays, S-FLAG-Strep-RNF111 purified from cells as described in the previous section and incubated in 20 µl ubiquitylation assay buffer (50 mM Tris, pH 7.5, 5 mM MgCl2, 2 mM NaF, 2 mM ATP, and 0.6 mM DTT) supplemented with 60 ng E1, 300 ng E2 (Ubc13–Mms2 complex or UbcH5c), and 5 µg HA-ubiquitin (all obtained from Boston Biochem) for 1 h at 37°C. Reactions were stopped by addition of Laemmli sample buffer, resolved by SDS-PAGE, and immunoblotted with the HA antibody.

For *in vitro* SUMOylation and STUbL assays, XPC-GFP ectopically expressed in U2OS cells was captured on GFP-Trap resin and incubated with 100 ng SAE1/2, 200 ng Ubc9, and 3 µg SUMO2 (all obtained from Boston Biochem) in ubiquitylation assay buffer for 1 h at 37°C. The beads were washed extensively in EBC buffer and incubated with extracts of U2OS cells transfected with WT or mutant versions of S-FLAG-Strep-RNF111 for 2 h at 4°C. The immobilized material was then washed in EBC and processed for immunoblotting or subjected to *in vitro* ubiquitylation assay as described in the previous section.

For surface plasmon resonance analysis, recombinant His6-tagged fragments (WT and *SIM) of human RNF111 (encompassing amino acids 282–411) were expressed in Escherichia coli and purified on an ÄKTAxpress system (GE Healthcare). The His6-tag was removed with tobacco etch virus protease, and the RNF111 fragments were further purified using reverse-phase chromatography on an UltiMate 3000 system (Dionex), using C18 columns (Phenomenex). Eluted proteins were lyophilized, and their masses were verified by SDS-PAGE and MS. Poly-SUMO2 chains (3-8) were immobilized on a CM5 sensor chip using standard amine-coupling chemistry. Before titration experiments, the RNF111(282–411) fragments were dialyzed in running buffer (10 mM Hepes, pH 7.4, 150 mM NaCl, and 0.005% P20). After each titration point, the surface was regenerated using 10 mM glycine, pH 2.5. All data were collected on an instrument (T200; Biacore) at 25°C and analyzed using the T200 evaluation software (Biacore), in which the data were fitted to a steady-state model.

UDS and XPC-GFP accumulation kinetics assays

UDS was performed as described previously[38,39]. In brief, MEFs were seeded on coverslips 3 d before the UDS assay and cultured in medium without serum to reduce the number of S-phase cells. Cells were exposed to 16 J/m2 UV-C and labeled with 5-ethynyl,2'-deoxyuridine (EdU) for 3 h. Subsequently, cells were fixed with 3.7% formaldehyde, and EdU incorporation was visualized using Alexa Fluor 594 nm (Click-iT) according to manufacturer's protocol (Invitrogen).

UDS was quantified in ≥ 75 cells by measuring the overall nuclear fluorescence using ImageJ software (National Institutes of Health). Images were obtained using a microscope (LSM-700; Carl Zeiss).

Kinetic study of XPC-GFP accumulation was performed in SV40-transformed XP4PA cells stably expressing XPC-GFP as described previously[40]. In brief, cells were cultured on 25-mm quartz coverslips (SPI Supplies) and imaged on a laser-scanning confocal microscope (SP5; Leica) using an Ultrafluar quartz 100×, 1.35 NA glycerol immersion lens (Carl Zeiss) at 37°C and 5% CO2. Imaging medium was the same as culture medium. For UV-C laser irradiation, a 2-mW pulsed (7.8 kHz) diode pumped solid-state laser emitting at 266 nm (DPSL; Rapp OptoElectronic) was connected to the microscope (SP5) with all-quartz optics. Treated nuclei were imaged using the same scanning speed, zoom factor, and laser power. Images were acquired using the LAS AF software (Leica). Data analysis was performed using the ImageJ software package. Measured fluorescence levels were determined in the specific region of the damage in the nucleus over time and corrected for background values. Resulting curves show the relative amount of protein in the damaged area over time and were normalized to 1 for the data points before damage.

Supplemental figures

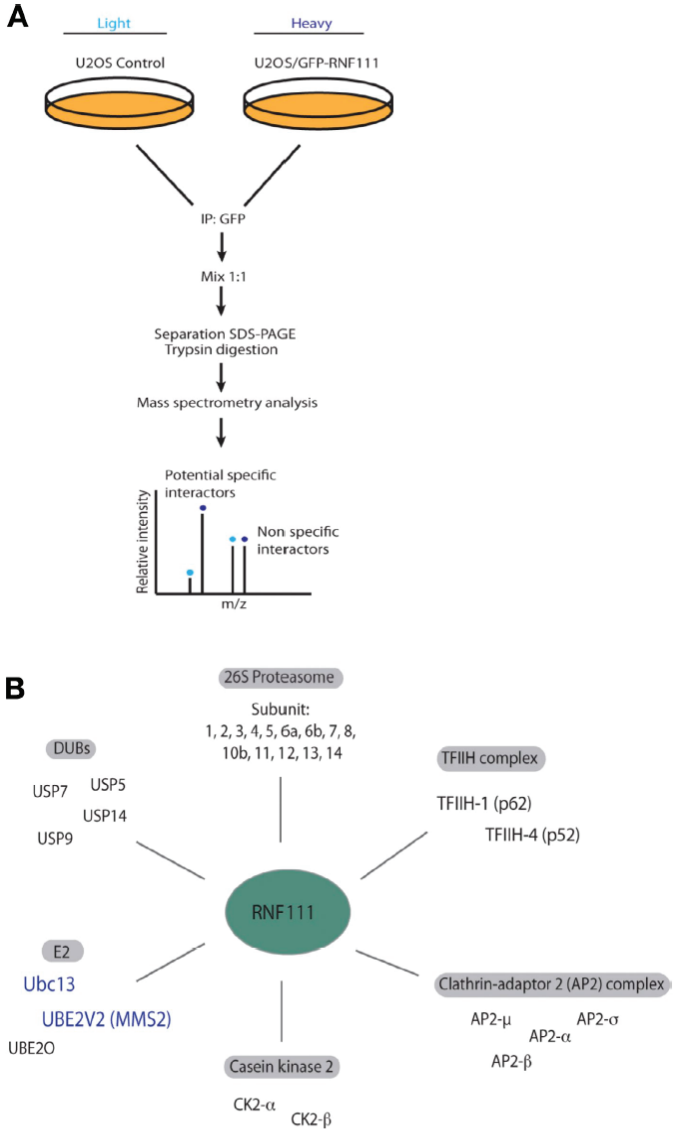

Figure S1. Analysis of cellular RNF111-interacting proteins. (A) MS-based analysis of RNF111-interacting proteins. U2OS or U2OS/GFP-RNF111 cells grown in light or heavy SILAC medium, respectively, were lysed and subjected to GFP IP. Subsequently, samples were combined, resolved by SDS-PAGE, and analyzed by MS. SILAC (heavy/light) ratios for individual proteins were determined. m/z, mass per charge. **(B)** Overview of selected proteins with high SILAC (heavy/light) ratios identified by the experimental approach outlined in A. DUB, deubiquitylating enzyme.

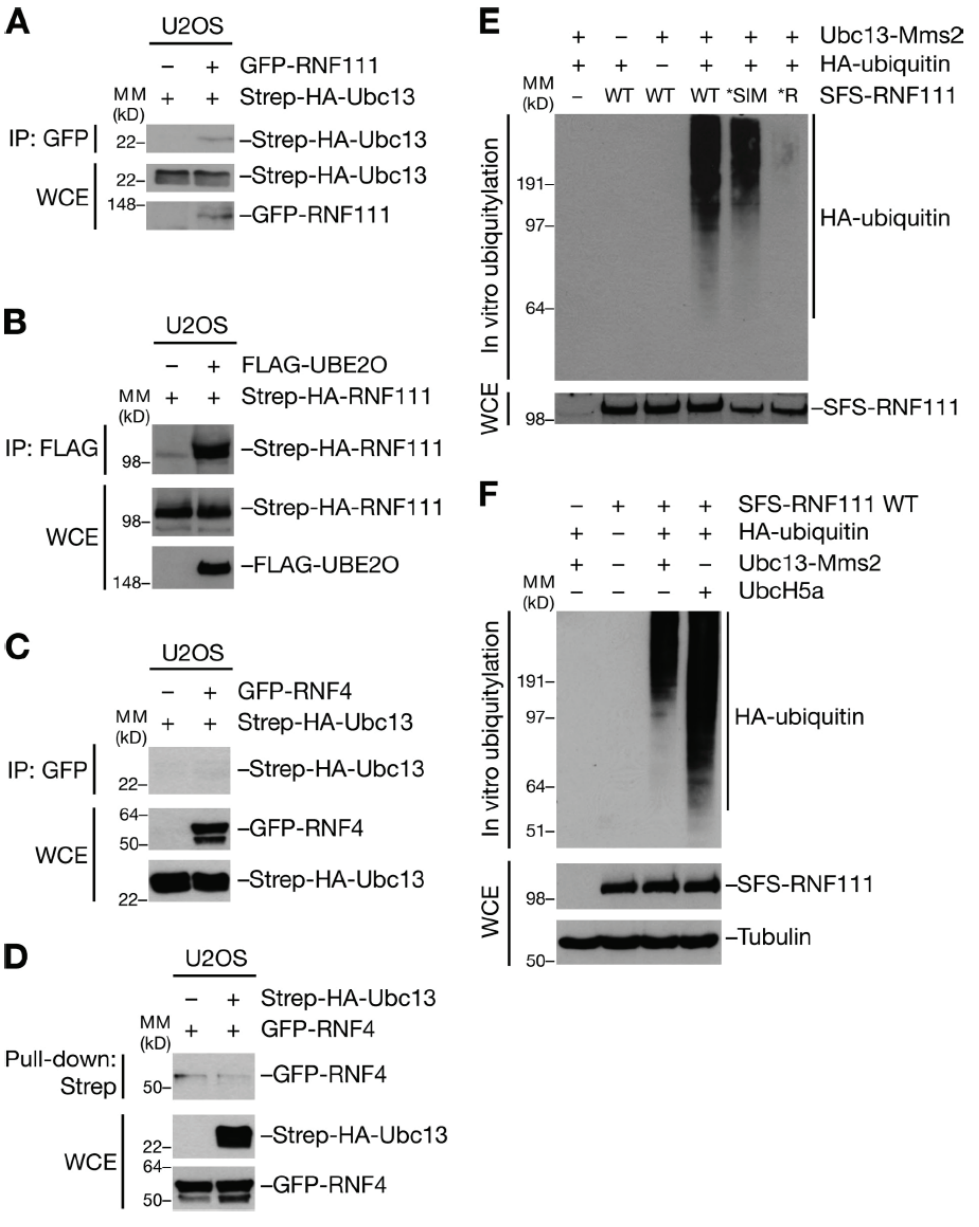

Figure S2. RNF111 promotes Ubc13-Mms2-dependent ubiquitylation. (A) U2OS cells were cotransfected with indicated combinations of GFP-RNF111 and Strep-HA-Ubc13 plasmids. Whole cell extracts (WCE) were subjected to GFP IP followed by immunoblotting with HA antibody. **(B)** U2OS cells were cotransfected with the indicated combinations of FLAG-UBE2O and Strep-HA-RNF111 plasmids. Whole cell extracts were subjected to FLAG IP followed by immunoblotting with HA antibody. **(C)** As in A, except that cells were transfected with combinations of GFP-RNF4 and Strep-HA-Ubc13 antibodies. **(D)** As in C, except that extracts were subjected to Strep-Tactin pull-down followed by immunoblotting with the GFP antibody. **(E)** Extracts of U2OS cells sequentially transfected with RNF111 siRNA and S-FLAG-Strep–tagged RNF111 (SFS-RNF111) plasmids as indicated were subjected to Strep-Tactin

pull-down. Bound complexes were incubated with ubiquitylation reaction mixture containing E1, Ubc13-Mms2 complex, and HA-ubiquitin as indicated and washed extensively, and RNF111 auto-ubiquitylation activity was analyzed by immunoblotting with HA antibody. **(F)** As in E, except that UbcH5a was used as an E2 enzyme instead of Ubc13-Mms2 where indicated. MW, molecular weight.

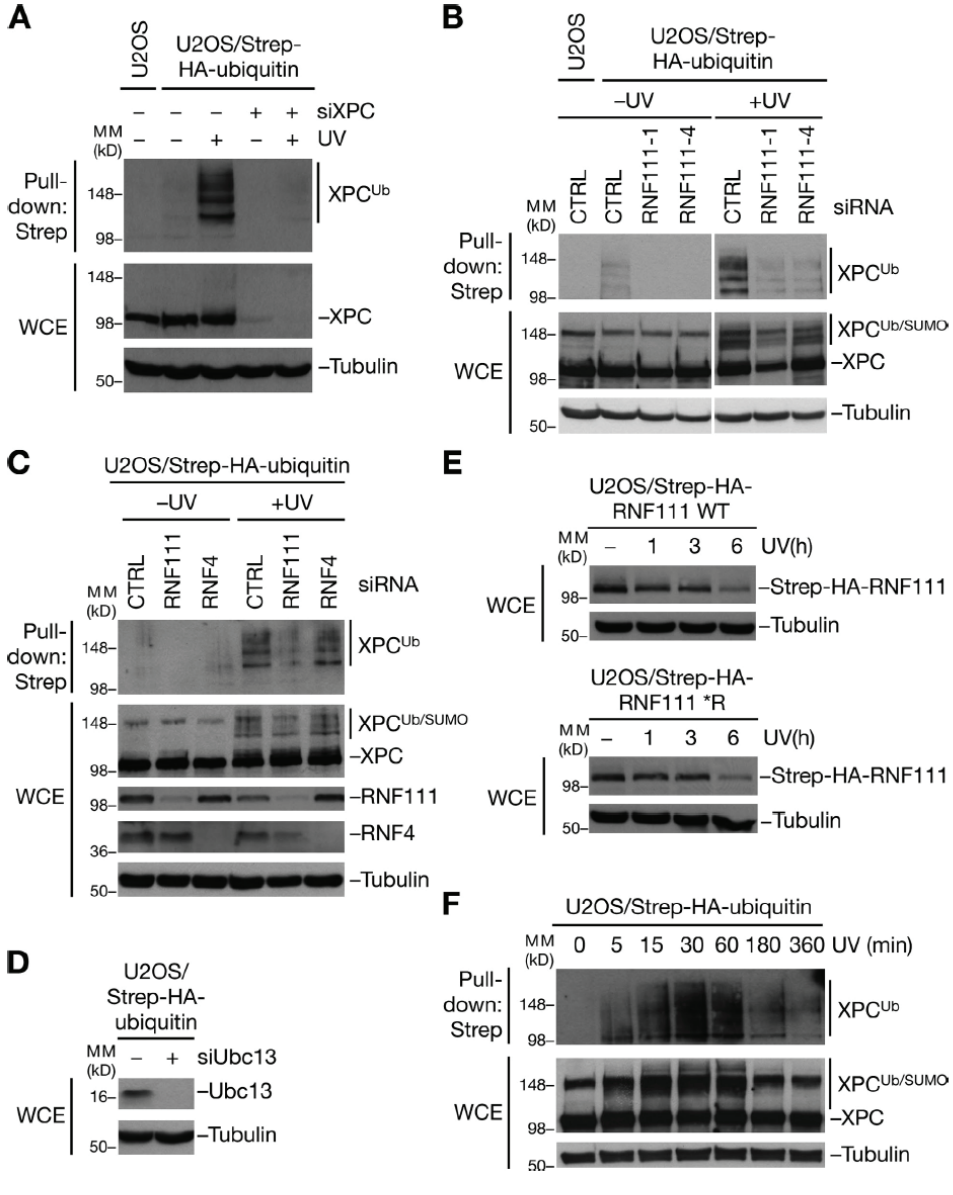

Figure S3. RNF111 promotes UV-induced ubiquitylation of XPC. (A) U2OS or U2OS/Strep-HA-ubiquitin cells transfected with control (-) or XPC siRNAs were exposed or not exposed to UV as indicated and collected 1 h later, and XPC ubiquitylation was analyzed by immunoblotting Strep-Tactin pull-downs of whole cell extracts (WCE) with XPC antibody. **(B)** As in A, except that cells were transfected with indicated control (CTRL) or RNF111 siRNAs. **(C)** As in A, except that cells were transfected with indicated control, RNF111, or RNF4 siRNAs. **(D)** Knockdown efficiency of Ubc13 siRNA. U2OS/Strep-HA-ubiquitin cells were

transfected with control (-) or Ubc13 siRNAs, collected 72 h later, and analyzed by immunoblotting with the Ubc13 antibody. **(E)** U2OS cell lines stably expressing Strep-HA-tagged RNF111 WT or *R mutant were collected at the indicated times after exposure to UV and analyzed by immunoblotting with HA antibody. **(F)** Time course analysis of UV-induced XPC ubiquitylation. U2OS/Strep-HA-ubiquitin cells were collected at the indicated times after exposure to UV, and XPC ubiquitylation was analyzed as in A. MW, molecular weight.

References

1. Kerscher, O., Felberbaum, R. & Hochstrasser, M. Modification of proteins by ubiquitin and ubiquitin-like proteins. *Annu Rev Cell Dev Biol* **22**, 159-80 (2006).
2. Gareau, J.R. & Lima, C.D. The SUMO pathway: emerging mechanisms that shape specificity, conjugation and recognition. *Nat Rev Mol Cell Biol* **11**, 861-71 (2010).
3. Komander, D. & Rape, M. The ubiquitin code. *Annu Rev Biochem* **81**, 203-29 (2012).
4. Matic, I. *et al.* Site-specific identification of SUMO-2 targets in cells reveals an inverted SUMOylation motif and a hydrophobic cluster SUMOylation motif. *Mol Cell* **39**, 641-52 (2010).
5. Tatham, M.H. *et al.* Polymeric chains of SUMO-2 and SUMO-3 are conjugated to protein substrates by SAE1/SAE2 and Ubc9. *J Biol Chem* **276**, 35368-74 (2001).
6. Chen, Z.J. & Sun, L.J. Nonproteolytic functions of ubiquitin in cell signaling. *Mol Cell* **33**, 275-86 (2009).
7. Al-Hakim, A. *et al.* The ubiquitous role of ubiquitin in the DNA damage response. *DNA Repair (Amst)* **9**, 1229-40 (2010).
8. Schwartz, D.C., Felberbaum, R. & Hochstrasser, M. The Ulp2 SUMO protease is required for cell division following termination of the DNA damage checkpoint. *Mol Cell Biol* **27**, 6948-61 (2007).
9. Golebiowski, F. *et al.* System-wide changes to SUMO modifications in response to heat shock. *Sci Signal* **2**, ra24 (2009).
10. Yin, Y. *et al.* SUMO-targeted ubiquitin E3 ligase RNF4 is required for the response of human cells to DNA damage. *Genes Dev* **26**, 1196-208 (2012).
11. Bergink, S. & Jentsch, S. Principles of ubiquitin and SUMO modifications in DNA repair. *Nature* **458**, 461-7 (2009).
12. Bekker-Jensen, S. & Mailand, N. The ubiquitin- and SUMO-dependent signaling response to DNA double-strand breaks. *FEBS Lett* **585**, 2914-9 (2011).
13. Hecker, C.M., Rabiller, M., Haglund, K., Bayer, P. & Dikic, I. Specification of SUMO1- and SUMO2-interacting motifs. *J Biol Chem* **281**, 16117-27 (2006).
14. Prudden, J. *et al.* SUMO-targeted ubiquitin ligases in genome stability. *EMBO J* **26**, 4089-101 (2007).
15. Sun, H., Leverson, J.D. & Hunter, T. Conserved function of RNF4 family proteins in eukaryotes: targeting a ubiquitin ligase to SUMOylated proteins. *EMBO J* **26**, 4102-12 (2007).
16. Galanty, Y., Belotserkovskaya, R., Coates, J. & Jackson, S.P. RNF4, a SUMO-targeted ubiquitin E3 ligase, promotes DNA double-strand break repair. *Genes Dev* **26**, 1179-95 (2012).
17. Miyazono, K. & Koinuma, D. Arkadia--beyond the TGF-beta pathway. *J Biochem* **149**, 1-3 (2011).
18. Episkopou, V. *et al.* Induction of the mammalian node requires Arkadia function in the extraembryonic lineages. *Nature* **410**, 825-30 (2001).
19. Sun, H. & Hunter, T. Poly-small ubiquitin-like modifier (PolySUMO)-binding proteins identified through a string search. *J Biol Chem* **287**, 42071-83 (2012).
20. Sugasawa, K. *et al.* UV-induced ubiquitylation of XPC protein mediated by UV-DDB-ubiquitin ligase complex. *Cell* **121**, 387-400 (2005).
21. Wang, Q.E. *et al.* DNA repair factor XPC is modified by SUMO-1 and ubiquitin following UV irradiation. *Nucleic Acids Res* **33**, 4023-34 (2005).
22. Povlsen, L.K. *et al.* Systems-wide analysis of ubiquitylation dynamics reveals a key role for PAF15 ubiquitylation in DNA-damage bypass. *Nat Cell Biol* **14**, 1089-98 (2012).
23. Mavrakis, K.J. *et al.* Arkadia enhances Nodal/TGF-beta signaling by coupling phospho-Smad2/3 activity and turnover. *PLoS Biol* **5**, e67 (2007).
24. Nishi, R. *et al.* UV-DDB-dependent regulation of nucleotide excision repair kinetics in living cells. *DNA Repair (Amst)* **8**, 767-76 (2009).
25. Koinuma, D. *et al.* Arkadia amplifies TGF-beta superfamily signalling through degradation of Smad7. *EMBO J* **22**, 6458-70 (2003).
26. Levy, L. *et al.* Arkadia activates Smad3/Smad4-dependent transcription by triggering signal-induced SnoN degradation. *Mol Cell Biol* **27**, 6068-83 (2007).
27. Nagano, Y. *et al.* Arkadia induces degradation of SnoN and c-Ski to enhance transforming growth factor-beta signaling. *J Biol Chem* **282**, 20492-501 (2007).
28. Bekker-Jensen, S. *et al.* HERC2 coordinates ubiquitin-dependent assembly of DNA repair factors on damaged chromosomes. *Nat Cell Biol* **12**, 80-6; sup pp 1-12 (2010).

29. Hoogstraten, D. *et al.* Versatile DNA damage detection by the global genome nucleotide excision repair protein XPC. *J Cell Sci* **121**, 2850-9 (2008).
30. Sands, A.T., Abuin, A., Sanchez, A., Conti, C.J. & Bradley, A. High susceptibility to ultraviolet-induced carcinogenesis in mice lacking XPC. *Nature* **377**, 162-5 (1995).
31. Danielsen, J.M. *et al.* Mass spectrometric analysis of lysine ubiquitylation reveals promiscuity at site level. *Mol Cell Proteomics* **10**, M110 003590 (2011).
32. Danielsen, J.R. *et al.* DNA damage-inducible SUMOylation of HERC2 promotes RNF8 binding via a novel SUMO-binding Zinc finger. *J Cell Biol* **197**, 179-87 (2012).
33. Ong, S.E. *et al.* Stable isotope labeling by amino acids in cell culture, SILAC, as a simple and accurate approach to expression proteomics. *Mol Cell Proteomics* **1**, 376-86 (2002).
34. Michalski, A. *et al.* Mass spectrometry-based proteomics using Q Exactive, a high-performance benchtop quadrupole Orbitrap mass spectrometer. *Mol Cell Proteomics* **10**, M111 011015 (2011).
35. Cox, J. & Mann, M. MaxQuant enables high peptide identification rates, individualized p.p.b.-range mass accuracies and proteome-wide protein quantification. *Nat Biotechnol* **26**, 1367-72 (2008).
36. Cox, J. *et al.* Andromeda: a peptide search engine integrated into the MaxQuant environment. *J Proteome Res* **10**, 1794-805 (2011).
37. Poulsen, M., Lukas, C., Lukas, J., Bekker-Jensen, S. & Mailand, N. Human RNF169 is a negative regulator of the ubiquitin-dependent response to DNA double-strand breaks. *J Cell Biol* **197**, 189-99 (2012).
38. Limsirichaikul, S. *et al.* A rapid non-radioactive technique for measurement of repair synthesis in primary human fibroblasts by incorporation of ethynyl deoxyuridine (EdU). *Nucleic Acids Res* **37**, e31 (2009).
39. Schwertman, P. *et al.* UV-sensitive syndrome protein UVSSA recruits USP7 to regulate transcription-coupled repair. *Nat Genet* **44**, 598-602 (2012).
40. Dinant, C. *et al.* Activation of multiple DNA repair pathways by sub-nuclear damage induction methods. *J Cell Sci* **120**, 2731-40 (2007).

Chapter 4

SUMO and ubiquitin-dependent XPC exchange drives nucleotide excision repair

van Cuijk L*, van Belle GJ*, Turkyilmaz Y, Poulsen SL, Janssens RC, Sabatella M, Lans H, Mailand N, Houtsmuller AB, Vermeulen W, Marteijn JA

Manuscript in preparation
*These authors contributed equally

Chapter 5

A bimodal switch regulates priority for repair of active genes under mild genotoxic stress

van Belle GJ, van Cuijk L, Vuist IM, Geverts B, van Royen ME, Verschure PJ, Marteijn JA, Vermeulen W, Houtsmuller AB

Manuscript in preperation

Chapter 6

Differential binding kinetics of replication protein A during replication and the pre- and post-incision steps of nucleotide excision repair

van Cuijk L*, Gourdin MA*, Tresini M, Luijsterburg MS, Nigg AL, Giglia-Mari G, Houtsmuller AB, Vermeulen W and Marteijn JA

Published in DNA repair 2014 December 24:46-56
*These authors contributed equally

Abstract

The ability of replication protein A (RPA) to bind single-stranded DNA (ssDNA) underlines its crucial roles during DNA replication and repair. A combination of immunofluorescence and live cell imaging of GFP-tagged RPA70 revealed that RPA, in contrast to other replication factors, does not cluster into replication foci, which is explained by its short residence time at ssDNA. In addition to replication, RPA also plays a crucial role in both the pre- and post- incision steps of Nucleotide Excision Repair (NER). Pre-incision factors like XPC and TFIIH accumulate rapidly at locally induced UV-damage and remain visible up to 4 h. However, RPA did not reach its maximum accumulation level until 3 h after DNA damage infliction and a chromatin-bound pool remained detectable up to 8 h, probably reflecting its role during the post-incision step of NER. During the pre-incision steps of NER, RPA could only be visualized at DNA lesions in incision deficient XP-F cells, however without a substantial increase in residence time at DNA damage. Together our data show that RPA is an intrinsically highly dynamic ssDNA-binding complex during both replication and distinct steps of NER.

Introduction

Replication protein A (RPA), the major eukaryotic single-stranded DNA binding protein, is required for several DNA metabolic processes including replication, repair, recombination and checkpoint activation. RPA is a heterotrimer consisting of 70, 32 and 14 kDa subunits and binds ssDNA with a 5' to 3' polarity[1,2]. RPA was initially identified as a crucial replication factor that, together with replication factor C (RFC) and proliferating cell nuclear antigen (PCNA), regulates the loading and processivity of different DNA polymerases onto the chromatin[3].

During replication in eukaryotes the trimeric sliding clamp PCNA, is loaded around the DNA at the 3'-OH end of the nascent DNA strand by the pentameric complex RFC in an RPA- and ATP-dependent manner in order to facilitate the tethering and processing of DNA polymerases δ and ε[4,5]. In eukaryotes, DNA replication is initiated and propagated from hundreds to thousands of replication sites that, together with associated replication factors, cluster into 'replication foci'. The location, number and size of these replication foci vary throughout S-phase. Three distinct replication patterns can be distinguished, that correspond to DNA synthesis in early S -phase (small and discrete foci), mid S-phase (perinucleolar and perinuclear large foci) and late S-phase (large foci)[6].

Besides their function in replication RPA, PCNA and RFC are also essential for Nucleotide Excision Repair (NER), a "cut-and-patch" mechanism that by the coordinated action of more than 30 different proteins, removes a wide variety of helix-distorting DNA lesions, including UV-induced DNA damages like cyclobutane pyrimidine dimers (CPD) and 6-4 pyrimidine-pyrimidone photoproducts (6-4-PP)[7]. NER can be sub-divided into two pathways which are activated by distinct recognition mechanisms. (1) Global genome NER (GG-NER) recognizes DNA damage throughout the genome via the concerted action of two damage recognizing complexes; XPC/HR23B/centrin complex and UV-DDB complex[7-9]. (2) Transcription coupled NER (TC-NER) is only active on the transcribed strand of active genes[10] and is initiated by the stalling of elongating RNA polymerase II on DNA lesions[11]. Following damage recognition, GG-NER and TC-NER converge into a common pathway by recruiting the ten-subunit transcription factor TFIIH that verifies the lesion and locally unwinds the DNA double helix around the lesion[12]. RPA then binds to the undamaged DNA strand and, together with XPA, stabilizes open complex formation, thereby stimulating and coordinating the incision by the endonucleases ERCC1-XPF and XPG[2,13,14]. A 24-32-nucleotide DNA fragment is excised and the undamaged strand is used as a template for DNA repair synthesis[15]. Finally the DNA is sealed by LigaseIII-XRCC1 or Ligase I[16]. *In vitro* and *in situ* experiments have revealed that, following dual incision, RPA remains bound to the DNA substrate where it initiates the recruitment of RFC, PCNA and either the DNA polymerase pol ε, or pol κ and δ[17-19].

In contrast to PCNA and RFC, which only play a role in the post-incision steps of NER, RPA is implicated in both the pre-incision and post-incision steps. In this paper, we compared the spatio-temporal distribution of RPA, RFC and PCNA, using immunofluorescence and live cell microscopy of the GFP-tagged versions of the three replication proteins, to uncover the dynamic interactions of these factors with the DNA template in different maintenance processes.

Material and methods

Cell culture and transfection

All cell lines were cultured under standard conditions at 37°C and 5% CO_2 in a humidified incubator. U2OS cells and SV40-immortilized MRC5 cells were grown in a 1:1 mixture of Ham's F10 and DMEM (Lonza), supplemented with 10% fetal calf serum (FCS) and 1% penicillin-streptomycin (PS). Human primary wild type control fibroblasts (C5RO) and XPF deficient fibroblasts (XP51RO) were cultured in Ham's F10 supplemented with 15% FCS and 1% PS. C5RO and XP51RO cells were grown to confluence and then incubated for 5 days with medium containing 0.5% FCS to induce quiescence.

A retroviral plasmid encoding RPA70-GFP was stably expressed in U2OS, SV40-immortilized MRC5, C5RO and XP51RO cells. Additionally, a cDNA encoding GFP-PCNA was stably expressed either by retroviral infection in C5RO hTERT[20] or by transfection[21] in SV40 immortilized MRC5. Cell lines expressing other fluorescent tagged proteins were used as described previously: RFC140-GFP[22], XPCGFP[23] and GFP-XPA[24].

Thirty min before irradiation cells were treated with 100 mM hydroxyurea and 10 µM cytosine-β-arabinofuranoside to inhibit DNA synthesis. For global and local UV-irradiation cells were washed with PBS and subsequently exposed to a UV-C germicidal lamp (254 nm, Philips) at the indicated dose[25]. To apply local UV-damage cells were UV-irradiated through an isopore membrane filter (Millipore), containing 5 µm pores.

Western blotting

For western blotting, primary mouse antibodies against RPA (B-6/sc-28304, Santa Cruz Biotechnology, Inc) and GFP (11 814 460 001, Roche) were used in combination with Alexa Fluor 795 donkey anti-mouse antibodies (LI-COR). Antibody complexes were visualized using the Odyssey CLx Infrared Imaging System (LI-COR Biosciences).

Immunofluorescence

Cells were fixed using 2% paraformaldehyde supplemented with 0.1% Triton X-100. Samples were processed as described previously[24]. For GFP staining, cells were permeabilized with 0.5% Triton X-100 for 30 sec prior to fixation. The following primary antibodies were used: anti-Ki67 (Ab833, Abcam), anti-XPC[26], anti-TFIIH p89 (s-19, Santa Cruz Biotechnology), anti-6-4pp (64M-2, Cosmo Bio), anti-RPA32 (ab2175, Abcam), anti-GFP (ab290, Abcam) and combined with secondary antibodies labeled with ALEXA fluorochromes 488 or 594 (Invitrogen; The Jackson Laboratory) for visualization. Samples were finally embedded in DAPI vectashield (Vector Laboratories). Anti-XPA (FL-273, Santa Cruz Biotechnology) or mouse anti-CPD (TDM-2, MBL International) was used as marker of local UV-damage, depending on the species in which the other antibody was raised. Co-localization was defined as an > 2 fold increase in fluorescent intensity at the LUD and quantified by counting at least 40 cells. Edu (5-ethynyl-2'-deoxyuridine) incorporation was visualized using Click-iT Alexa Fluor 647 according to the manufacturer's protocol (Invitrogen). Optical images were obtained using a Zeiss LSM 510 META confocal microscope equipped with 63x oil Plan-Apochromat 1.4 NA oil immersion lens (Carl Zeiss Inc.) and a pinhole aperture setting of 2.0 airy units.

Live cell confocal laser-scanning microscopy

Confocal laser scanning microscopy images were obtained using a Zeiss LSM 510 microscope equipped with a 25 mW Argon laser (488 and 561 nm) and 63x oil Plan-Apochromat 1.4 NA oil immersion lens (Carl Zeiss Inc.).

Kinetic studies of GFP-tagged RPA, PCNA, RFC, XPC and XPA accumulation were executed as described previously[27]. Cells were grown in glass bottom dishes (MatTek, Ashland, Massachusetts, USA) and irradiated with a UV-C source containing four UV-lamps (Philips TUV 9W PL-S) above the microscope stage. For induction of local damage, cells were UV-irradiated through a polycarbonate mask (Millipore Billerica, Massachusetts, USA) with pores of 5 µm and subsequently irradiated for 39 seconds ($100J/m^2$)[28,29] and monitored for up to 5 h. Fluorescence intensity was normalized between 0 and 100%. Assembly kinetics were measured on a Zeiss Axiovert 200M wide field fluorescence microscope, equipped with a 100x Plan-Apochromat (1.4 NA) oil immersion lens (Zeiss, Oberkochen, Germany), a Cairn Xenon Arc lamp with monochromator (Cairn research, Kent, U.K.) and an objective heater and climate chamber. Images were recorded with a cooled CCD camera (Coolsnap HQ, Roper Scientific, USA) using Metamorph 6.1 imaging software (Molecular devices, Downingtown, PA, USA). Cells were examined in microscopy medium (137 mM NaCl, 5.4 mM KCl, 1,8 mM $CaCl_2$, 0.8 mM $MgSO_4$, 20 mM D-glucose and 20 mM HEPES) at 37°C.

To determine protein mobility FRAP was performed as described[30]. Indicated areas were photobleached by two iterations using 100% 488 nm laser power. The recovery of fluorescence in the photobleached area was monitored for the indicated times. Data was normalized to the overall fluorescence of the cell before bleaching.

Half nucleus bleaching combined with FLIP-FRAP was performed as described previously[22]. Half of the nucleus was bleached and subsequently the fluorescence recovery in the bleached area and the loss of fluorescence in the non-bleached area was measured for up to 4 min. For data analysis the difference in fluorescence signal between FLIP and FRAP before bleaching was set at 0 and the difference between FLIP and FRAP after bleaching was normalized to 1. The mobility of a protein was determined as the time necessary for FLIP-FRAP to return to 0.

FLIP analysis was performed by continuously photobleaching a third of a locally-irradiated nucleus opposite to the site of damage with 100% 488 nm laser intensity, as described previously [27,28,31]. Fluorescence in the locally irradiated area was monitored with normal laser intensity until fluorescence was completely lost. All values were background corrected.

Results

Differential nuclear localization of RFC140, PCNA and RPA70 during the cell cycle

To study the spatio-temporal distribution of core DNA replication factors implicated in the DNA damage response (DDR) we first analyzed the localization of RPA, RFC and PCNA in unperturbed living cells. We used cell lines that stably express GFP-tagged RFC[22] and PCNA[32] and generated cells that stably express RPA70-GFP. Immunoblot analysis showed that full-length RPA70-GFP is expressed at physiological levels (Fig. 1A). RPA70-GFP shows a homogeneous nuclear distribution, with lower expression in nucleoli in addition to a varying number of sub-nuclear structures with higher local concentrations. This distribution pattern is similar to endogenous

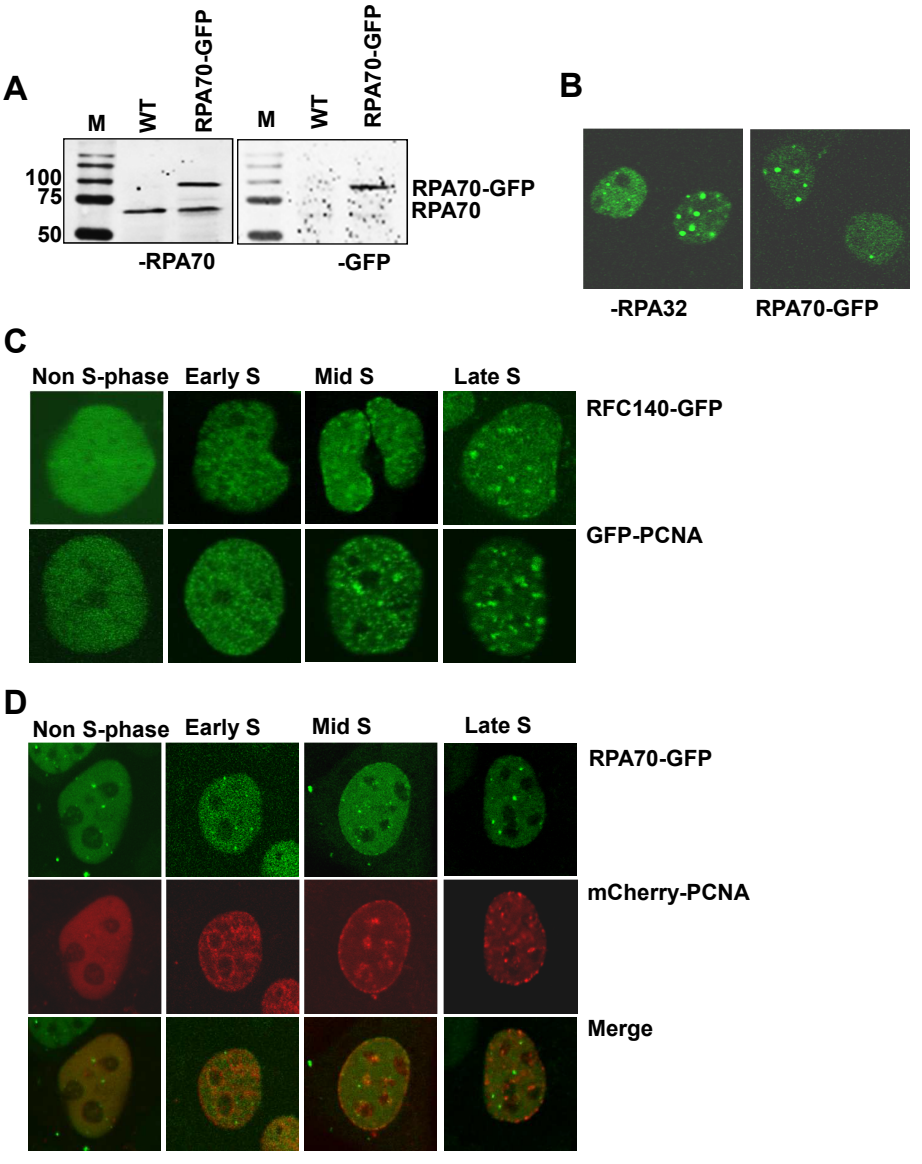

Figure 1: Characterization and subcellular localization of RPA70-GFP
(A) Comparison of the RPA70-GFP and the endogenous RPA70 protein levels. Equal amounts of lysates of U2OS cells stably expressing RPA70-GFP and WT U2OS cells were immunoblotted and probed with antibodies against RPA70 and GFP. The protein marker is indicated with M. The expression levels of RPA70-GFP and endogenous RPA70 are comparable. Experiment was performed twice. **(B)** A representative image of a comparison of RPA localization in fixed U2OS cells (left) and U2OS cells stably expressing RPA70-GFP (right). Endogenous RPA was visualized in WT cells using an antibody specific for the RPA32 subunit. RPA70-GFP shows a similar nuclear distribution to endogenous RPA, with a lower expression in nucleoli and a higher expression in sub-nuclear foci. Experiment was performed at least four times. **(C)** Representative images of living MRC5 cells stably expressing RFC140-GFP and GFP-PCNA, experiment was performed twice. The replication factors display a homogenous localization in cells in G1- and G2-phase

of the cell cycle but distinct focal patterns in specific stages of the S-phase. **(D)** Representative images of living MRC5 cells stably co-expressing RPA70-GFP and mCherry-PCNA. RPA70-GFP displays a similar localization throughout the cell cycle as defined by mCherry-PCNA as S-phase marker. Experiment was performed twice.

RPA as shown by immunofluorescence (Fig. 1B). Sub-nuclear structures with higher local concentrations were independent of the cell cycle phase and were previously described to co-localize with promyelocytic leukemia (PML) body markers[33,34].

Within an asynchronously growing cell population we observed, in approximately 40% of the cells expressing RFC140-GFP and GFP-PCNA, the typical S-phase focal distribution (Fig. 1C)[22,35]. Interestingly, in contrast to these factors, the typical 'replication foci' were not observed in RPA70-GFP expressing cells. To verify that the absence of replication foci in these cells was not due to the imaging conditions or to a strong reduction in the relative number of S-phase cells, we investigated the cell cycle dependent distribution of RPA70-GFP in cells coexpressing mCherry-PCNA to identify cells in S-phase[36]. We observed no focal accumulation of RPA70-GFP although these cells clearly showed mCherry-PCNA foci indicating that these cells were in S-phase (Fig. 1D). Thus far RPA-foci in S-phase cells could only be detected in fixed cells, using antibodies directed against endogenous RPA[37]. These data suggest that RPA, although an essential replication factor, is not visibly clustered into replication foci in living cells. In line with our observations, the *in vivo* localization GFP-RPA32, was previously investigated and also no replication foci of this RPA subunit were observed in living S-phase cells[38,39].

GFP-PCNA, RPA70-GFP and RFC140-GFP mobility

Despite the proven involvement of PCNA, RFC and RPA in replication[40], RPA does not cluster in replication foci. This apparent discrepancy in subcellular localization may be explained by their different binding times. Previous FRAP studies have shown that in non-S-phase cells the mobility of GFP-PCNA and RFC140-GFP is mainly determined by free diffusion[21,22]. To compare the dynamic properties of these two proteins with those of RPA in living cells, we applied an adapted FRAP procedure, designated FLIP-FRAP. This procedure is specifically suited to determine subtle differences in overall nuclear mobility[31]. The mobility curves of GFP-PCNA and RPA70-GFP in non-S-phase cells were comparable (Fig. 2A), with a half-life of approximately 7,5s. RFC140-GFP showed a much longer half-life of approximately 30s (Fig. 2A). The slower diffusion of RFC140-GFP is likely related to the molecular shape and size of the RFC complex, which is almost twice the molecular weight of either the PCNA trimer or the RPA hetero-trimer. Although the mobilities of PCNA and RPA appeared very similar in non-S-phase cells, a striking difference was observed in S-phase cells (Fig. 2B). As expected from earlier studies[21,41], the mobility of GFP-PCNA during S-phase ($t_{1/2}$=40s) was significantly slower than in non-S-phase cells ($t_{1/2}$=7,5s), which is most likely caused by a relatively long PCNA binding in replication factories. Interestingly, the dynamics of RPA70-GFP in non-S-phase cells was similar to that determined in S-phase cells. The striking differences in the mobility between PCNA ($t_{1/2}$=40s) and RPA ($t_{1/2}$=7,5s) in S-phase are most likely explained by the very short binding time of RPA70-GFP molecules to DNA replication substrates and/or factors, while PCNA is bound significantly longer. This suggested transient association would also explain the lack of clearly visible RPA70-GFP replication foci in S-phase cells in live-cell imaging experiments.

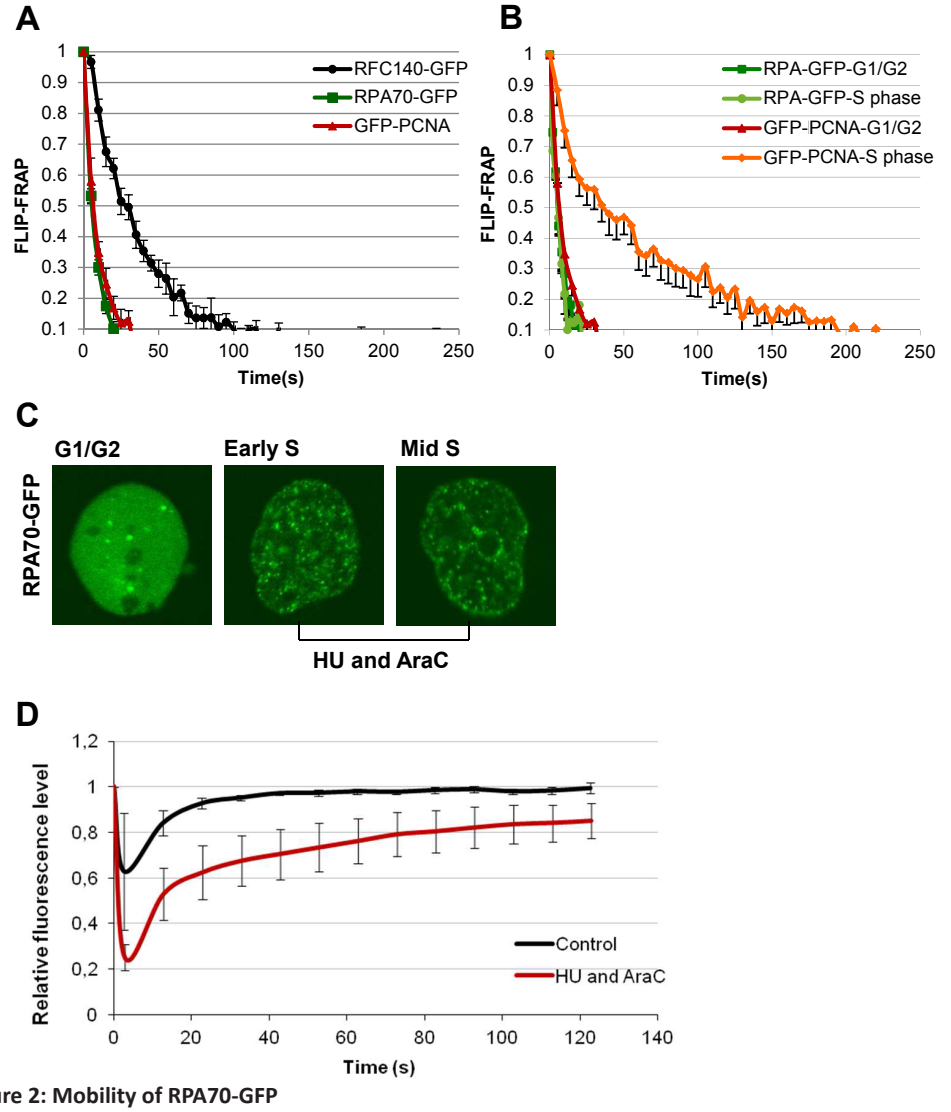

Figure 2: Mobility of RPA70-GFP

(A) FLIP-FRAP analysis in untreated MRC5 cells expressing RFC140-GFP, C5RO cells expressing GFP-PCNA and MRC5 cells expressing RPA70-GFP(At least 8 cells were analyzed, mean ± SEM). Half of the nucleus was bleached with 100% laser power. The loss of fluorescence was measured (FLIP) in the unbleached area and recovery of fluorescence (FRAP) was monitored in the bleached area of the cell. The difference between FLIP and FRAP was normalized to 1 directly after the bleach pulse. The diffusion curves show that RFC140-GFP diffuses much slower than the other replication factors. **(B)** FLIP-FRAP analysis in MRC5 RPA70-GFP and C5RO GFP-PCNA in S-phase versus G1- or G2-phase cells (N=8, mean ± SEM). GFP-PCNA is immobilized during S-phase, while RPA70-GFP kinetics is similar throughout the cell cycle. RPA70-GFP expressing MRC5 cells in S-phase were identified by co-expression of the S-phase marker mCherry-PCNA. **(C)** Representative pictures of living MRC5 RPA70-GFP cells that were exposed to HU and AraC for 30min. In the presence of DNA synthesis inhibitors, RPA70-GFP is visible at replication foci. **(D)** Quantitative FRAP analysis on MRC5 cells stably expressing RPA70GFP in the presence and absence of the DNA synthesis inhibitors HU and AraC. The fluorescence in a small square within the nucleus was bleached and the fluorescence recovery was measured and normalized to pre-bleach intensity (N=5, mean ±SEM).

RPA is immobilized at HU/AraC inhibited replication forks

To investigate whether the dynamic association of RPA70-GFP in replication foci is indeed too transient to be visualized using live cell imaging, we attempted to slow-down its DNA binding kinetics by inhibiting DNA synthesis using hydroxyurea (HU) and cytosine-β-arabinofuranoside (AraC). Upon treatment, a large number of cells exhibited clear S-phase foci (Fig. 2C), indicating that RPA70-GFP protein is biologically active and capable of binding at replication sites. This observation is in line with previous reports, which also showed pronounced focal localization of RPA32-GFP upon treatment of cells with the DNA polymerase-inhibitor, aphidicolin[38].

The presence of RPA70 at replication foci upon replication inhibition might be explained by an increased amount of substrate or an increased binding time of RPA to ssDNA. Therefore, we measured the mobility of RPA70-GFP by photobleaching upon replication inhibition by HU and AraC. A small square within nuclei was photo-bleached and the subsequent recovery of fluorescence, which reflects the effective diffusion rate, was monitored (Fig. 2D). Inhibition of replication fork progression induces an overall slower mobility of RPA70-GFP in the nucleus, likely caused by the transient immobilization of a fraction of RPA molecules at inhibited replication forks. Interestingly, our data suggest that during normal replication the coating of ssDNA with RPA is a highly dynamic process in which individual RPA molecules swiftly bind to and dissociate from its substrate most probably mediated by active DNA polymerases.

RPA70-GFP accumulates for up to 8 hours at sites of local UV damage

RPA, PCNA and RFC are not solely involved in DNA replication but also in several DNA repair processes such as NER. In order to obtain information on the dynamic interactions of these replication factors with DNA damage, we determined the assembly kinetics of RPA and RFC and compared it with the previously determined kinetics of PCNA as well as that of the pre-incision NER factors, XPC and XPA[27]. Accumulation of NER factors at sites of local UV-damage (LUD) was investigated in a population of asynchronous living cells expressing the fluorescent tagged versions of these proteins. The DNA damage recognition factor XPC started to accumulate at sites of LUD immediately after DNA damage infliction. For the down-stream pre-incision factor XPA a slight delay in accumulation was observed. As RPA is present at the same pre-incision step during NER as XPA[42,43], similar accumulation kinetics were expected. However, RPA accumulation was slower than that of XPA. RPA reached a maximum accumulation after 200 min, resembling the accumulation kinetics of the repair replication factors PCNA and RFC (Fig. 3A and Fig. S1). Although it is known that RPA functions in the pre-incision step of NER[44], these data suggest that the visible RPA accumulation is mainly derived from its function in the post-incision step of NER.

Accumulation of RPA at sites of LUD at later time points after UV-irradiation may represent replication-stress in cells that were in S-phase at the moment of damage infliction or that entered this phase despite the presence of DNA damage, rather than reflecting its activity during the NER reaction. To further dissect this possibility, local UV-irradiated cells were incubated with the thymidine analogue EdU. Cells that were in S-phase during the experiment were detected by EdU incorporation. Accumulation of RPA at sites of LUD, using XPA as a damage marker, is visible in both S-phase and non S-phase cells (Fig. 3B). This suggests that RPA accumulation at sites of LUD reflects NER replication sites and is not solely caused by

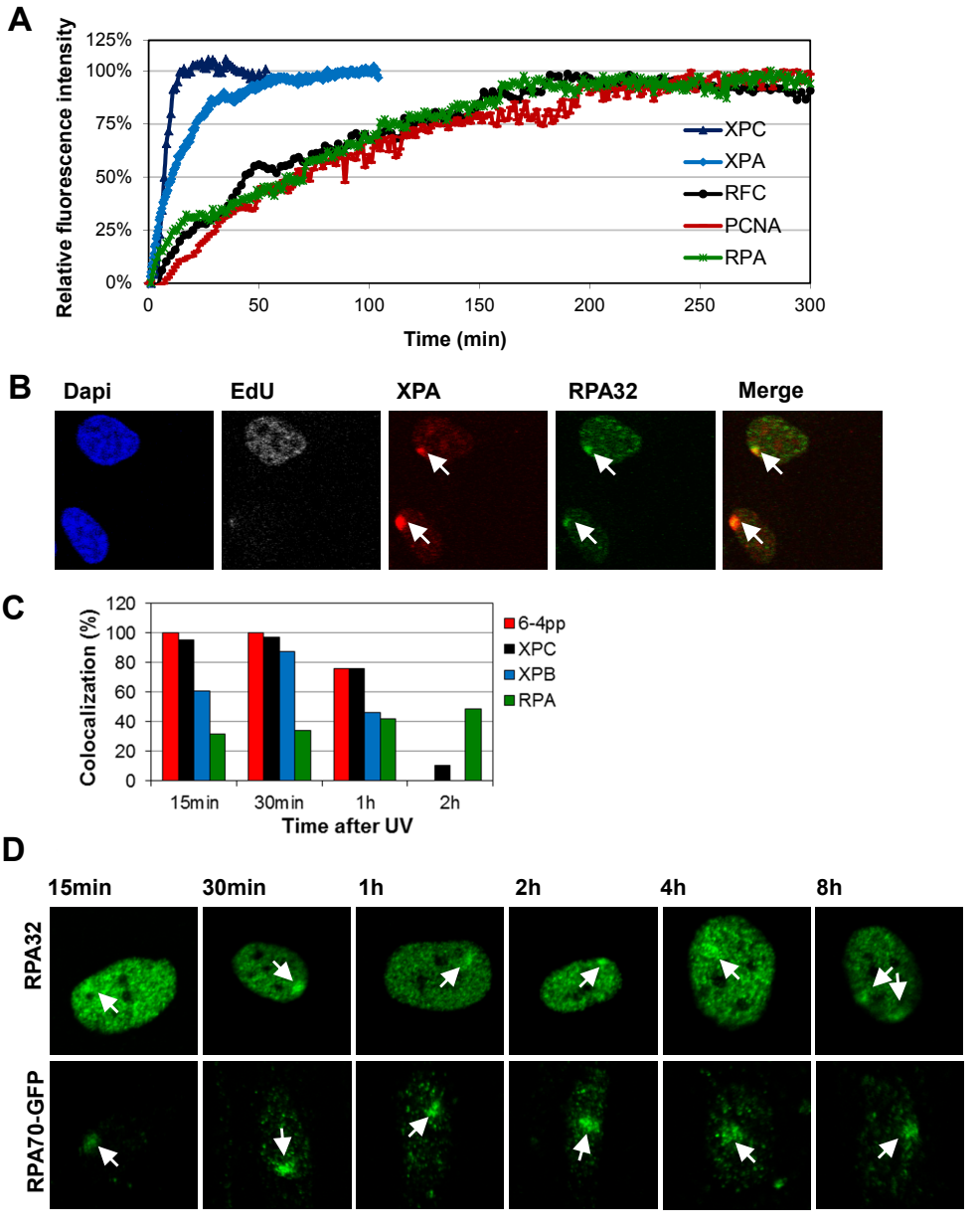

Figure 3: Accumulation kinetics of pre- and post-incision factors at sites of local UV damage
(A) Cells stably expressing XPC-GFP (N=12), GFP-XPA (N=7), RFC140-GFP (N=7), GFP-PCNA (N=5) and RPA70-GFP (N=5) were locally UV-irradiated (100 J/m^2) through 5 µm diameter pores. GFP fluorescence intensities at the site of UV-damage were measured by real time imaging until a maximum was reached. Relative fluorescence was normalized to 0 (before damage) and 100% (maximum level of fluorescence). **(B)** U2OS cells were exposed to local UV-damage (60 J/m^2) and directly after damage incubated for 30 min in medium containing EdU. S-phase cells were identified by EdU incorporation, visualized by Alexa 647. Cells were immunostained for RPA32 and XPA. RPA accumulates at LUD in both S-phase and non-S-phase cells. Arrows indicate local damage. Experiment was performed twice. **(C)** Quantification of co-

localization of the indicated proteins at LUD with a damage marker at various time points after local UV irradiation (40 J/m^2). XPA was used as damage marker for 6-4PP and RPA stainings, whereas CPD was used as damage marker for XPC and XPB stainings. Co-localization was defined as ≥ 2-fold increase in intensity at LUD and analyzed in 40 cells, experiment was performed twice. **(D)** Representative pictures of RPA in locally UV-irradiated (40 J/m^2) quiescent C5RO cells visualized with anti-RPA32 and quiescent C5RO cells stably expressing RPA70-GFP. RPA is visible at the site of damage up to 8 h after UV. Arrows indicate LUD. Experiment was performed twice.

replication stress.

To confirm these observations we also studied the accumulation of RPA and other pre-incision NER factors, XPC and XPB in quiescent cells, where no replication processes occur, as shown by the absence of Ki67 staining (Fig. S2A). Cells were fixed at various time-points post UV-irradiation (15 min, 30 min, 1 hour and 2 hours) and immunostained for 6-4PP, XPC, XPB and RPA. As expected, the pre-incision factors XPC and XPB accumulated at sites of LUD shortly after damage infliction (within 15 min) and started to disappear after 2 hours following the removal of 6-4PP (Fig. 3C, and Fig. S2B-D). In contrast, while only a faint RPA signal could be detected at sites of LUD at the earliest time point (15 min), a stronger signal was detected at one hour after UV and remained visible up to 8 hours post UV irradiation (Fig.3C and D). These data suggest that the long-lasting accumulation of RPA is related to post-incision events of NER and is not solely caused by stalled replication forks at sites of UV-damage.

Dynamics of RPA70-GFP in the pre- and post-incision steps of NER

As shown above, RPA can be visualized at sites of LUD at later time points post-UV relative to other pre-incision NER factors, despite the fact that it is absolutely required during the pre-incision step[44,45]. This late accumulation at sites of LUD suggests that the binding time of RPA in the pre-incision NER step is too short to result in detectable accumulation at sites of LUD, which is in line with the observation that RPA is not visible at replication foci (Fig. 1D). To reveal RPA binding to pre-incision NER intermediates we made use of a specific XPF mutant cell line, XP51RO. Due to a missense mutation in XPF this endonuclease is mis-localized in the cytoplasm and therefore cannot execute the essential 5' incision during NER[46]. Since these XP-F cells are devoid of dual incision events, no post-incision repair replication associated RPA accumulation is expected.

Despite the absence of incision, co-localization of RPA32 to sites of LUD was higher in XPF mutant cells than in wild type cells at all time points (Fig. 4A). In addition, RPA signal-intensity at sites of LUD was higher in XP-F cells. Similar results were observed for the GFP-tagged version of RPA70 (Fig. S3). Thus, due to absence of the ERCC1/XPF mediated incision, the stronger RPA signal at LUD could be explained by an extended lifetime and/or an increased number of unwound and RPA coated pre-incision NER-intermediates. To determine the dynamic association of RPA in non-processed pre-incision NER complexes, we compared, using FRAP, the mobility of RPA70-GFP, in UV-irradiated XP-F and wild type cells. In XPF mutant cells, we observed a small transient immobilization of RPA70-GFP upon UV-damage, which was not present in wild type cells (Fig. 4B). This difference however, is most likely too small to account for the increased signal of RPA in XP-F cells. Probably XP-F cells accumulate more pre-incision NER intermediates (RPA substrates) at any given time, resulting

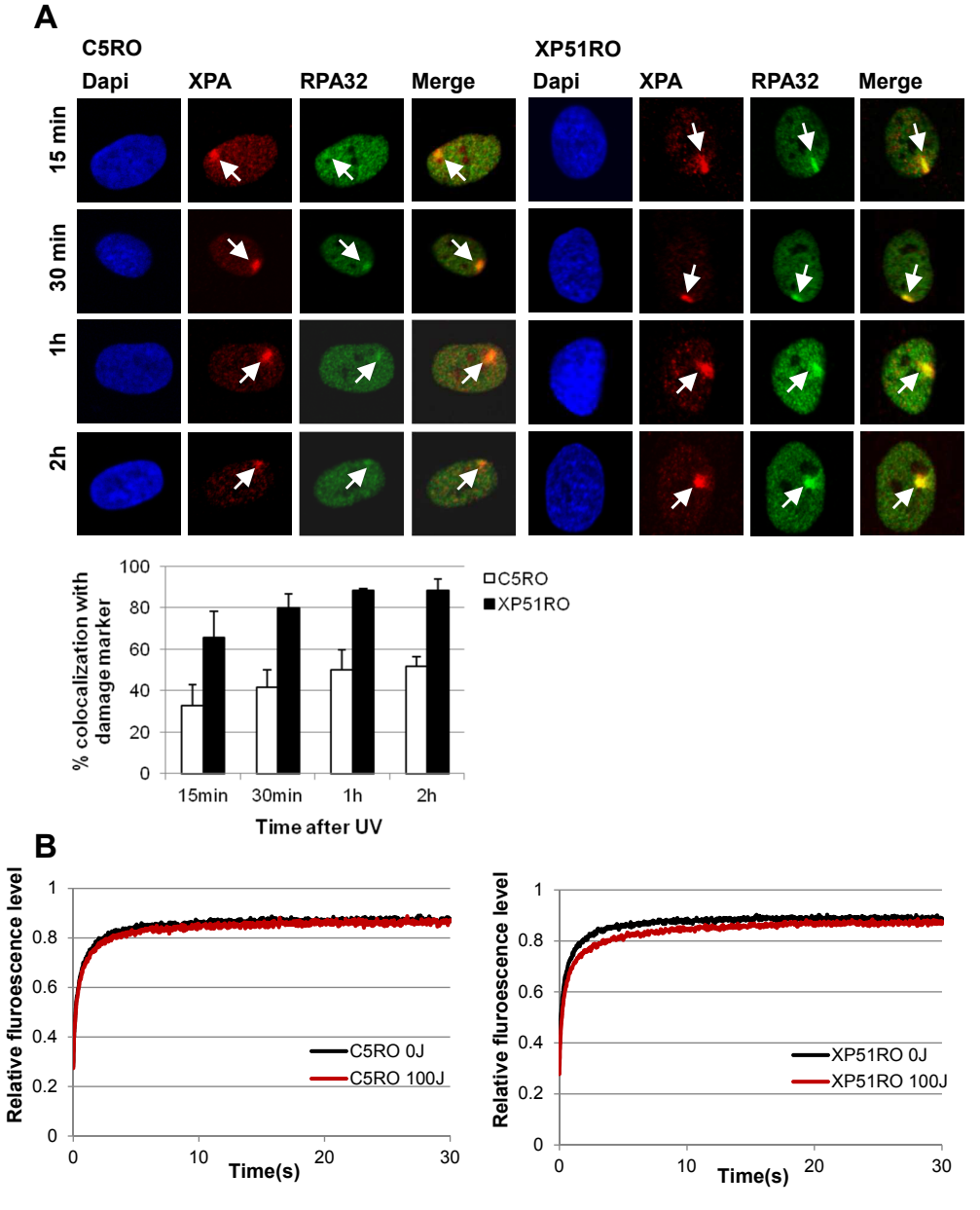

Figure 4: Dynamics of RPA in XPF deficient cells
(A) Quiescent C5RO and XP51RO (XPF deficient) cells were local UV irradiated (40 J/m^2). Cells were fixed at the indicated time points after UV and immunostained for RPA32 and XPA. Arrows indicate local damage sites. The percentage of colocalization of RPA32 with XPA after LUD is plotted in the graph. At least 40 cells with LUD were analyzed in three independent experiments (mean ± SD). **(B)** FRAP analysis of RPA70-GFP in non-damaged and global UV-irradiated (100 J/m^2) C5RO and XP51RO (XPF deficient) cells. FRAP was performed directly after UV-treatment. The recovery was normalized to pre-bleach intensity (N=24, from two independent experiments).

in a higher RPA signal. Together these data show that RPA displays a remarkable highly dynamic association with DNA during the assembly of the pre-incision NER complex. The binding kinetics are that short that they could not be revealed under standard live-cell imaging conditions in NER proficient cell lines.

In contrast to other pre-incision factors, but similarly to RFC, RPA is present for a prolonged time at sites of DNA damage[22]. This different kinetic behavior is probably derived from its function in the post-incision steps of NER. To further decipher the mode of action of RPA70-GFP during the post-incision steps of NER, we used the DNA synthesis inhibitors HU/AraC. Upon treatment with HU/AraC, repair associated DNA synthesis is inhibited and NER induced ssDNA remains, which represents post-incision intermediates[22]. Under these conditions it is possible to study RPA kinetics specifically at the post-incision steps of NER. Cells were treated with HU/AraC or mock treated 30 min prior to LUD infliction, and fixed one hour later. During the entire procedure cells were cultured in the presence of EdU. UV-irradiated areas were visualized using CPD immunostaining. In response to an UV-dose of 30 J/m^2 RPA70-GFP accumulation is not detectable at sites of LUD, independent of the cell cycle phase (Figure 5A, Top panel). Note that in the non-replicating cell the DNA repair replication is active as shown by the EdU incorporation at LUD. Despite this clear mark of DNA synthesis, under these conditions no local RPA accumulation is visible. However, when DNA synthesis was blocked with HU and AraC, as shown by the lack of EdU incorporation, RPA70-GFP accumulation at sites of LUD was clearly detected (Fig. 5A, Lower panel). The same was observed for the endogenous protein visualized using an antibody against RPA32 (Fig. S4). This could be explained either by an increase in the number of binding sites for RPA or by a more stable association of RPA with ssDNA.

To gain more insight into the dynamic association of RPA with sites of HU/AraC-inhibited repair replication, we performed a FLIP experiment at sites of LUD to measure the off-rate of RPA from sites of DNA damage. One hour after local UV irradiation, an area in the nucleus representing approximately one third of the nuclear volume located opposite of the LUD was continuously bleached. The intensity of fluorescence in the local damage was measured[47]. The time it takes to lose the fluorescent signal at LUD by this procedure is a measurement for the dissociation rate of the RPA-GFP molecules. The average binding time of RPA70-GFP molecules was longer (~2-fold) in the presence of inhibitors than in cells with processive DNA repair synthesis (Fig. 5B), suggesting that the DNA polymerases involved in DNA repair synthesis have an important impact on the residence time of RPA at the ssDNA gap. In summary these data demonstrate that RPA presents differential kinetic properties in pre- and post-incision steps of NER.

Discussion

Dynamics at replication sites

The DNA synthesis step of DNA replication of the genome requires the concerted action of many proteins including: DNA polymerases, the polymerase clamp (PCNA), the clamp loading complex (RFC), and the single-stranded DNA-binding protein complex (RPA)[40]. Replication factors, such as PCNA and RFC show specific distribution patterns throughout the S-phase known as replication foci or replisomes (Fig. 1C)[35]. In line with this, PCNA and RFC become

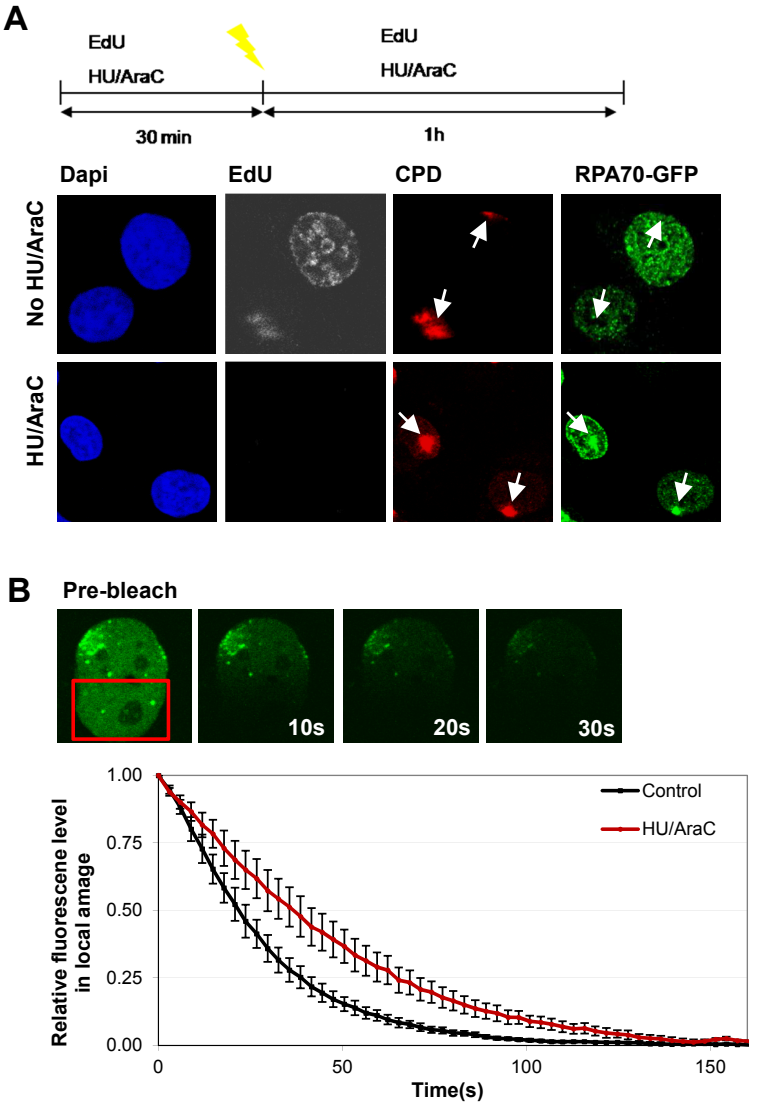

Figure 5: Dynamics of RPA70-GFP at sites of LUD upon HU/AraC treatment
(A) A representative image of RPA70-GFP expressing U2OS cells that were mock treated or incubated with HU and AraC for 30 min before local UV-irradiation (30 J/m^2). Cells were fixed 1 hour after UV exposure. S-phase cells were identified by EdU incorporation, visualized by Alexa647 or by localization of RPA70-GFP. The UV-irradiated areas were visualized using an antibody specific for CPDs. In the presence of DNA synthesis inhibitors RPA70-GFP accumulation is visible at LUD in both S-phase and non-S-phase cells. Arrows indicate local damage. Experiment was performed twice. **(B)** Dissociation kinetics of RPA70-GFP from LUD in mock or HU and AraC treated cells (30min). MRC5 RPA70-GFP cells were locally UV-irradiated (100 J/m^2) and one third of the nucleus was continuously bleached. The decrease of fluorescence in the LUD was quantified (N ≥ 12**,** from two independent experiments; mean ± SEM). The residence time of RPA70-GFP at LUD is longer in cells treated with DNA synthesis inhibitors.

less mobile during S-phase compared to G1- or G2-phases of the cell cycle (Fig. 2B)[21]. Interestingly, and in contrast to PCNA and RFC, the 2 largest subunits of replication protein A (RPA70 and RPA32) are not visible in replication foci in living cells (Fig. 1D)[38,41]. Thus far, RPA has only been detected in replication foci upon fixation followed by immunofluorescence[37]. In this procedure the bound RPA at sites of replication is fixed and unbound RPA is most likely washed away enabling detection under such conditions. However, in living cells RPA does not visibly accumulate in replication foci, despite its established role in this process, which is likely due to the fast turnover of RPA molecules at replication sites. The dwell time of RPA at replication sites is in the same order of its respective diffusion rate (Fig. 2B), indicating that the ssDNA-RPA interaction is too transient to induce RPA steady-state levels above background.

DNA synthesis inhibitors such as HU and AraC have been shown to block DNA polymerases at replication forks, resulting in an increase of ssDNA patches[48], which are coated by RPA. Under these conditions, RPA accumulates in replication foci (Fig. 2C), indicating that RPA70-GFP is functional and binds at sites of replication. Similar results have been observed for GFP-RPA32 in cells treated with the DNA synthesis inhibitor aphidicolin[38,39]. DNA synthesis inhibition results in an excess of ssDNA[48], thereby increasing the amount of RPA-binding substrates, which partially explains the clear presence of RPA at sites of blocked replication. In addition, RPA mobility is greatly reduced upon inhibition of the DNA polymerases (Fig. 2D). These data further corroborate that although RPA coats ssDNA at sites of replication, it is not visible at replication foci in living cells in unperturbed conditions because it is swiftly displaced by the elongating DNA polymerases during replication[49]. It is however important to note that even when RPA is bound at the ssDNA patches induced by a replication block, it still binds transiently, indicating that it is an intrinsic property of RPA to continuously associate and dissociate from ssDNA, independently of DNA polymerases. These results are in line with the rapid RPA turnover on ssDNA *in vitro*[50]. In contrast to RPA, PCNA binds more stably at replication forks, most likely remaining at the site of replication until replication is completed[41]. This difference in residence time at the replication fork between RPA and PCNA likely explains why PCNA can be observed at replication sites in living cells, while RPA cannot.

RPA promotes two mechanistically distinct steps in NER

RPA plays a key role in the pre- as well as post-incision steps of NER. Intriguingly, while RPA binding kinetics is similar to the assembly kinetics of the replication factors PCNA and RFC, they are very different to those of the pre-incision NER factors XPC, XPB and XPA. Pre-incision factors accumulate rapidly after UV-irradiation and their bound steady-state levels decrease within 2 hours (Fig. 3C and Fig. S2B-D)[27], closely following the repair kinetics of 6-4 photoproducts. Conversely, RPA reaches it maximum only after 3 hours and is still visible up to 8 hours at sites of local UV-damage (Fig. 3A and D).

Treatment of cells with DNA synthesis inhibitors, which also disturbs DNA synthesis during the gap-filling stage of NER, resulted in a more abundant accumulation of RPA at sites of DNA damage, which is likely due to longer residence times on the chromatin (Fig. 5B). On the contrary, the residence time of the pre-incision factors XPA and ERCC1 is not retarded by inhibition of DNA synthesis[27]. This suggests that the observed localization of RPA at LUD is mainly derived from its function in repair synthesis during the post-incision step of NER. In line

with our results, previous studies showed that inhibition of either the DNA repair synthesis or ligation step of NER, results in prolonged presence of RPA at sites of LUD, while other pre-incision factors are still able to dissociate and relocate to other damage sites[19]. While Overmeer *et al. 2011* report that RPA remains bound at sites of DNA damage and does not relocate to engage new repair sites upon inhibition of DNA repair synthesis, our FRAP data clearly shows that, although its mobility is greatly reduced, RPA can still bind to and dissociate from the DNA continuously.

In XPF-deficient cells, incision does not take place and pre-incision NER intermediates accumulate[46]. These intermediates contain unwound DNA structures to which RPA binds. In these cells RPA accumulation at early time points was observed in a higher percentage of cells, more closely resembling the accumulation kinetics of other pre-incision factors. This demonstrates that although not clearly visible in repair proficient cells, RPA can be visualized in pre-incision NER intermediates. Interestingly, despite the accumulation of pre-incision NER-intermediates in XPF-deficient cells, RPA mobility was only minimally reduced, indicating that RPA binds to and dissociates from NER intermediates at almost similar rates to that in wild-type cells. This indicates that the rapid binding and dissociation of RPA in the pre-incision step of NER, just like during normal replication, is an intrinsic property of RPA. These data suggest that the binding time of RPA in the pre-incision steps of NER is too brief to be visualized in NER proficient cells.

The two major DNA lesions induced by UV-irradiation display different repair kinetics: while local induced 6-4PPs are repaired (depending on the dose) within ~2 to 4 hours; CPD repair is not achieved within 24 hours[51]. Previous studies showed that accumulation of NER factors to LUD follow the repair kinetics of 6-4PP[27,51]. It is unlikely that RPA accumulation to LUD at late time points is due to repair of 6-4PPs. It is more probable that RPA is involved in other processes, for example those linked to the persistent presence of CPD lesions. It is possible that accumulation of RPA at late time points after UV is a result of replication stress due to replication fork stalling at UV-lesions in cells that were in S-phase at the moment of damage infliction or that moved into this phase despite the presence of DNA damage. However RPA accumulation at late time points is also observed in non-S-phase cells (Fig. 3B) and quiescent cells, where no replication occurs (Fig. 3D). These results suggest that RPA accumulation to LUD at late time points marks post-incision NER sites. This hypothesis is supported by the fact that - like RPA - PCNA and RFC also localize to sites of LUD in quiescent cells up to 8 hours post-irradiation[22].

Whether the ssDNA NER intermediates, formed by the joint action of the XPF/ERCC1 and XPG nucleases, are alone responsible for this long-lasting RPA accumulation at sites of damage is questionable; especially since NER intermediates are short ssDNA gaps, (~30 nt long) which can, most likely, bind only one RPA trimer. Moreover, the ssDNA NER intermediates are likely very short lived, being rapidly refilled by DNA polymerases during DNA repair synthesis, which might take place even before incision 3' to the UV-lesion[15]. Recent studies have shown that the exonuclease activity of EXO1 is implicated in the processing of NER intermediates, thereby generating long stretches of ssDNA that are coated by RPA[52,53]. This can also happen in non-cycling cells under specific conditions that might occur when the normally short-lived ssDNA NER intermediates persist. Examples of such conditions are when the damage load in

the cell is so high that the concentration of NER factors might become limiting, or during the collision of two opposing NER reactions when the opposing lesion is blocking the progression of NER-induced gap filling synthesis. Indeed, a possible explanation for the accumulation of RPA, PCNA and RFC at late time points after UV-irradiation is that lesions that are difficult to repair are processed to long ssDNA gaps by the exonuclease activity of EXO1 to overcome these lesions. In line with this, others have shown that EXO1 accumulation is also increased at sites of DNA damage in situations where more RPA accumulates, for example upon inhibition of the gap-filling step of the NER reaction[53].

In summary, RPA displays differential dynamics during replication and at sites of NER. It binds ssDNA transiently during replication and the pre-incision steps of NER, but has a more stable association during the post-incision steps of NER and in response to replication stress. RPA is known to recruit ATR through its binding partner ATRIP in order to induce checkpoint activation and cell cycle arrest in response to both replication stress and UV damage[48]. If there are no obstacles during replication, RPA binding does not induce checkpoint activation. In line with this, studies in yeast have shown that very low doses of UV do not induce checkpoint activation[54]. We speculate that the differential dynamic behavior of RPA might be an important control factor for checkpoint activation. Binding of RPA during replication and pre-incision steps of NER is too transient to induce checkpoint activation, whereas the more stable association of RPA during replication stress and the post-incision steps of NER recruits ATR and ATRIP thereby activating a cellular response to cope with the damage.

Supplementary information

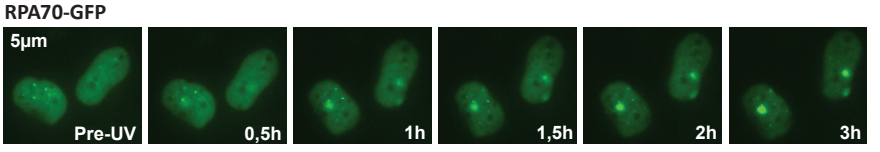

Figure S1. Representative pictures of cells stably expressing RPA70-GFP at several time points after local UV-C irradiation (100 J/m^2 through 5µm diameter pores).

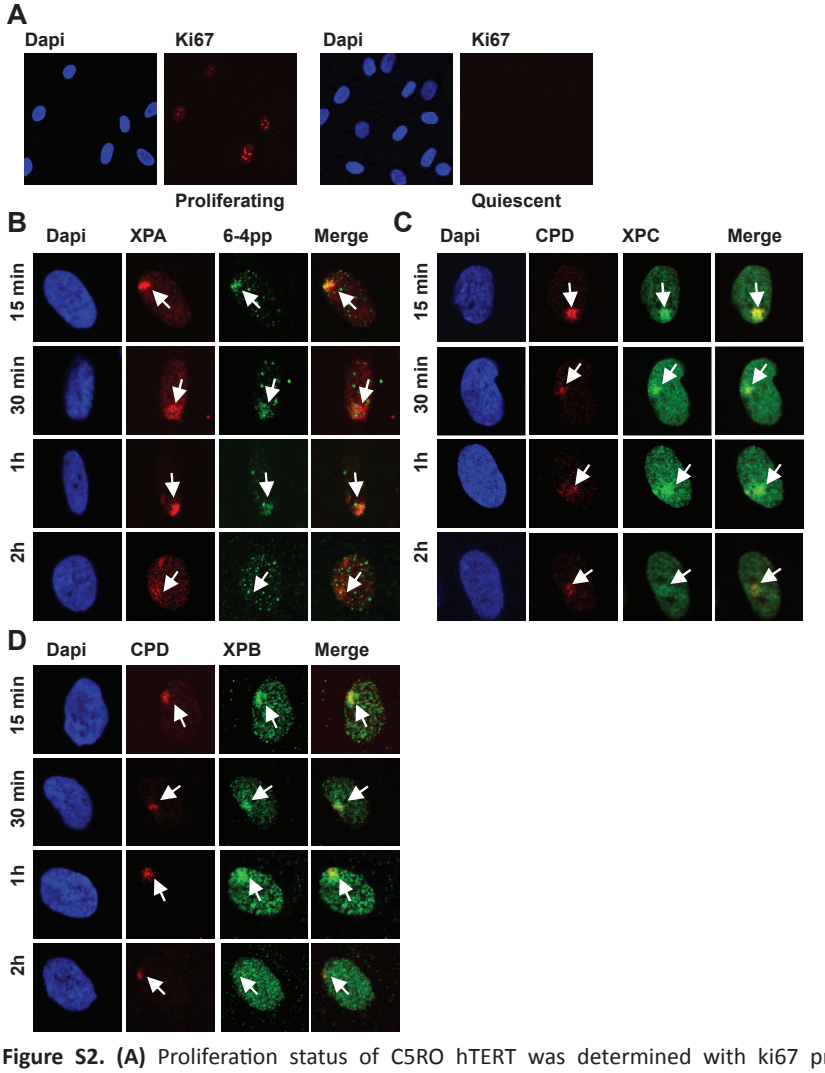

Figure S2. (A) Proliferation status of C5RO hTERT was determined with ki67 proliferation marker. Proliferating cells are positive for ki67 (left panel), while quiescent cells are ki67 negative (right panel). Experiment was performed four times. **(B-D)** Representative pictures of quiescent C5RO cells that were locally UV-irradiated (40 J/m^2). Cells were fixed at different time points after UV and stained for 6-4PP (B), XPC (C), and XPB (D). LUD were visualized using a XPA (in B) or CPD (in C and D) antibody. Arrows indicate local damage sites. Experiment was performed at least two times.

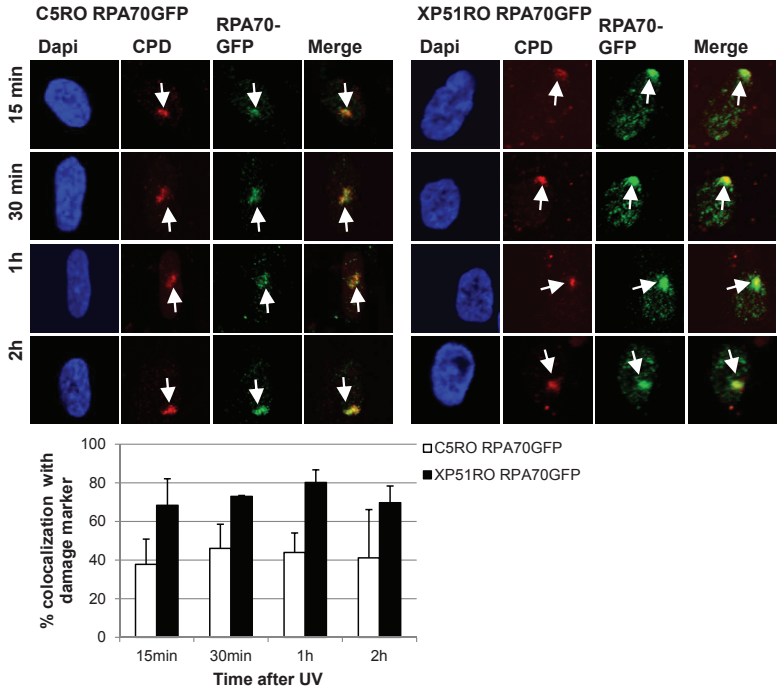

Figure S3. Quiescent C5RO and XP51RO (XPF deficient) cells expressing RPA70-GFP were locally UV-irradiated (40 J/m^2) and fixed at indicated time points. The UV-irradiated areas were visualized by CPD counterstaining. Arrows indicate local damage sites. The percentage of colocalization of RPA70-GFP with CPD is shown in the graph. At least 40 LUDs were scored in two independent experiments (mean ± SD).

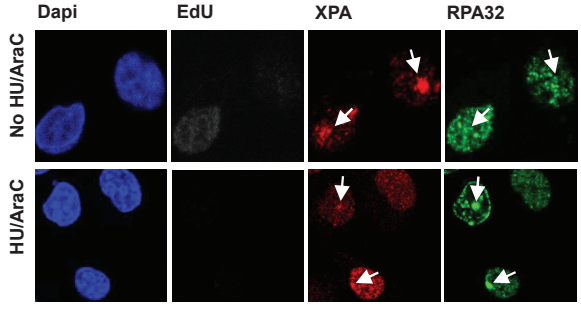

Figure S4. U2OS cells were mock or HU and AraC treated 30 min before local UV-irradiation (30 J/m^2) and incubated with the thymidine analogue EdU. Cells were fixed 1 hour after UV-treatment and immunostained for XPA and RPA32 S-phase cells were identified by EdU incorporation, visualized by Alexa647 or by localization of RPA32 in replication foci. Arrows indicate LUD. In the presence of DNA synthesis inhibitors RPA32 localizes to LUD in both S-phase and non-S-phase cells. Experiment was performed twice.

References

1. Wold, M.S. Replication protein A: a heterotrimeric, single-stranded DNA-binding protein required for eukaryotic DNA metabolism. *Annu Rev Biochem* **66**, 61-92 (1997).
2. de Laat, W.L. *et al.* DNA-binding polarity of human replication protein A positions nucleases in nucleotide excision repair. *Genes Dev* **12**, 2598-609 (1998).
3. Iftode, C., Daniely, Y. & Borowiec, J.A. Replication protein A (RPA): the eukaryotic SSB. *Crit Rev Biochem Mol Biol* **34**, 141-80 (1999).
4. Moldovan, G.L., Pfander, B. & Jentsch, S. PCNA, the maestro of the replication fork. *Cell* **129**, 665-79 (2007).
5. Majka, J. & Burgers, P.M. The PCNA-RFC families of DNA clamps and clamp loaders. *Prog Nucleic Acid Res Mol Biol* **78**, 227-60 (2004).
6. O'Keefe, R.T., Henderson, S.C. & Spector, D.L. Dynamic organization of DNA replication in mammalian cell nuclei: spatially and temporally defined replication of chromosome-specific alpha-satellite DNA sequences. *J Cell Biol* **116**, 1095-110 (1992).
7. Scharer, O.D. Nucleotide excision repair in eukaryotes. *Cold Spring Harb Perspect Biol* **5**, a012609 (2013).
8. Sugasawa, K. *et al.* Xeroderma pigmentosum group C protein complex is the initiator of global genome nucleotide excision repair. *Mol Cell* **2**, 223-32 (1998).
9. Moser, J. *et al.* The UV-damaged DNA binding protein mediates efficient targeting of the nucleotide excision repair complex to UV-induced photo lesions. *DNA Repair (Amst)* **4**, 571-82 (2005).
10. Fousteri, M. & Mullenders, L.H. Transcription-coupled nucleotide excision repair in mammalian cells: molecular mechanisms and biological effects. *Cell Res* **18**, 73-84 (2008).
11. Vermeulen, W. & Fousteri, M. Mammalian transcription-coupled excision repair. *Cold Spring Harb Perspect Biol* **5**, a012625 (2013).
12. Volker, M. *et al.* Sequential assembly of the nucleotide excision repair factors in vivo. *Mol Cell* **8**, 213-24 (2001).
13. Matsunaga, T., Park, C.H., Bessho, T., Mu, D. & Sancar, A. Replication protein A confers structure-specific endonuclease activities to the XPF-ERCC1 and XPG subunits of human DNA repair excision nuclease. *J Biol Chem* **271**, 11047-50 (1996).
14. He, Z., Henricksen, L.A., Wold, M.S. & Ingles, C.J. RPA involvement in the damage-recognition and incision steps of nucleotide excision repair. *Nature* **374**, 566-9 (1995).
15. Staresincic, L. *et al.* Coordination of dual incision and repair synthesis in human nucleotide excision repair. *EMBO J* **28**, 1111-20 (2009).
16. Moser, J. *et al.* Sealing of chromosomal DNA nicks during nucleotide excision repair requires XRCC1 and DNA ligase III alpha in a cell-cycle-specific manner. *Mol Cell* **27**, 311-23 (2007).
17. Riedl, T., Hanaoka, F. & Egly, J.M. The comings and goings of nucleotide excision repair factors on damaged DNA. *EMBO J* **22**, 5293-303 (2003).
18. Ogi, T. *et al.* Three DNA polymerases, recruited by different mechanisms, carry out NER repair synthesis in human cells. *Mol Cell* **37**, 714-27 (2010).
19. Overmeer, R.M. *et al.* Replication protein A safeguards genome integrity by controlling NER incision events. *J Cell Biol* **192**, 401-15 (2011).
20. van Veelen, L.R. *et al.* Analysis of ionizing radiation-induced foci of DNA damage repair proteins. *Mutat Res* **574**, 22-33 (2005).
21. Essers, J. *et al.* Nuclear dynamics of PCNA in DNA replication and repair. *Mol Cell Biol* **25**, 9350-9 (2005).
22. Overmeer, R.M. *et al.* Replication factor C recruits DNA polymerase delta to sites of nucleotide excision repair but is not required for PCNA recruitment. *Mol Cell Biol* **30**, 4828-39 (2010).
23. Hoogstraten, D. *et al.* Versatile DNA damage detection by the global genome nucleotide excision repair protein XPC. *J Cell Sci* **121**, 2850-9 (2008).
24. Rademakers, S. *et al.* Xeroderma pigmentosum group A protein loads as a separate factor onto DNA lesions. *Mol Cell Biol* **23**, 5755-67 (2003).
25. Mone, M.J. *et al.* Local UV-induced DNA damage in cell nuclei results in local transcription inhibition. *EMBO Rep* **2**, 1013-7 (2001).

26. Ng, J.M. *et al.* A novel regulation mechanism of DNA repair by damage-induced and RAD23-dependent stabilization of xeroderma pigmentosum group C protein. *Genes Dev* **17**, 1630-45 (2003).
27. Luijsterburg, M.S. *et al.* Stochastic and reversible assembly of a multiprotein DNA repair complex ensures accurate target site recognition and efficient repair. *J Cell Biol* **189**, 445-63 (2010).
28. Luijsterburg, M.S. *et al.* Dynamic in vivo interaction of DDB2 E3 ubiquitin ligase with UV-damaged DNA is independent of damage-recognition protein XPC. *J Cell Sci* **120**, 2706-16 (2007).
29. Mone, M.J. *et al.* In vivo dynamics of chromatin-associated complex formation in mammalian nucleotide excision repair. *Proc Natl Acad Sci U S A* **101**, 15933-7 (2004).
30. Houtsmuller, A.B. & Vermeulen, W. Macromolecular dynamics in living cell nuclei revealed by fluorescence redistribution after photobleaching. *Histochem Cell Biol* **115**, 13-21 (2001).
31. Hoogstraten, D. *et al.* Rapid switching of TFIIH between RNA polymerase I and II transcription and DNA repair in vivo. *Mol Cell* **10**, 1163-74 (2002).
32. Sabbioneda, S. *et al.* Effect of proliferating cell nuclear antigen ubiquitination and chromatin structure on the dynamic properties of the Y-family DNA polymerases. *Mol Biol Cell* **19**, 5193-202 (2008).
33. Park, J., Seo, T., Kim, H. & Choe, J. Sumoylation of the novel protein hRIP{beta} is involved in replication protein A deposition in PML nuclear bodies. *Mol Cell Biol* **25**, 8202-14 (2005).
34. Groth, A. *et al.* Regulation of replication fork progression through histone supply and demand. *Science* **318**, 1928-31 (2007).
35. Somanathan, S., Suchyna, T.M., Siegel, A.J. & Berezney, R. Targeting of PCNA to sites of DNA replication in the mammalian cell nucleus. *J Cell Biochem* **81**, 56-67 (2001).
36. Soria, G. *et al.* DNA damage induced Pol eta recruitment takes place independently of the cell cycle phase. *Cell Cycle* **8**, 3340-8 (2009).
37. Murti, K.G., He, D.C., Brinkley, B.R., Scott, R. & Lee, S.H. Dynamics of human replication protein A subunit distribution and partitioning in the cell cycle. *Exp Cell Res* **223**, 279-89 (1996).
38. Solomon, D.A., Cardoso, M.C. & Knudsen, E.S. Dynamic targeting of the replication machinery to sites of DNA damage. *J Cell Biol* **166**, 455-63 (2004).
39. Gorisch, S.M. *et al.* Uncoupling the replication machinery: replication fork progression in the absence of processive DNA synthesis. *Cell Cycle* **7**, 1983-90 (2008).
40. Waga, S., Bauer, G. & Stillman, B. Reconstitution of complete SV40 DNA replication with purified replication factors. *J Biol Chem* **269**, 10923-34 (1994).
41. Sporbert, A., Gahl, A., Ankerhold, R., Leonhardt, H. & Cardoso, M.C. DNA polymerase clamp shows little turnover at established replication sites but sequential de novo assembly at adjacent origin clusters. *Mol Cell* **10**, 1355-65 (2002).
42. Stigger, E., Drissi, R. & Lee, S.H. Functional analysis of human replication protein A in nucleotide excision repair. *J Biol Chem* **273**, 9337-43 (1998).
43. Li, L., Lu, X., Peterson, C.A. & Legerski, R.J. An interaction between the DNA repair factor XPA and replication protein A appears essential for nucleotide excision repair. *Mol Cell Biol* **15**, 5396-402 (1995).
44. Coverley, D. *et al.* Requirement for the replication protein SSB in human DNA excision repair. *Nature* **349**, 538-41 (1991).
45. Aboussekhra, A. *et al.* Mammalian DNA nucleotide excision repair reconstituted with purified protein components. *Cell* **80**, 859-68 (1995).
46. Ahmad, A. *et al.* Mislocalization of XPF-ERCC1 nuclease contributes to reduced DNA repair in XP-F patients. *PLoS Genet* **6**, e1000871 (2010).
47. Pines, A. *et al.* PARP1 promotes nucleotide excision repair through DDB2 stabilization and recruitment of ALC1. *J Cell Biol* **199**, 235-49 (2012).
48. Zou, L. & Elledge, S.J. Sensing DNA damage through ATRIP recognition of RPA-ssDNA complexes. *Science* **300**, 1542-8 (2003).
49. Hubscher, U. & Seo, Y.S. Replication of the lagging strand: a concert of at least 23 polypeptides. *Mol Cells* **12**, 149-57 (2001).
50. Gibb, B. *et al.* Protein dynamics during presynaptic-complex assembly on individual single-stranded DNA molecules. *Nat Struct Mol Biol* (2014).

51. Marteijn, J.A. *et al.* Nucleotide excision repair-induced H2A ubiquitination is dependent on MDC1 and RNF8 and reveals a universal DNA damage response. *J Cell Biol* **186**, 835-47 (2009).
52. Giannattasio, M. *et al.* Exo1 competes with repair synthesis, converts NER intermediates to long ssDNA gaps, and promotes checkpoint activation. *Mol Cell* **40**, 50-62 (2010).
53. Sertic, S. *et al.* Human exonuclease 1 connects nucleotide excision repair (NER) processing with checkpoint activation in response to UV irradiation. *Proc Natl Acad Sci U S A* **108**, 13647-52 (2011).
54. Hishida, T., Kubota, Y., Carr, A.M. & Iwasaki, H. RAD6-RAD18-RAD5-pathway-dependent tolerance to chronic low-dose ultraviolet light. *Nature* **457**, 612-5 (2009).

Chapter 7

General discussion

Appendix

Summary

The integrity of DNA is constantly threatened by endogenously produced cellular metabolites and environmental genotoxic agents. DNA damage interferes with cellular functioning as it disturbs vital DNA-dependent processes, including transcription and replication. Persistent DNA lesions may alter genetic information or induce cell death, which contributes to malignant transformation and accelerated ageing, respectively. To protect against these deleterious effects organisms have evolved the DNA Damage Response (DDR), consisting of multiple DNA repair pathways and DNA damage signaling processes that control cell fate. One of these DNA repair processes, Nucleotide Excision Repair (NER), is responsible for the repair of different structurally unrelated DNA lesions that destabilize the DNA double helix, including UV-induced cyclobutane pyrimidine dimers and 6-4 pyrimidine-pyrimidone photoproducts. NER comprises two damage recognition sub-pathways: Global genome NER (GG-NER), which detects and removes DNA lesions located anywhere in the genome, whereas transcription coupled NER (TC-NER) specifically targets DNA lesions in the transcribed strand of active genes. NER involves the action of more than 30 proteins to recognize and remove damage from DNA. To ensure proper coordination of multiple NER factors, this process requires a tight regulation, which is commonly achieved by post-translational modifications (PTMs). Recent evidence suggests that within NER protein ubiquitylation seems to play a prominent role in controlling this process, although their significance for regulating NER and the molecular mechanism that drives these PTMs are currently unknown. This thesis focuses on protein modifications by ubiquitin in the damage recognition steps of NER. Protein ubiquitylation can - amongst others - influence the stability, activity, localization and interactions of a protein. Several NER factors have already been shown to be ubiquitylated in response to UV. **Chapter 1** provides a general introduction to the DDR and ubiquitylation. In addition, an overview of the current knowledge of ubiquitin-mediated regulation of the damage recognition in NER has been included.

To identify (novel) ubiquitin modifications involved in the UV-induced DDR mass spectrometry can be used. Quantitative proteomic strategies, including stable isotope labeling by amino acids in cell culture (SILAC) enable the identification and quantification of ubiquitylation sites in response to a specific stimulus on a proteome-wide level. However, identification of ubiquitylation sites is challenging due to their low abundance in protein mixtures. In **Chapter 2** we combined SILAC-based proteomics with a method to specifically isolate ubiquitylated peptides in order to identify UV-induced changes in the ubiquitylation status of proteins. Approximately, 400 UV-responsive ubiquitylation sites were identified on 310 proteins. Most of these proteins play a role in DNA repair, chromatin remodeling, transcription, RNA splicing, translation and the ubiquitin proteasome system. Among proteins with increased ubiquitylation sites we identified the well established ubiquitylated NER factors, especially those involved in damage recognition, indicating the high level of regulation during NER initiation. In addition, we identified multiple ubiquitylated peptides of the thus far unknown ubiquitin target, histone H1. UV-induced ubiquitylation of histone H1 was validated by biochemical experiments. These results suggest a role for histone H1 ubiquitylation in the UV-DDR and have initiated further studies on the functional significance and molecular mechanism of the H1 ubiquitination during the UV-DDR.

Chapter 3 describes the identification and characterization of RNF111, a SUMO-

targeted ubiquitin E3 ligase (STUbL) that is required for GG-NER. STUbLs facilitate direct crosstalk between modifications by small ubiquitin-like modifier (SUMO) and ubiquitin. RNF111 was identified in a search for proteins containing SUMO-interacting motifs (SIMs). RNF111 uses three adjacent SIMs for the specific recognition of proteins modified with poly-SUMO2/3 chains. Quantitative mass spectrometry indicated that RNF111 interacts with the E2 ubiquitin-conjugating enzyme UBC13, which specifically promotes K63-linked chain formation. In addition, we demonstrate that RNF111 - together with UBC13 - targets SUMOylated XPC, the main damage recognition factor of GG-NER. We showed that RNF111 controls NER by regulating the recruitment of XPC to DNA damage. Follow up research, as described in **Chapter 4**, on the molecular function of RNF111 during NER revealed that DNA repair is not fully defective but its progression is rather delayed in the absence of functional RNF111. Live cell imaging experiments showed that RNF111-mediated ubiquitylation stimulates the release of XPC from DNA lesions. In addition, we demonstrate that this ubiquitin-dependent release of XPC is required for the stable incorporation of the NER endonulcleases XPG and ERCC1/XPF to progress the NER reaction. These data provide evidence for a novel NER regulatory mechanism, involving SUMOylation-dependent ubiquitylation of the DNA damage sensor XPC that controls its binding to damaged DNA and is essential for a coordinated handover between XPC and the structure-specific endonuclease XPG. Failure to release XPC by RNF111 at the appropriate time impedes progression of the later steps.

In **Chapter 5** we further focus on XPC dynamics during NER initiation. FRAP analysis revealed that binding of XPC to damaged DNA in living cells, in contrast to other NER factors, presents a switch-like behavior dependent on the received UV-dose. At low UV-doses (0-4 J/m^2) XPC only binds transiently to sites of DNA damage and recruitment of the core NER factors seems to predominantly depend on functional TC-NER. However, above this threshold (~4 J/m^2) the DNA binding affinity of XPC switches to a more stable association to sites of DNA damage and subsequent activation of GG-NER. These data suggest a molecular switch that may prioritize at low UV-doses the repair of toxic transcription blocking DNA lesions over lesions located in non-transcribed parts of the genome. Knockdown of the ubiquitin E3 ligase CUL4A abolished the switch-like behavior of XPC, indicating that XPC ubiquitylation may be required to establish the switch. Mutating one of the UV-induced ubiquitylation sites (K174) of XPC that we have identified in **Chapter 2,** resulted in a similar linear UV-dose dependent behavior as observed for CUL4A knockdown. Taken together we identified a novel ubiquitin-dependent molecular switch that suppresses GG-NER at low dose to prioritize TC-NER. Intriguingly, pathway choice between TC-NER of GG-NER is thus not only determined by the location of lesions, but also by the amount of lesions.

In **Chapter 6** we investigate the dynamic behavior of another NER factor; replication protein A (RPA). RPA binds single stranded DNA (ssDNA) and is an essential DNA replication factor that is also involved in different DNA repair pathways, including NER. Using a combination of immunofluorescence and live cell imaging of GFP-tagged RPA70 we showed that RPA, in contrast to the replication factors PCNA and RFC, does not cluster into replication foci, most likely due to it short residence time at ssDNA. In addition, RPA is the only NER factor known to function in both the pre- and post-incision steps of NER. While pre-incision factors accumulate rapidly at locally UV-induced DNA damage and start to disappear 2 h after DNA damage

induction, RPA reaches its maximum accumulation only after 3 h and remains detectable up to 8 h post UV, probably reflecting its role during the post-incision step of NER. RPA binding to the pre-incision NER complexes could only be visualized in the absence of incision, i.e. in XPF-deficient cells, without a substantial increase in residence time. These data indicate that RPA is an intrinsically highly dynamic protein.

Finally, in **Chapter 7** the main findings derived from the experimental work described in this thesis are summarized and their contribution towards the further understanding of the regulation of damage recognition in NER is being discussed. In addition, possible directions for future research regarding ubiquitin-mediated regulation of NER are provided.

Samenvatting

DNA bevat alle genetische informatie voor de ontwikkeling en het functioneren van ieder organisme. DNA bestaat uit twee strengen nucleotiden (letters) die met elkaar vervlochten zijn in de vorm van een dubbele helix. De volgorde van de letters vormt een code, die via een tijdelijke kopie (RNA) vertaald wordt naar de verschillende bouwstenen (eiwitten) in de cel. Eiwitten regelen alle processen in de cel. Het is dus van groot belang dat er geen fouten in de code (DNA) ontstaan.

DNA wordt echter continu aangetast door schadelijk factoren, zoals bijproducten die vrijkomen bij cellulaire stofwisseling, chemicaliën en UV-straling in zonlicht. Het directe gevolg van DNA-schade is de verstoring van vitale processen in de cel zoals de verdubbeling van DNA (replicatie) ten behoeve van celdeling, en de aanmaak van RNA (transcriptie) voor de productie van eiwitten. Opeenhoping van DNA-schade vermindert cel vitaliteit en kan leiden tot versnelde celdood wat bijdraagt aan de veroudering van een organisme. Daarnaast kan DNA-schade leiden tot veranderingen in de genetische code (mutaties) en het ontstaan van kanker veroorzaken. Ons lichaam is echter uitgerust met verschillende DNA-herstelmechanismen en signaleringssystemen, de DNA-schade respons (DNA Damage Response, DDR) - die de genetische code in het DNA beschermt.

Nucleotide excisie herstel (Nucleotide Excision Repair, NER) is een DNA-herstelmechanisme dat verantwoordelijk is voor de reparatie van DNA-schades, die de structuur van de dubbele DNA helix verstoren. Dit type DNA-schade wordt onder andere veroorzaakt door UV-straling aanwezig in zonlicht. NER kan DNA-schade op twee verschillende manieren verwijderen: globaal genoom NER (GG-NER) en transcriptie gekoppeld NER (TC-NER). Deze sub-mechanismen verschillen slechts in de manier van schadeherkenning. GG-NER tast continu het hele genoom af (al het DNA in een cel) op zoek naar DNA-schades, terwijl TC-NER specifiek schades herkent die transcriptie blokkeren. Er zijn in totaal meer dan 30 eiwitten betrokken bij het functioneren van NER. Het is van groot belang dat de betrokken eiwitten hun functie op de juiste plaats en tijd uitvoeren. Dit vereist een goede organisatie en regulatie. Complexe processen zoals NER worden vaak gereguleerd door kleine chemische veranderingen aan eiwitten (post-translationele modificatie, PTM). In veel gevallen wordt er een kleine functionele groep aan eiwitten gekoppeld, bijvoorbeeld bij fosforylering of methylering. Ook kunnen eiwitten aangepast worden met kleine eiwitten. Een heel bekend voorbeeld is ubiquitine, dat met behulp van drie enzymen (E1, E2 en E3) gebonden wordt aan eiwitten. Deze koppeling wordt ubiquitinering genoemd en kan eigenschappen, zoals stabiliteit en activiteit van het aangepaste eiwit veranderen. Recente bevindingen duiden erop dat ubiquitinering een belangrijke rol speelt in de regulatie van NER. Dit proefschrift beschrijft de regulatie van DNA-schadeherkenning in NER door ubiquitine. In **hoofdstuk 1** worden de onderwerpen DNA-schade respons en ubiquitinering geïntroduceerd. Daarnaast wordt er een actueel overzicht gegeven over de rol van ubiquitine in DNA-schadeherkenning door NER.

Een techniek om (nieuwe) eiwit veranderingen (modificaties) met ubiquitine te identificeren is massa-spectrometrie (MS). Eiwitten worden in kleine stukjes (peptiden) geknipt om vervolgens de massa hiervan te bepalen. Peptiden met een ubiquitine modificatie hebben een unieke massa verandering die gebruikt kan worden om de modificatie en de plaats te identificeren. Kwantitatieve MS methoden maken het mogelijk om ubiquitine

modificaties, veroorzaakt door een specifieke stimulus, te identificeren en kwantificeren. Het is echter niet eenvoudig om ubiquitine modificaties te detecteren, omdat slechts een klein deel van alle eiwitten geubiquitineerd wordt. In **hoofdstuk 2** hebben we kwantitatieve MS gecombineerd met een methode om geubiquitineerde peptiden te isoleren om een efficiëntere detectie mogelijk te maken. Deze strategie hebben we gebruikt om UV-specifieke ubiquitine modificaties te identificeren. In totaal hebben we ongeveer 400 UV-afhankelijke ubiquitine modificaties op 310 verschillende eiwitten geïdentificeerd. Een groot deel van deze eiwitten speelt een belangrijke rol in biologische processen als DNA reparatie, chromatine reorganisatie, transcriptie, translatie en het ubiquitine proteasome systeem. In de groep eiwitten met een toename in ubiquitine modificaties zijn bekende NER eiwitten geïdentificeerd. De grootste verandering is gemeten voor de eiwitten die DNA-schade herkennen - onder andere XPC - en dit benadrukt de sterke regulatie van NER, en met name de DNA-schadeherkenning. Daarnaast hebben we ook, tot voor kort onbekende ubiquitine modificaties op het histon H1 eiwit geïdentificeerd. Biochemische experimenten hebben bevestigd dat histon H1 inderdaad UV-afhankelijk geubiquitineerd wordt. Deze resultaten laten zien dat ubiquitinering van histon H1 mogelijk een rol speelt in de DDR. De functie en het moleculaire mechanisme van histon H1 ubiquitinering in de DDR worden momenteel verder onderzocht.

Hoofdstuk 3 beschrijft de identificatie en karakterisering van het E3 enzym RNF111 dat nodig is voor het functioneren van GG-NER. RNF111 behoort tot een speciale klasse E3 enzymen, die specifiek eiwitten herkennen die gemodificeerd zijn met een ubiquitine analoog, SUMO. Een E3 enzym uit deze klasse wordt een “SUMO-targeted ubiquitin E3 ligase” (STUbL) genoemd. STUbLs vormen een belangrijke link tussen SUMO- en ubiquitine- modificaties. RNF111 is geïdentificeerd in een zoektocht naar eiwitten met SUMO-bindende motieven (SUMO-interacting motif, SIM). RNF111 heeft drie aangrenzende SIMs en herkent specifiek eiwitten gemodificeerd met SUMO-ketens (geSUMOyleerde eiwiten). Kwantitatieve MS heeft aangetoond dat RNF111 bindt aan het E2 enzym UBC13, dat de vorming van ubiquitine ketens via lysine (K) 63 katalyseert. Daarnaast hebben we laten zien dat RNF111 in samenwerking met UBC-13 K63-ubiquitine ketens kan vormen op SUMO gemodificeerd XPC, het eiwit wat verantwoordelijk is voor het herkennen van DNA-schade en activatie van GG-NER. Bovendien tonen onze bevindingen aan dat RNF111 GG-NER reguleert door de bindingseigenschappen van XPC voor DNA-schade te veranderen. Vervolg onderzoek naar de moleculaire functie van RNF111 in NER, beschreven in **hoofdstuk 4**, wijst uit dat NER in de afwezigheid van RNF111 niet compleet defect is maar vertraagd. Microscopie op levende cellen heeft laten zien dat XPC ubiquitinering door RNF111 nodig is om ervoor te zorgen dat XPC los laat van het DNA. Het loslaten van XPC van DNA-schade is belangrijk zodat de eiwitten die het DNA inknippen (endonucleases XPG en ERCC1/XPF), om DNA-schade te verwijderen, kunnen binden. Deze bevinding vormt het bewijs voor een nieuw moleculair mechanisme dat de DNA-bindingseigenschappen van XPC reguleert met behulp van SUMO- en ubiquitine- modificaties. Dit is essentieel voor een gecoördineerde overdracht van beschadigd DNA van XPC naar XPG. In het geval dat XPC niet op het juiste moment loslaat van beschadigd DNA belemmert dit de voortgang NER en de reparatie van het DNA.

In **hoofdstuk 5** bestuderen we de dynamiek (beweging) van XPC eiwitten tijdens de schadeherkenning stap van NER. Door XPC te voorzien van een fluorecent label hebben

we ontdekt dat XPC DNA-schade bindt afhankelijk van de hoeveelheid UV-straling die de cel ontvangt (UV-dosis). Bij een lage UV-dosis (0-4 J/m^2) bindt XPC slechts heel kort (transient) aan beschadigd DNA en is de werking van de latere NER factoren compleet afhankelijk van het andere mechanisme, TC-NER. Echter bij een dosis boven de 4 J/m^2 schakelt XPC over naar een stabielere binding wat leidt tot de activatie van GG-NER. Deze data suggereert dat er een soort moleculaire schakelaar is die prioriteit geeft aan de reparatie van DNA-schades die transcriptie blokkeren ten opzichte van DNA-schades elders in het DNA bij lage UV-dosis. Vermindering van de hoeveelheid Cul4A, een ubiquitine E3 ligase, of het verwijderen van één van de ubiquitine plaatsen (K174) in XPC, geïdentificeerd in **hoofdstuk 2**, heft het schakelgedrag van XPC echter op. Dit resultaat laat zien dat XPC ubiquitinering nodig is om het schakelgedrag mogelijk te maken. Samengevat, hebben we een nieuw ubiquitine afhankelijk mechanisme ontdekt, dat GG-NER bij lage UV-dosis onderdrukt om prioriteit te geven aan de reparatie van DNA-schades die transcriptie blokkeren (TC-NER). De keuze tussen GG-NER en TC-NER is dus niet alleen afhankelijk van de plaats van schade, maar ook van de hoeveelheid UV-straling.

In **hoodstuk 6** doen we onderzoek naar de dynamiek van een ander NER eiwit, replicatie eiwit A (Replication protein A, RPA). RPA bindt aan enkelstrengs DNA en speelt een belangrijke rol in DNA replicatie en verschillende DNA-herstelmechanismen, inclusief NER. Een combinatie van immunofluorescentie en microscopie in levende cellen met fluorescerend RPA toont aan dat RPA eiwitten, in tegenstelling tot andere replicatie eiwitten zoals PCNA en RFC, niet clusteren in replicatie foci (een plaats in de cel waar veel DNA wordt vermenigvuldigd). Dit is te verklaren door de zeer korte verblijftijd van RPA op het enkelstrengs DNA tijdens replicatie. RPA is het enige NER eiwit dat zowel een functie heeft voor en na het inknippen van DNA (pre- en post-incisie NER). Pre-incisie eiwitten zoals XPC verzamelen direct op de plaats van DNA-schade en gaan weg binnen twee uur. Opeenhoping van RPA is echter pas zichtbaar op de plaats van DNA-schade na 3 uur en is te detecteren tot 8 uur na blootstelling aan UV. Deze opeenhoping van RPA moleculen reflecteert zeer waarschijnlijk de functie van RPA tijdens post-incisie NER. RPA opeenhoping tijdens pre-incisie NER kunnen we alleen zichtbaar maken in cellen waar geen incisie plaats kan vinden door XPF. De verblijftijd van RPA op het DNA verandert echter niet in deze cellen en blijft zeer kort. Deze resultaten bewijzen dat RPA een zeer dynamisch eiwit is.

In **hoofdstuk 7** worden de belangrijkste bevindingen van dit proefschrift samengevat en bediscussieerd. We laten zien hoe onze bevindingen bijdragen aan het inzicht in de regulatie van DNA-schadeherkenning door NER. Daarnaast worden er mogelijkheden besproken voor toekomstig onderzoek naar ubiquitine modificaties die NER kunnen reguleren.

Curriculum Vitae

Loes van Cuijk was born on January 7th 1986 in Oosterhout (NB), The Netherlands. She graduated from secondary school at Theresialyceum in Tilburg in 2004. She continued her education at the Radboud University Nijmegen, studying Molecular Life Sciences. As part of the master program she carried out two internships. She performed the first internship at the department of Tumor Immunology under supervision of Prof.dr. J de Vries. The second internship she conducted in the group Genome dynamics and stability of Prof.dr. M. Tijsterman. After obtaining her master degree in 2009, she started her PhD research at the Erasmus MC, 2010-2014. The work was performed at the department of Genetics under supervision of Dr. J.A.F. Marteijn and Prof.dr. W. Vermeulen. The results of the research are described in this thesis. In November 2014 she started a Traineeship Regulatory Afffairs at Zwiers Regulatory Consultancy.

List of publications

Poulsen SL, Hansen RK, Wagner SA, **van Cuijk L**, van Belle GJ, Streicher W, Wikström M, Choudhary C, Houtsmuller AB, Marteijn JA, Bekker-Jensen S, Mailand N. RNF111/Arkadia is a SUMO-targeted ubiquitin ligase that facilitates the DNA damage response. *J Cell Biol* 201, 797-807 (2013)

van Cuijk, L., Vermeulen, W. & Marteijn, J.A. Ubiquitin at work: The ubiquitous regulation of the damage recognition step of NER. *Exp Cell Res* 329, 101-109 (2014).

Gourdin AM*, **van Cuijk L***, Tresini M, Luijsterburg MS, Nigg AL, Giglia-Mari G, Houtsmuller AB, Vermeulen W, Marteijn JA. Differential binding kinetics of replication protein A during replication and the pre- and post-incision steps of nucleotide excision repair. *DNA Repair* 24, 46-56 (2014)

van Cuijk, L*, van Belle GJ *, Turkyilmaz Y[1], Poulsen SL, Janssens RC, Sabatella M, Lans H, Mailand N, Houtsmuller AB, Vermeulen W, Marteijn JA. *Manuscript in preparation.*

van Belle GJ, **van Cuijk L**, Vuist IM, Geverts B, van Royen ME, Verschure PJ, Marteijn JA, Vermeulen W, Houtsmuller AB. A bimodal switch regulates priority for repair of active genes under mild genotoxic stress. *Manuscript in preparation.*

A

PhD portfolio

Name	Loes van Cuijk
PhD period	2010-2014
Promotor	Wim Vermeulen
Co-promotor	Jurgen Marteijn

General courses

Safely Working in the Laboratory	2010
ML-I (work permit for GMOs)	2007
ML-II (work permit for Adenovirus and Lentivirus)	2010
CDB Course	2010
Genetics course	2010
Biochemistry and biophysics course	2010
Literature course	2011
Biomedical English Writing and Communication	2013

Specific courses

Confocal microscopy	2010
Genome Maintenance and Cancer	2010
In vivo imaging from molecule to organism	2010
The Microscopic Image Analysis: From Theory to Practice	2011
Technology facilities	2011
Image J	2011

Seminars and workshops

3rd Annual CGC scientific meeting Utrecht, The Netherlands.	2010
17th MGC workshop Cologne, Germany.	2010
20th MGC Symposium Leiden, The Netherlands.	2010
CGC/CBG meeting “Molecular Mechanisms in Cancer” Amsterdam, The Netherlands.	2010
18th MGC workshop Maastricht, The Netherlands. Poster presentation.	2011
21th MGC Symposium Rotterdam, The Netherlands.	2011

19th MGC workshop Düsseldorf, Germany. Oral presentation.	2012
22th MGC workshop Leiden, The Netherlands.	2012
23th MGC workshop Rotterdam, The Netherlands.	2013

(Inter)national conferences

Responses to DNA damage:from molecular mechanism to human disease Egmond aan Zee, The Netherlands. Poster presentation.	2011
9th Dutch chromatin meeting Groningen, The Netherlands. Poster presentation.	2011
Copenhagen biosciemce conferences: PTMs in cell signaling Copenhagen, Denmark. Poster presentation.	2012

Teaching

Bachelor student	2012
Junior science program	2012
Werkcollege Genetica	2012
Bachelor student	2013
Master student	2013

Dankwoord

Met het einde in zicht typ ik de laatste bladzijden van het proefschrift. Het was soms hard werken, vooral het laatste jaar heb ik heel wat avonduren achter de microscoop en computer doorgebracht. Maar het is de moeite waard geweest, want ik kan mijn proefschrift met trots aan jullie presenteren. Het was een uitdagende tijd waarin ik veel heb geleerd, veel mensen heb leren kennen, maar ook vooral mezelf. Ik kan met veel voldoening terugkijken op deze periode en wil graag alle mensen bedanken, die ieder op hun eigen wijze een bijdrage hebben geleverd aan dit proefschrift. Ik wil een aantal mensen graag in het bijzonder bedanken.

Allereerst mijn copromotor Jurgen. Ik had me geen betere begeleider kunnen wensen. Ik heb erg veel van je geleerd. Niet alleen op het gebied van wetenschap, maar ook dat ik af en toe dingen met een korreltje zout / minder serieus mag nemen. Je deur stond niet alleen open voor vragen, maar ook een praatje (en dat heb je geweten ;)). Je doelgerichte werkwijze, en positieve instelling waren erg verfrissend, en zijn erg belangrijk geweest voor de publicaties. Net als de correcties (tekeningen) van je kinderen. Ook de laatste maanden was je erg betrokken, je nam zelfs taken van mijn paranimf over. Jurgen, bedankt voor deze mooie tijd.

Wim het is een eer om als eerste te promoveren met jou als promotor. Onze meetings waren een bron voor nieuwe ideeën. Je kritische blik en feedback waren zeer waardevol. Op de momenten dat het tegen zat had je altijd wel advies en een opbeurend woordje. Je hebt een zeer gevarieerde groep weten op te bouwen waar altijd een goede sfeer hangt, mede dankzij de labuitjes en BBQ's bij jou en Hannie thuis. Ik ben altijd met veel plezier naar het lab gekomen.

Jan bedankt voor de kans om mijn promotieonderzoek binnen de afdeling Genetica uit te voeren. Je enthousiasme voor wetenschap is uitzonderlijk. Ik hoop dat je de komende jaren nog veel mensen weet te inspireren met deze aanstekelijke eigenschap. Ook Jasperina en Marieke waren de afgelopen jaren onmisbaar. Bedankt voor jullie interesse en het soepel laten verlopen van administratieve zaken rondom mijn promotie.

Daarnaast wil ik de leescommissie, Claire, Titia en Leon bedanken voor het kritisch lezen van het proefschrift en de feedback. Ook wil ik de overige commissieleden, Jan, Adriaan, Jeroen en Alfred bedanken voor de tijd die zij besteed hebben aan (de voorbereiding van) mijn verdediging.

Hoofdstuk 2 was er niet geweest zonder de mensen van de mass spec faciliteit. Jeroen, Dick en Karel heel erg bedankt voor jullie hulp bij het opzetten van de di-Gly experimenten en het snelle meten van mijn samples. Karen jij maakte de vele kolomuren gezellig.

Ook Bert Jaap verdient een aparte vermelding in mijn dankwoord. Vanaf het begin waren we maatjes en hebben we veel samengewerkt. Dit werd wat minder toen ik van ATR naar ubiquitine switchte, maar RNF111 bracht ons onderzoek weer samen. Uit de hoofdstukken 3 t/m 5 blijkt dat we een succesvol team zijn. Verder kwam je vaak naar ons lab voor de gezelligheid en TAART. Je bent dan ook deel van onze groep geworden.

Yasemin en Roel, ook jullie bedankt voor je bijdrage aan de resubmissie van het RNF111 paper.

And not to forget my colleagues from the lab. First my “old buddies”, Petra, Maikel, Ozge and Kasper. Petra you showed me around in the lab and introduced me to the world of ubiquitin. You and Maikel made sure we could always have fun; I will never forget our Friday afternoon “dance on the lab table” drinks. Ozge you have a warm personality. Thanks for always listening to me and your advice to negotiate for my promotion party; you became more Dutch than you want to admit;). Kasper the one that reminds me of home (Brabant), you were always there to help me when I was yelling at my computer. And then the core of the lab: Hannes, Arjan and Nils. Although the majority of the lab transformed from men to women, you managed to maintain your humor in the lab, my compliments. Joris thanks for the conversations at the coffee machine when I needed a break. Also my new buddies, Imke, Serena, Yasemin, Mariangela, Barbara, Cristina and Franzi made sure I enjoyed my time in the lab. One of my favourite moments was our trip to the Efteling. Jana although we just met before I left, I enjoyed your company in the office. During the years many people came and went to reinforce our lab, Charlie, Daniel, Maria, Herve, Gisella, Florian, Rianne, David, Gossia, Angela, Loes, Marinke, Esther, Mireille, Aida, Mervyn, Marloes, Aranka, Quirine, Weike, Alice, Mark and Tiago. Thank you all for the nice time, I wish you all the best.

Nee Karen, ik ben je niet vergeten je verdient gewoon je eigen stukje. Jij was toch wel mijn maatje op het lab. Ik kon altijd bij je terecht of je nu op het lab wormen aan het pikken was of bezig met andere “saaie” taken. Ik heb het erg leuk gevonden om samen met jou één van de labuitjes te organiseren. Heel veel succes met je “projectje”in het zonnige Gouda. Ik kom graag een keer BBQ-en als het klaar is.

Ook tijdens de laatste fase sta ik er gelukkig niet alleen voor. Imke en Anouk, ik ben trots dat jullie mijn paranimfen willen zijn. Imke jouw aanwezighied op het lab was een garantie voor gezelligheid. Na het vertrek van Petra en Maikel zorgde jij er onder andere voor dat de vrijdagmiddag borrels bleven bestaan, hoewel dit niet een gemakkelijke taak was. Ik hoop dat we nog vaak een drankje zullen doen. Verder wil ik je graag bedanken voor je bijdrage aan Hoofdstuk 2. En ik vertrouw erop dat het een mooi feestje gaat worden.

Anouk, mijn grote kleine zusje, of ik nu wel of niet ga trouwen één ding is zeker je bent in ieder geval 17 april mijn bruidsmeisje ;). Vanaf de basisschool was je stiekem al een grote zus voor mij, want kom je aan Loes dan kom je aan Anouk. Daarom ben ik ook blij dat jij tijdens mijn verdediging aan mijn zijde staat. Ook jij weet van feesten, dus al met al een zeer geschikte paranimf.

Natuurlijk zijn er ook mensen buiten het lab die ik graag wil bedanken. Allereerst mijn vrienden uit Nijmegen jullie zorgden voor de nodigde afleiding en “gedwongen” ontspanning. Zonder alle weekendjes, feestjes en etentjes zou ik de uitgang van het Erasmus MC niet meer hebben kunnen vinden.

Mijn schoonfamilie Wim, Marloe, Casper, Audrey, Opa en Oma Bult, na jaren promotie hectiek is het einde in zicht. De vakantie in Cyprus, uitjes en gourmetavondjes waren altijd erg gezellig. Wel twijfel ik na al die jaren of de bombe echt bestaat. Bedankt voor jullie interesse in mijn werk, begrip en bemoedigende woorden tijdens deze drukke periode.

Dais mijn “echte grote zus” ik ben trots op jou en Isabella. Geweldig dat je nu samen met Tjeerd gesetteld bent in jullie nieuwe huis. Het is fantastisch om Isabella te zien opgroeien. Als kinderen maakten we samen met Anouk en Lucien de buurt onveilig. Ik herinner me vooral iets met een schans. Stiekem mis ik de tijd dat we zoveel met zijn drietjes optrokken. Maar gelukkig heb ik binnenkort weer meer vrije tijd, ik voel een Lady’s night aankomen.

Opa, de laatste jaren bekend als opi (ongelofelijk pientere ik), ik wil u en oma (aan wie ik het proefschrift opdraag) ook graag bedanken. Jullie zijn altijd heel erg betrokken geweest. Ik kon altijd bij jullie terecht en heb mooie herinneringen aan onze gezamenlijke vakanties en vele logeerpartijtjes. We delen de passie voor spelletjes, ik hoop dat we nog vaak een potje mogen keezen/ pipi-en.

Over spelletjes gesproken, dan mag ik zeker niet mijn 30 seconds maatje Max vergeten. Aan 1 woord of gebaar hebben we genoeg. Wanneer gaan we weer gamen?!

Pap en Mam ik weet dat jullie ontzettend trots op mij zijn, maar ik mag mijn handen dichtknijpen met jullie als ouders. Jullie hebben mij altijd gesteund, gestimuleerd en advies gegeven waar mogelijk. Het is soms zwaar dat ik niet om de hoek woon en even binnen kan wippen als ik daar zin heb. Ik vind het erg fijn dat als ik thuis kom, nog steeds het gevoel heb dat ik echt thuis kom. Ik geniet enorm van onze wandelingen in het bos. Bedankt dat jullie er altijd voor me zijn, als klaagmuur, luisterend oor of gewoon voor de gezelligheid. Ik kijk al uit naar onze trip naar Rome. Pap en Mam bedankt voor alles.

Lieve Remko, eindelijk klaar. Jij hebt me altijd steun en stabiliteit gegeven. Je weet me altijd op te vrolijken en aan het lachen te maken. Ik ben een sterker persoon met jou aan mijn zijde. Ik vind het heerlijk om na een drukke werkdag bij jou thuis te komen. Bedankt voor alle mooie momenten en avonturen die we de afgelopen jaren hebben beleefd, dat er nog velen mogen volgen. Ofwel, Remko ik hou van jou.

Loes